

**Biotrophic Development of *Ustilago maydis*
and the Response of Its Host Plant Maize**

(Die biotrophe Entwicklung von *Ustilago maydis*
und die Reaktion seiner Wirtspflanze Mais)

Dissertation



zur

Erlangung des Doktorgrades
der Naturwissenschaften
(Dr.rer.nat)

dem Fachbereich Biologie
der Philipps-Universität Marburg
vorgelegt von

Ramon Wahl
aus Kreuztal

Marburg/Lahn 2009

Vom Fachbereich Biologie
der Philipps-Universität Marburg als Dissertation
angenommen am: _____

Erstgutachter: Herr PD. Dr. Michael Feldbrügge
Zweitgutachter: Herr Prof. Dr. Jörg Kämper

Tag der mündlichen Prüfung am: _____

Erklärung

Ich versichere, daß Ich meine Dissertation mit dem Titel “Biotrophic Development of *Ustilago maydis* and the Response of Its Host Plant Maize” selbständig, ohne unerlaubte Hilfe angefertigt und mich dabei keiner anderen als der von mir ausdrücklich bezeichneten Quellen und Hilfen bedient habe.

Die Dissertation wurde in der jetzigen oder einer ähnlichen Form noch bei keiner anderen Hochschule eingereicht und hat noch keinen sonstigen Prüfungszwecken gedient.

(Ort/Datum)

Ramon Wahl

Die Untersuchungen zur vorliegenden Arbeit wurden von September 2005 bis März 2008 in Marburg am Max-Planck-Institut für terrestrische Mikrobiologie in der Abteilung für Organismische Interaktionen und von April 2008 bis Juni 2009 am Karlsruher Institut für Technologie in der Abteilung für Genetik unter der Betreuung von Herrn Prof. Dr. Jörg Kämper durchgeführt

Teile dieser Arbeit sind in folgenden Artikeln veröffentlicht oder zur Veröffentlichung eingereicht:

Wahl, R., Doehlemann, G., Horst, R.J., Voll, L.M., Usadel, B., Poree, F., Stitt, M., Pons-Kühnemann, J., Sonnewald, U., Kahmann, R., Kämper, J. (2008) Reprogramming a maize plant: transcriptional and metabolic changes induced by the fungal biotroph *Ustilago maydis*. *Plant J.* 56(2):181-95.

Wahl, R., and Kämper, J. (2009) The *Ustilago maydis* *b* mating type locus controls hyphal proliferation and expression of secreted virulence factors *in planta*. *Mol Microbiol.* submitted

Wahl, R., Wippel, K., Kämper, J., and Sauer, N. (2009) A novel high affinity sucrose transporter is required for fungal virulence and avoids extracellular glucose signaling in biotrophic interactions. *PLoS Biol.* submitted

Summary

Fungal plant pathogens affect the quality of food and feed produced from infected plants and cause substantial yield losses every year. Especially fungi infecting cereal crops represent an enormous threat. The biotrophic fungus *Ustilago maydis* is the causative agent of the smut disease on maize. Molecular pathways essential for the initiation of fungal pathogenicity, like mating of two compatible sporidia, the establishment of an infectious dikaryon and the penetration process leading to plant infection are intensively studied in *U. maydis*. However, the strategies used by the fungus to proliferate within the plant and to deal with the hostile environment, are vastly unknown. This dissertation investigates the complex molecular interplay between *Ustilago maydis* and its host plant in more detail, focusing on three different aspects.

In *U. maydis* the initiation of sexual development and pathogenicity is controlled by two homeodomain proteins bE and bW, which form an active transcription factor after fusion of two compatible sporidia. By constructing temperature-sensitive bE proteins, I was able to demonstrate that also the proliferation of *U. maydis* within the plant is regulated by the b mating type transcription factor (2.1). The inactivation of the bW/bE complex within the plant stops fungal development and leads to the deregulation of secreted proteins, which are believed to interfere with plant defense responses.

U. maydis establishes a compatible biotrophic relationship with its host. To analyze the plant cell responses towards this forced interaction, global expression analysis and metabolic profiling were performed monitoring a time-course of infection (2.2). Expression analyses revealed an initial recognition of *U. maydis* by the maize plant, leading to the induction of basal plant defense responses. After *U. maydis* has penetrated the plant these defense responses are suppressed, suggesting an active interference with the plant immune system. Moreover, during disease progression *U. maydis* infected maize leaves do not develop into photosynthetically active source tissues, but maintain the characteristics of a nutrient sink. Like typical plant nutrient sinks the infected area is supplied with sucrose that is feeding the fungus.

As nutrient availability determines the fitness of the pathogen, it also determines the pathogen's success to conquer the plant. Thus, biotrophic fungi like *U. maydis* have to develop strategies to feed on nutrients provided by a living host plant. By identifying two *U. maydis* sugar transporters, Srt1 and Hxt1, as necessary for full

fungal virulence, I was able to analyze which plant-derived carbohydrates are crucial for biotrophic development (2.3; 2.4). Srt1, a novel kind of sucrose transporter, is exclusively expressed during infection. Its unusual high sucrose affinity is well suited to compete with plant-derived sucrose uptake systems at the plant/fungus interfacen (2.3). Hxt1 utilizes hexoses glucose, fructose and mannose, and with lower affinity also galactose and xylose. Deletion of *hxt1* reduces fungal pathogenicity, influences growth and hampers monosaccharide-dependent gene regulation. Moreover, expression analysis revealed that Hxt1 has a dual function as monosaccharide-transporter and -sensor (2.4). As double-deletion mutants of *hxt1* and *srt1* fail to induce severe disease symptoms, both uptake of sucrose and its cleavage products glucose and fructose are crucial for *in planta* development of *U. maydis* (2.4).

U. maydis is recognized by the maize plant already prior to infection, resulting in the induction of basal plant defense responses. However, as soon as the fungus penetrates the plant these defense responses are manipulated by *U. maydis*, most probably caused by the action of fungal secreted proteins interfering with recognition and defense pathways. During disease progression, the infected maize tissue remains a sucrose-dependent nutrient sink, which lacks photosynthetic activity. This sink supplies *U. maydis* with sucrose and hexoses utilized by Srt1 and Hxt1 to promote fungal growth. Initiation and maintenance of the biotrophic interaction, including the expression of secreted proteins necessary to manipulate the host, are regulated by a complex transcription cascade, which is controlled by the bE/bW heterodimer. The b-cascade not only regulates fungal proliferation and differentiation, but also adapts the fungal needs towards changing plant tissues.

Zusammenfassung

Pflanzenpathogene Pilze beeinträchtigen die Qualität von Nahrungsmitteln für Mensch und Tier und verursachen jedes Jahr erhebliche Ernteaufschläge. Speziell Pilze, die Getreidepflanzen infizieren, stellen ein erhebliches wirtschaftliches Problem dar. Der biotrophe Pilz *Ustilago maydis* ist der Erreger des Maisbeulenbrandes. Für die Initiation pilzlicher Pathogenität essentielle molekulare Mechanismen, wie die Fusion zweier kompatibler Sporidien, die Etablierung des infektiösen Dikaryons sowie des Penetrationsprozesses, welcher die Infektion der Pflanze einleitet, werden in *U. maydis* intensiv erforscht. Die Details, wie sich der Pilz in der Pflanze ausbreitet und sich an die unwirtliche Pflanzenumgebung anpasst, sind jedoch weitgehend unbekannt. Diese Dissertation untersucht das molekulare Wechselspiel zwischen *Ustilago maydis* und seiner Wirtspflanze und verfolgte dabei drei verschiedenen Ansätze.

Die Initiation der sexuellen Entwicklung und Pathogenität wird in *U. maydis* von den beiden Homeodomänproteinen bE und bW kontrolliert, welche einen aktiven Transkriptionsfaktor nach Fusion zweier kompatibler Sporidien bilden. Durch Konstruktion von temperatursensitiven bE-Proteinen war es möglich zu zeigen, dass auch innerhalb der Pflanze die Entwicklung von *U. maydis* von dem b-Heterodimer reguliert wird (2.1). Eine Inaktivierung des bW/bE-Komplexes innerhalb der Pflanze stoppt das pilzliche Wachstum und führt zu einer Deregulation von sekretierten Proteinen, welche wahrscheinlich die Abwehrmechanismen der Pflanze manipulieren.

U. maydis etabliert ein enges, biotrophes Abhängigkeitsverhältnis mit seinem Wirt. Um die Reaktion der Pflanzenzellen während dieser Interaktion zu untersuchen, wurden globale Expressions- und Metabolomanalysen über den gesamten Infektionsverlauf durchgeführt (2.2). Die Expressionsanalysen zeigten eine frühe Erkennung von *U. maydis* durch die Maispflanze, welche grundlegende Abwehrreaktion induziert. Nach Penetration der Pflanze durch *U. maydis* werden diese Abwehrreaktionen unterdrückt, was auf einen aktiven Eingriff des Pilzes in das pflanzliche Immunsystem hindeutet. Weiterhin zeigten die Analysen, dass sich mit *U. maydis* infizierte Maisblätter nicht zu photosynthetisch aktiven Geweben entwickeln, sondern ihre Nährstoffe aus anderen Teilen der Pflanze beziehen. Zur Deckung des Kohlenhydratbedarfs wird typischerweise Saccharose in solche Gewebe importiert, was sich auch in den infizierten Bereichen beobachten lässt.

Da die Nährstoffverfügbarkeit die Fitness eines Pathogens bestimmt, ist sie auch ausschlaggebend für die erfolgreiche Entwicklung innerhalb der Wirtspflanze. Entsprechend müssen biotrophe Pilze wie *U. maydis* Strategien entwickeln, um sich von den Nährstoffen des Wirtes zu ernähren. Durch die Identifizierung von Srt1 und Hxt1, zwei für die pathogene Entwicklung von *U. maydis* notwendigen Zuckertransportern, war es mir möglich zu analysieren, welche pflanzlichen Kohlenhydrate entscheidend für die biotrophe Entwicklung sind (2.3; 2.4). Srt1, ein neuartiger Saccharosetransporter, wird ausschließlich während der Infektion exprimiert. Durch seine ungewöhnlich hohe Affinität zu Saccharose ist Srt1 bestens geeignet, um mit pflanzlichen Saccharosetransportsystemen zu konkurrieren (2.3). Hxt1 transportiert die Hexosen Glukose, Fruktose und Mannose, und mit niedrigerer Affinität auch Galaktose und Xylose. Die Deletion von *hxt1* reduziert die Pathogenität von *U. maydis*, beeinflusst sein Wachstum und behindert Monosaccharid-abhängige Genregulation. Expressionsanalysen in *hxt1*-Deletionsmutanten zeigten, dass Hxt1 als Monosaccharidtransporter und -sensor fungiert (2.4). Da *hxt1* und *srt1* Doppeldeletionsmutanten nahezu überhaupt keine Krankheitssymptome nach Infektion induzieren, ist sowohl die Aufnahme von Saccharose als auch die ihrer Spaltprodukte notwendig für die pathogene Entwicklung von *U. maydis*.

Die Pflanze erkennt *U. maydis* bereits auf der Pflanzenoberfläche, woraufhin sie Abwehrmechanismen einleitet. Nach Infektion mit *U. maydis* werden diese Reaktionen manipuliert, wahrscheinlich durch die Aktivität sekretierter, pilzlicher Proteine. Während der Krankheitsentwicklung ist das infizierte Maisgewebe von Nährstoffimport abhängig, da es keine photosynthetische Aktivität aufweist. Der Kohlenhydratbedarf wird hierbei von Saccharose gedeckt, welche direkt (Srt1) und indirekt (Hxt1) von *U. maydis* aufgenommen wird und als Nahrungsquelle dient. Die Einleitung und Aufrechterhaltung der biotrophen Interaktion, sowie die Expression von sekretierten Proteinen, die für die Manipulation des Wirtes notwendig sind, werden von einer komplexen Transkriptionskaskade reguliert, die durch das bW/bE-Heterodimer kontrolliert wird. Die b-Kaskade reguliert somit nicht nur das Wachstum und die Differenzierung des Pilzes, sondern auch seine Anpassung an verschiedene Pflanzengewebe.

Index

1. General Introduction	1
1.1 The Maize Pathogen <i>Ustilago maydis</i>	1
1.2 <i>Ustilago maydis/Zea mays</i>: A Model System to Study Mechanism of Compatibility	4
1.3 Plant Pathogen Interactions	6
1.3.1 The Plant Immune System	6
1.3.2 Small Secreted Effectors: The Pathogens Tools to Manipulate Its Host ...	8
1.3.3 Carbon Acquisition of Fungal Pathogens during Plant Infection.....	10
1.4 Focus of this Work	12
2. Results	14
2.1 The <i>Ustilago maydis b</i> Mating Type Locus Controls Hyphal Proliferation and Expression of Secreted Virulence Factors <i>in Planta</i>	14
2.1.1 Introduction	16
2.1.2 Results	18
2.1.3 Discussion	25
2.1.4 Experimental Procedures	29
2.1.5 Supplementary Information.....	35
2.2 Reprogramming a Maize Plant: Transcriptional and Metabolic Changes Induced by the Fungal Biotroph <i>Ustilago maydis</i>	37
2.2.1 Introduction	39
2.2.2 Results	41
2.2.3 Discussion	53
2.2.4 Experimental Procedures	57
2.2.5 Supplementary Information.....	61
2.3 A Novel High Affinity Sucrose Transporter is Required for Fungal Virulence and Avoids Extracellular Glucose Signaling in Biotrophic Interactions	63
2.3.1 Introduction	65
2.3.2 Results	67
2.3.3 Discussion	74
2.3.4 Experimental Procedures	77
2.3.5 Supplementary Information.....	81
2.4 Hxt1, a Monosaccharide Transporter and Sensor Required for Virulence of the Maize Pathogen <i>Ustilago maydis</i>	83
2.4.1 Introduction	85
2.4.2 Results	88

2.4.3 Discussion	99
2.4.4 Experimental Procedures	105
2.4.5 Supplementary Information.....	110
3. Research Perspectives.....	112
3.1 b-mediated Transcriptome Adaptation during Biotrophic Development.....	112
3.2 Fungal Sugar Transporters and Their Contribution to Feed <i>U. maydis</i> and to Reprogram the Host Metabolism	114
4. Literature.....	118
5. Supplementary Material.....	138
Authors Contributions	139

1. General Introduction

The General Introduction focuses on the lifestyle of *Ustilago maydis* and highlights the advantages and disadvantages of the model pathosystem *Ustilago maydis/Zea mays*. Furthermore, it reviews the current knowledge about molecular mechanisms of plant pathogen interactions.

1.1 The Maize Pathogen *Ustilago maydis*

Biotrophic fungi usually require a high degree of specification towards their host plants to successfully establish a close interaction. The biotroph *Ustilago maydis* is specialized to infect only two *Zea mays* species, maize and teosinte (*Zea mays ssp. mays* and *ssp. mexicana*). During its dimorphic lifecycle, *U. maydis* changes from saprophytic to biotrophic growth, which is accompanied by a morphological transition from yeast to hypha. In the saprophytic stage, the haploid yeast cells (sporidia) grow by budding (Figure 1.1-1A). Fusion of two sexually compatible sporidia results in a filamentously growing dikaryon (Figure 1.1-1A). This fusion event and the establishment of the infectious dikaryon is mediated by the two mating type loci *a* and *b* (Figure 1.1-1A; Banuett and Herskowitz, 1989; Spellig *et al.*, 1994b).

The *a* locus encodes a pheromone receptor system that regulates cell-to-cell recognition and the fusion of two compatible sporidia (Bölker *et al.*, 1992; Hartmann *et al.*, 1996). The *b* locus encodes two unrelated homeodomain proteins bE and bW that trigger an intracellular recognition event. bE and bW dimerize, when originating from different alleles, and form an active transcription factor which maintains the dikaryon and initiates pathogenic development (Kämper *et al.*, 1995; Romeis *et al.*, 2000; Brachmann *et al.*, 2003). The initiation of pathogenicity via a functional bE/bW complex has been shown conclusively. Its role during subsequent biotrophic development is described in Section 2.1.

The dikaryotic hypha is the infectious form of *U. maydis*. Initially, only the apical cell of the hypha is filled with cytoplasm leaving behind empty fungal sections (Banuett and Herskowitz, 1994). Cell division is stalled until the fungus has invaded its host plant by means of a specialized infection structure (Figure 1.1-1A; Snetselaar and Mims, 1992; Snetselaar and Mims, 1993; Banuett and Herskowitz, 1994). This appressoria-like structure marks the point of penetration into the host cell, which is most likely facilitated by concentrated secretion of cell wall degrading enzymes that soften the plant cell wall (Christensen, 1963; Snetselaar and Mims, 1992; Snetselaar

and Mims, 1993; Doehlemann *et al.*, 2008b). In contrast, fungi that develop true appressoria use mechanical force by generating high turgor pressure within the appressorial cell to enter the plant (reviewed by Deising *et al.*, 2000).

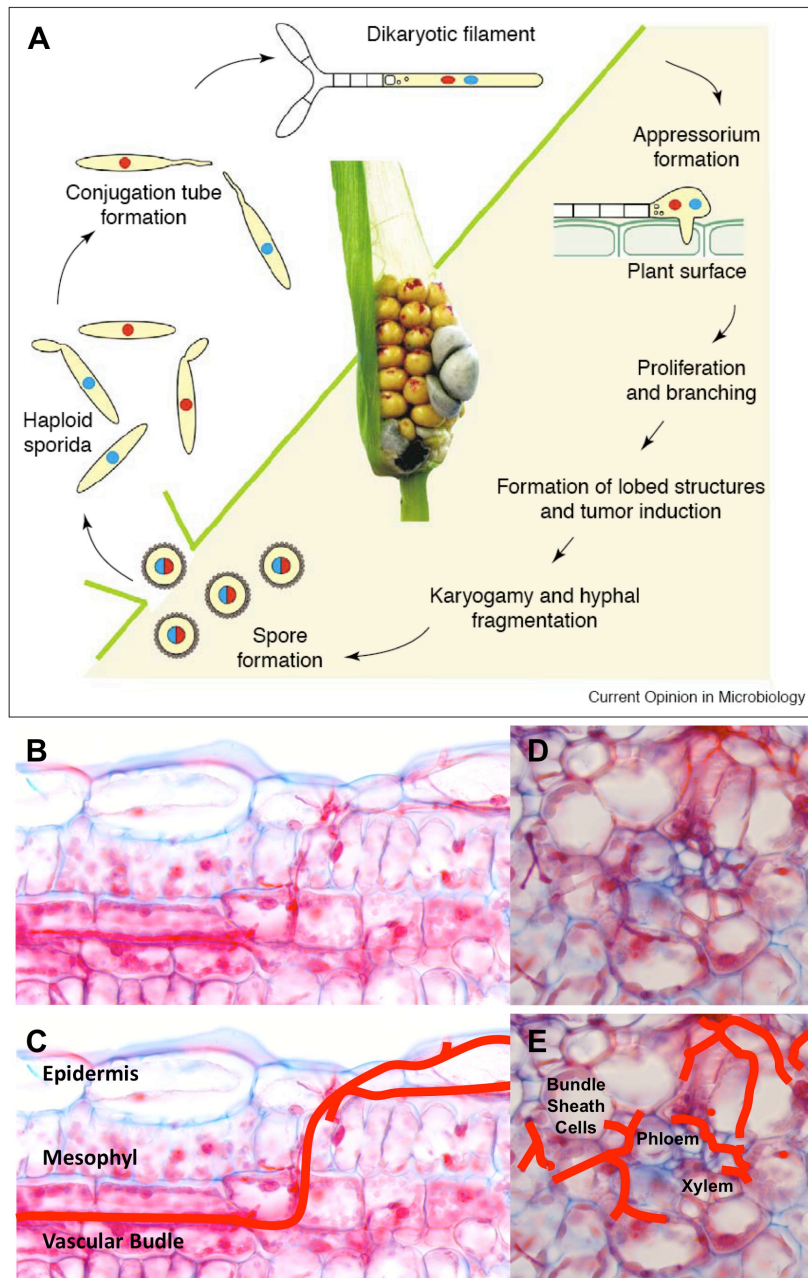


Figure 1.1-1 Life cycle of *Ustilago maydis*. (A) Life cycle of *U. maydis* published by Feldbrügge *et al.* (2004). The area shaded in light yellow indicates processes that are strictly dependent on the plant. Blue and red nuclei indicate different a and b mating types and are used to visualize the haploid, dikaryotic and diploid phases during the life cycle. In the centre of the diagram an infected corn ear with typical disease symptoms is shown. In the lower part of the tumor the black teliospores are visible. When the diploid spores germinate they undergo meiosis and produce haploid sporidia. (B) and (C) show a longitudinal section through a *U. maydis* infected maize leave 7 dpi. In (C) fungal hyphae are highlighted in red, visualizing that proliferation of *U. maydis* is directed to the vascular bundles after penetration (R. Wahl and M. Rath, unpublished data). (D) and (E) show a cross section of an *U. maydis* infected maize leave. In (E) fungal hyphae are highlighted in red, showing massive spreading within the vascular bundle (R. Wahl and M. Rath, unpublished data).

During plant penetration by *U. maydis* the host plasma membrane invaginates and surrounds the invading hypha (Snetselaar and Mims, 1992). An interaction zone develops between plant and fungal membranes that is thought to be involved in the exchange of signaling molecules. During the *U. maydis* infection this interaction zone also seems to be involved in nutrient uptake as the fungus does not develop specialized feeding structures like the haustoria found after rust and downy mildew infection.

Recently, a comprehensive genome analysis has revealed that *U. maydis* is poorly equipped with plant cell wall degrading enzymes (Doehlemann *et al.*, 2008b). Indeed, the fungus has sufficient plant cell wall degrading enzymes to soften and penetrate the plant cell walls; however, it is unlikely that *U. maydis* feeds on carbohydrates derived from this digestion (Doehlemann *et al.*, 2008b). It was observed that *U. maydis* hyphae prefer to proliferate in the vascular bundles, the nutrient transport routes in plants (Figure 1.1-1B-E; R. Wahl and M. Rath, unpublished data), suggesting that *U. maydis* primarily feeds on the nutrients transported in these tissues. Sections 2.3 and 2.4 shed new light on the nature of the carbon sources and the mode of their uptake by *U. maydis* during *in planta* growth (Feldbrügge *et al.*, 2004; Klosterman *et al.*, 2007; Doehlemann *et al.*, 2008b). Moreover, Section 2.2 describes how the maize metabolism is reprogrammed to promote biotrophic development of *U. maydis*.

Although *U. maydis* hyphae traverse plant cells, the plant tissue remains alive, there is no apparent host defense response during the infection process and, to date, no resistant corn or teosinte lines are known. The analysis of the *U. maydis* genome sequence revealed the presence of clustered genes encoding secreted proteins that are induced during the biotrophic stage (Kämper *et al.*, 2006). Several of these clusters are required for pathogenic development, but their distinctive functions have not been identified (Kämper *et al.*, 2006). After *U. maydis* infection an active suppression of maize defense responses was observed (see section 2.2). It has been discussed that secreted *U. maydis* effector proteins are responsible for this interference with the host defense mechanisms.

At later stages of infection, hyphae grow both intra- and intercellularly (Banuett and Herskowitz, 1996). Ongoing hyphal proliferation results in the formation of plant galls (commonly designated as tumors) (Figure 1.1-1A). As *Ustilago maydis* infects juvenile, meristematic tissue, tumors preferably appear only at the maize cobs, but also at leaves and other aerial parts of the plant (Christensen, 1963; Snetselaar and

Mims, 1992; Snetselaar and Mims, 1993). Tumor development is associated with both plant cell enlargement and enhanced cell divisions, processes normally triggered by the plant hormones auxin and gibberellin. However, Reineke *et al.* (2008) reported that production of the auxin indole-3-acetic acid by *U. maydis* is not crucial for the formation of plant tumors (Reineke *et al.*, 2008).

Within these tumors the hyphal cells start to differentiate. The hyphae become fragmented and round up until finally, upon karyogamy, the diploid teliospores are formed (Figure 1.1-1A; Banuett and Herskowitz, 1996). The biotrophic stage of *U. maydis* is completed after the tumor breaks open and the black teliospores are spread out by wind or the distribution of maize kernels for example (Figure 1.1-1A). The fungal spores are very resistant to environmental stress and able to remain dormant in the soil for several years. When they are getting attached to new juvenile, meristematic plant tissues again, a basidium is formed, meiosis and mitosis take place and new sporidia are released (Figure 1.1-1A). Finally, the life cycle of *U. maydis* is complete when two compatible sporidia meet and fuse continuing the cycle (Christensen, 1963).

1.2 Ustilago maydis/Zea mays: A Model System to Study Mechanism of Compatibility

Ustilago maydis belongs to the class of Ustilagomycetes, basidiomycete plant parasites called smuts. The term smut derives from the massive amount of black teliospores produced by this group of fungi during plant infection. The best characterized members of over 1,000 known species of smut fungi are those which are parasitic on cereal crops, like *Ustilago hordei*, *U. nigra* and *U. nuda* (barley), *U. scitaminea* (sugar cane), *U. avenae* and *U. kollerii* (oats), *U. tritici* and *Tilletia caries* (wheat), and *Sporisorium reilianum* and *Ustilago maydis* (maize). These biotrophic grass pathogens lead to significant annual crop losses and are therefore of economic interest. *U. maydis* generally infects about 2% of the maize plants in a field. Due to the large amount of maize grown in the United States, this equals to several 100 million U.S. dollars per year (reviewed by Martinez-Espinoza *et al.*, 2002).

U. maydis is not only a worthy model organism because of the economic importance of smut fungi. The fungus is closely related and has a biotrophic lifecycle comparable to rust fungi, another economic threat also belonging to the basidiomycota (Urodinomycetes; Singh *et al.*, 2006). These fungi are obligate biotrophs and, unlike

U. maydis, not cultivable under axenic conditions. Moreover, *U. maydis* is not only an interesting model to investigate economically harmful, but also beneficial fungi. Mycorrhizal fungi are biotrophic plant symbionts used to improve crop yields. Like rusts they are not amenable to directed reverse genetic approaches. Therefore, the *U. maydis* pathosystem provides insight towards elucidating the molecular processes that takes place in various obligate biotrophic systems.

The molecular interplay between basidiomycete pathogens and economic important crop plants is, despite its economic importance, relatively poor investigated. Most crop plants are monocotyledones grasses, like barley (*Hordeum vulgare*), wheat (*Triticum spp.*), rice (*Oryza sativa*) and maize, which are different from the extensively studied dicotyledones model plants like *Arabidopsis thaliana*, *Medicago truncatula* and *Nicotiana tabaccum*. Thus, maize, one of the most cultivated crop plants worldwide, represents another significant reason to study the *U. maydis/Zea mays* pathosystem. Recently, the genome sequence of maize was released (www.maizesequence.org), which transforms the *Ustilago/maize* interaction into a valuable system to study pathogen/crop interactions in more detail.

A further benefit of the *U. maydis* pathosystem is the short reproduction time of the fungus *in planta*, giving rise to fungal spores only 14 days after infection. Thus, the complete examination of the biotrophic stage is a fast process. Moreover, solopathogenic haploid *U. maydis* strains exist, which are able to infect the plant without a compatible mating partner further alleviating the investigation of biotrophic development (Bölker *et al.*, 1995; Kämper *et al.*, 2006).

The other great advantage of *U. maydis* as a model for pathogenic interactions is that the initial stages of plant infection can be simulated under axenic conditions. The pheromone dependent cell-to-cell recognition, the subsequent cell fusion and the b-dependent establishment of the infectious dikaryon can be monitored on charcoal containing media plates (Rowell, 1955; Puhalla, 1968). Moreover, inducible transcription of the b genes, controlled by arabinose or nitrate inducible promoters, allows the investigation of b-dependent gene expression in liquid culture (Brachmann *et al.*, 2001; Scherer *et al.*, 2006). Recently, Mendoza-Mendoza *et al.* (2009) described a method to induce appressoria formation in *U. maydis* after application of fatty acids on hydrophobic surfaces (Mendoza-Mendoza *et al.*, 2009).

U. maydis grows not only biotrophically within the plant, but also saprotrophically as haploid yeast that can be propagated in axenic culture with short generation times. The fact that *U. maydis* possesses a very efficient homologous recombination system

makes the fungus highly susceptible to genetic manipulation (reviewed in Holliday, 2004). In 2003, the genome of *U. maydis* was sequenced and extensively annotated making targeted genetic approaches easy to perform (<http://mips.gsf.de/genre/proj/ustilago/>; Kämper *et al.*, 2006). In addition to the standard toolbox of molecular and biochemical methods a custom made Affymetrix *Ustilago* genome array is available to perform global transcriptome analyses (Kämper *et al.*, 2006).

The investigation of the *Ustilago*/maize model system has the potential to quickly generate knowledge about how biotrophic plant pathosystems work, contributing to the protection of cultivated crops against pathogenic threats.

1.3 Plant Pathogen Interactions

1.3.1 The Plant Immune System

Disease resistance in plants relies to one end on a constant shield, which consists of physical barriers such as the wax cuticle and the epidermal cell walls, as well as chemical barriers like antimicrobial phytoanticipins. This shield is supposed to stop pathogens already on the plant surface prior to penetration or directly after penetration by avoiding the formation and establishment of infectious structures. When the pathogen is able to overcome the first layer of defense, an additional layer of defense is induced (reviewed by Dangl and Jones, 2001; Jones and Takemoto, 2004; Mysore and Ryu, 2004; Nürnberger and Lipka, 2005; Jones and Dangl, 2006).

The critical processes are the proper recognition of a pathogen and induction of adequate defense responses. As some of these responses have deleterious effects on the plant itself, they have to be tightly controlled. Induced responses include expression of specific pathogenicity related (PR) genes, production of secondary metabolites (i.e. phytoalexins), and the reinforcement of cell walls with callose and lignins. Additionally, so called hypersensitive responses (HR), as the production of reactive oxygen species (ROS) and localized cell death, can be induced. If these defense responses are effective, the plant is considered a non-host, which is resistant towards the specific pathogen (reviewed by Dangl and Jones, 2001; Jones and Takemoto, 2004; Mysore and Ryu, 2004; Nürnberger and Lipka, 2005; Jones and Dangl, 2006).

This basal plant defense machinery is induced by the recognition of conserved molecules that are commonly found in a variety of microbial species, but that are absent from the host species. Such pathogen associated molecular patterns (PAMPs) include bacterial, fungal and oomycete factors as chitin, β -glucans, ergosterol and flagellin (Baureithel *et al.*, 1994; Granado *et al.*, 1995; Ito *et al.*, 1997; Felix *et al.*, 1999; Yamaguchi *et al.*, 2000; Klarzynski *et al.*, 2000). In addition, plant cell wall degradation products appearing upon pathogen attack are used as endogenous elicitors to induce basal plant defense responses (Vorwerk *et al.*, 2004). PAMP-mediated recognition is triggered by so-called pattern recognition receptors (PRR), which are either plant plasma membrane spanning receptor-like kinases or receptor-like proteins lacking a kinase domain. Both of which can contain extracellular leucine-rich repeat (LRR)-domains or LysM-motifs for signal perception (reviewed by Dangl and Jones, 2001; Göhre and Robatzek, 2008).

Pathogens have managed to overcome the PAMP-induced basal resistance system of the plant by evolving virulence factors that are either enabling them to evade or to suppress plant defense responses (reviewed by Chang *et al.*, 2004; Abramovitch and Martin, 2004). In that case the plant is converted to a host plant, which is susceptible towards the pathogen. Yet, during co-evolution plants have developed specific disease resistances towards pathogens. Specific resistance proteins, cellular LRR receptor-like proteins or by transmembrane LRR receptor-like kinases (R proteins), recognize the corresponding virulence factors (or effectors) of pathogens in a gene-for-gene manner (Dangl and Jones, 2001; Espinosa and Alfano, 2004; Jones and Takemoto, 2004; Chang *et al.*, 2004; Abramovitch and Martin, 2004; Göhre and Robatzek, 2008).

R protein-mediated disease resistance is effective against biotrophic pathogens that are dependent on living host tissue, but not against necrotrophs that kill their hosts (see also 1.3.3). Activation of the salicylic acid (SA)-dependent signaling pathway upon pathogen recognition leads to expression of defense-related genes like PR1, to ROS production, and programmed cell death, resulting in depletion of nutrients to biotrophs (Seo *et al.*, 2001; Glazebrook *et al.*, 2003). In the case of necrotrophs, however, programmed cell death would be supportive for the life-style of the pathogen.

Additional plant hormone pathways induced upon pathogen attack are the ethylene (ET) and/or jasmonate (JA) pathways that are both also involved in response to wounding. These responses do not include cell death and are associated with

induction of tryptophan biosynthesis, the accumulation of secondary metabolites and the induction of plant genes encoding defensins, hevein-like proteins and chitinases (Penninckx *et al.*, 1998; Thomma *et al.*, 1998; Brader *et al.*, 2001; Glazebrook *et al.*, 2003). It has been suggested that plant defense responses may be specifically adapted to attacking pathogens, with SA-dependent defenses acting against biotrophs, and JA- and ET-dependent responses acting against necrotrophs (reviewed by Glazebrook, 2005; Wasternack, 2007).

1.3.2 Small Secreted Effectors: The Pathogens Tools to Manipulate Its Host

Plant pathogens need various sets of secreted proteins to support their life styles. Secreted plant cell wall degrading or modifying enzymes, for example, are involved in the penetration process and during the cell-to-cell passage to spread inside the plant (Toth and Birch, 2005; Kikot *et al.*, 2008; Doehlemann *et al.*, 2008b). Furthermore, secreted lytic proteases were found to modify host proteins in order to counter the host defense responses (Monod *et al.*, 2002; Xia, 2004; Shindo and Van der Hoorn, 2008). Secreted nucleases are thought to degrade plant RNAs and DNA to inhibit plant responses (Müller *et al.*, 2008). And finally, secreted metabolic enzymes such as invertases might be used by the pathogen to redirect the host metabolism towards its needs (Voegelé *et al.*, 2006; Horst *et al.*, 2008; Müller *et al.*, 2008).

In addition, pathogens possess a large variety of small secreted effector proteins with so far unknown function. In bacteria relatively small numbers of these genes are found, whereas oomycete and fungal genomes harbor several hundred genes coding for putative secreted proteins (Kamoun, 2006; Kämper *et al.*, 2006; Stavrinides *et al.*, 2008; Müller *et al.*, 2008; Tyler, 2009). The effectors are thought to be transferred into the host cell where they manipulate the hosts recognition and defense systems (reviewed by Morgan and Kamoun, 2007; Zhou and Chai, 2008; Birch *et al.*, 2008; Müller *et al.*, 2008).

Plant pathogenic bacteria live in the intercellular space of the plant and use conserved type III secretion systems to inject small secreted effector molecules directly into the host cells. These secreted effector molecules were shown to specifically modulate the above described recognition pathways and the hormone signaling of the plant (reviewed by Zhou and Chai, 2008). The *Pseudomonas syringae* effector AvrPtoB promotes the degradation of Fen and Prf, which are crucial components of programmed cell death (Rosebrock *et al.*, 2007). AvrRpt2 modulates

the auxin pathway to enhance plant susceptibility (Fu *et al.*, 2007). Another step of manipulating the host towards the needs of the pathogen was discovered for *Xanthomonas species*. The AvrBs3 family effectors contain nuclear-localization, DNA-binding and transcriptional activation domains. Thus, these effectors are able to enter the host nucleus and alter gene expression to enhance susceptibility towards the pathogen (Schornack *et al.*, 2006; Yang *et al.*, 2006; Sugio *et al.*, 2007; Römer *et al.*, 2007; Kay *et al.*, 2007; Kay and Bonas, 2009).

The secreted effectors of plant pathogenic oomycetes possess in addition to an N-terminal signal peptide, which is required for secretion from the pathogen, an RXLR motif followed by an acidic region (D/E residues) also found in malaria parasites (Rehmany *et al.*, 2005; Morgan and Kamoun, 2007; Birch *et al.*, 2008). After secretion of these oomycete effectors into the host apoplast, the RXLR leader sequence was shown to be required for targeting the effector protein into the cytoplasm of host cells (Whisson *et al.*, 2007). Yet, the mechanism as well as the machinery, which are required for the translocation of RXLR-containing effectors into the host cells are still unknown (Morgan and Kamoun, 2007; Birch *et al.*, 2008; Tyler, 2009). Birch *et al.* (2008) reported that the RXLR motif was also found in 315 *Arabidopsis thaliana* proteins of which 20 % were conserved or members of the endocytosis cycle, suggesting that endocytosis might be involved in the uptake of RXLR effector proteins by the host cells. Even though RXLR proteins were identified to influence virulence of the respective pathogen their function is largely unknown. Bos *et al.* (2006) were able to relate the function of the *Phytophthora infestans* RXLR effector Avr3 with INF1-induced cell death suppression in *Nicotiana benthamiana* (Bos *et al.*, 2006). Other oomycete effectors are thought to manipulate host gene expression like the above described bacterial effectors as they contain nuclear localization signals (NLS), however, functional proof is missing (Morgan and Kamoun, 2007).

The genome sequences of fungal plant pathogens often comprise of several hundred, some even close to a thousand secreted proteins with unknown function, which are in most cases pathogen specific (Dean *et al.*, 2005; Kämper *et al.*, 2006; Hane *et al.*, 2007). Except from a common N-terminal secretion signal peptide it is currently unknown how fungal effectors localize to their site of action within the host plant. Fungi lack a bacterial secretion machinery-like system and a common RXLR-like host targeting peptide has not been discovered yet. Nevertheless, the *Uromyces fabae* effector RTP1 was detected in the host cytoplasm suggesting a route for uptake and a function within the host cell (Kemen *et al.*, 2005). Several secreted

proteins were found to be crucial for fungal virulence (Jia *et al.*, 2000; Westerink *et al.*, 2004; Kemen *et al.*, 2005; Rooney *et al.*, 2005; Kämper *et al.*, 2006; Catanzariti *et al.*, 2006; Dodds *et al.*, 2006; Bolton *et al.*, 2008; Doehlemann *et al.*, 2009). Moreover, the virulence function of some of these effectors has been linked to interaction with the cognate R gene products or inhibition of proteases required for plant disease resistance (Jia *et al.*, 2000; Westerink *et al.*, 2004; Rooney *et al.*, 2005).

As effectors are directed to plant cells to overcome disease resistance, their genes are, like the cognate R genes from plants, subject to high evolutionary selection, causing a high degree of diversity (Win *et al.*, 2007). Putative functions are therefore hard to predict. However, the mere number of these effectors would lead one to expect a high level of functional redundancy, which might finally simplify the classification of this diverse group of proteins.

1.3.3 Carbon Acquisition of Fungal Pathogens during Plant Infection

Most of the research dealing with the molecular interaction of pathogens and their host plants has focused on the above described plant defense responses and the strategies of pathogens to enter their hosts. A far less studied, but not less important aspect of a phytopathogenic interaction is the nutrient acquisition of the pathogen within the host plant. As nutrient availability determines the fitness of the pathogen, it also determines the pathogen's success to conquer the plant. Fungal plant pathogens have developed two major strategies to acquire nutrients from their respective hosts. Necrotrophic fungi kill the plant cells after plant infection and feed on the host tissue as saprotrophs. In contrast, biotrophic fungi manipulate their hosts to feed on its resources, while keeping the plant cells alive. A third group of fungal pathogens, called hemibiotrophs, uses a combination of both strategies to complete their lifecycle. They first develop a biotrophic lifestyle to spread within the plant, and in a second phase switch to necrotrophism.

During a biotrophic interaction the pathogen has to develop well-adapted strategies to get access to nutrients, while the host tissue is staying alive. The obligate biotrophic rust and powdery mildew fungi, which are strictly dependent on the host tissue for growth and reproduction, form similar to symbiotic arbuscular mycorrhiza fungi specialized feeding structures to access plant derived nutrients (review by

Panstruga, 2003; Parniske, 2008). These so called haustoria are thought to function predominantly to promote fungal hexose and amino acid uptake.

In the *Uromyces fabae/Vicia fabae* interaction a hexose transporter (HXT1p) and three amino acid transporters (AAT1p, AAT2p and AAT3p) were found to be specifically expressed in haustoria (Hahn *et al.*, 1997; Voegelé *et al.*, 2001; Struck *et al.*, 2002; Struck *et al.*, 2004). Functional analysis revealed that HXT1p functions as a proton co-transporter specific for glucose and fructose. Furthermore, a haustoria-induced, secreted invertase of *U. fabae* was discovered, which is thought to act in combination with HXT1p by promoting the uptake of glucose and fructose through prior cleavage of sucrose (Voegelé, 2006). Yet, the importance of the transporters and the invertase of *U. fabae* for biotrophic development has never been addressed in the homologous system, as rusts are not amenable to reverse genetic approaches (Voegelé *et al.*, 2001).

The same holds true for the ectomycorrhizal fungi *Amanita muscaria*, *Tuber borchii*, and *Geosiphon pyriformis*. Although, hexose transporters were identified as specifically expressed during symbiosis in those fungi, their impact on fungal symbiosis is currently unknown (Nehls *et al.*, 1998; Schüssler *et al.*, 2006; Polidori *et al.*, 2007). Nevertheless, the uptake of sucrose-derived hexoses seems to be a common feature of plant pathogenic fungi, as it was not only observed in biotrophic but also in necrotrophic interactions. It is suggested that *Sclerotinia sclerotiorum*, a necrotroph of sunflower, uses a fungal invertase for sucrose cleavage and two hexose transporters, *Sshxt1* and *Sshxt2* for subsequent uptake of glucose and fructose during infection (Jobic *et al.*, 2007).

Apart from the strategy to differentiate specialized feeding structures, which is not realized by all fungal biotrophs, a biotrophic interaction is accompanied with the establishment of a metabolic sink. Plant sink tissues like roots are dependent on sucrose import from photosynthetically active source tissues (reviewed by Winter and Huber, 2000; Koch, 2004). Apoplastic invertase activity is described to influence a transition from source to sink tissue at fungal infection sites (reviewed by Panstruga, 2003; Hüchelhoven, 2005; Biemelt and Sonnewald, 2006). Both, secreted fungal invertases, as well as plant cell wall invertases have been found to be induced after fungal infection, and thought to mediate a source to sink transition (Heisteruber *et al.*, 1994; Chou *et al.*, 2000; Fotopoulos *et al.*, 2003).

Upon enhanced sucrose cleavage, sucrose export is reduced and in turn sucrose unloading in the vicinity of fungal hyphae is increased (Tetlow and Farrar, 1992;

Ayres *et al.*, 1996; Tang *et al.*, 1999). Increased sucrose uptake was observed in *Arabidopsis thaliana* leaves infected with powdery mildew (Fotopoulos *et al.*, 2003). Due to enhanced invertase activity the increased unloading of sucrose at infection sites comes along with elevated levels of free hexoses (von Schaewen *et al.*, 1990; Sonnewald *et al.*, 1991). As a result not only fungal hexose transporters are specifically expressed in sink tissues (Nehls *et al.*, 1998; Voegelé *et al.*, 2001; Schüssler *et al.*, 2006; Polidori *et al.*, 2007), but also plant hexose transporters are induced, most likely to compete with the fungal transporters (Tang *et al.*, 1996; Fotopoulos *et al.*, 2003).

In addition to this direct competition by plant hexose transporters, which should restrict carbon access of the pathogen, plants are able to sense “aberrant” pathogen-induced carbon compositions to trigger defense responses. Increased hexose levels were found to trigger PR gene expression and systemic acquired resistance (Herbers *et al.*, 1996b; Herbers *et al.*, 1996a; Rolland *et al.*, 2006). Likewise, enhanced invertase activity has been reported to influence PR genes expression (Heineke *et al.*, 1992; Roitsch *et al.*, 2003; Schaarschmidt *et al.*, 2007; Kocal *et al.*, 2008). In rice plants, elevated sucrose-levels led to PR gene expression and increased resistance against pathogens (Murillo *et al.*, 2003; Gómez-Ariza *et al.*, 2007). In general, the plant appears to be able to sense a pathogen-induced source to sink transition upon which a defense response reaction is performed. Accordingly, the pathogen has to develop strategies to cope with such recognition events based on the plants carbon level. To be successful the pathogen either has to block the induced defense responses or utilize the signaling carbohydrate molecules fast enough to not trigger a response.

1.4 Focus of this Work

The topic of this dissertation, “Biotrophic Development of *Ustilago maydis* and the Response of Its Host Plant Maize”, covers a broad range of subjects, which can be addressed from different angles to answer questions as: Why is there no effective plant defense response upon *U. maydis* infection? Is *U. maydis* actively interfering with plant defense responses? How does *U. maydis* manage to feed on the plant? Is there active reprogramming of the maize metabolism by the fungus and which carbon sources are taken up by the fungus? To answer these questions three different approaches were carried out, all of which are described in section 2.

Section 2.1 (The *Ustilago maydis* *b* Mating Type Locus Controls Hyphal Proliferation and Expression of Secreted Virulence Factors *in Planta*) addresses the function of the bE/bW heterodimer during biotrophic growth. The two unrelated homeodomain proteins bE and bW form an active transcription factor which was shown to initiate sexual development and pathogenicity (Kämper *et al.*, 1995; Romeis *et al.*, 2000; Brachmann *et al.*, 2003). By constructing temperature sensitive *b* alleles, I was able to show that the *b* heterodimer also controls *in planta* proliferation of *U. maydis* and regulates secreted effectors important for fungal virulence.

Section 2.2 (Reprogramming a Maize Plant: Transcriptional and Metabolic Changes Induced by the Fungal Pathogen *Ustilago maydis*) describes changes of the maize transcriptome and metabolome in response to *U. maydis* infection. Down-regulation of plant defense and cell death related genes after fungal penetration revealed an active interference with the plants immune system by *U. maydis*. Next to changes in hormone signalling, the interplay between fungus and host involved induction of antioxidant and secondary metabolism. The prevention of source leaf establishment after infection indicated that *U. maydis* relies on sugar import rather than on active photosynthesis to nourish on the plants resources.

Sections 2.3 and 2.4 (**2.3** - A Novel High Affinity Sucrose Transporter is Required for Fungal Virulence and Avoids Extracellular Glucose Signaling in Biotrophic Interactions; **2.4** - Hxt1, a Monosaccharide Transporter and Sensor Required for Virulence of the Maize Pathogen *Ustilago maydis*) elucidate which fungal sugar transporters and which types of carbon sources are important to promote growth of *U. maydis* during biotrophic development. I identified two sugar transporter genes, *srt1* and *hxt1* as required for fungal development *in planta*. Functional characterization revealed that Srt1 is specific for sucrose and Hxt1 has high affinities to hexoses, concluding that *U. maydis* nourishes on the plants transport sugar sucrose as well as its cleavage products.

The subsections describe specific topics, dealing with the complex interplay between *U. maydis* and its host plant maize. Next to research results and discussion, they include a detailed introduction and experimental procedures to explain why and how the underlying research was carried out.

2. Results

2.1 The *Ustilago maydis* b Mating Type Locus Controls Hyphal Proliferation and Expression of Secreted Virulence Factors in Planta

Ramon Wahl^{1,2} and Jörg Kämper^{1,2#}

¹ Max Planck Institute for Terrestrial Microbiology, D-35043 Marburg, Germany,

² Current Address: University of Karlsruhe, Institute of Applied Biosciences, D-76187 Karlsruhe, Germany

To whom correspondence should be send:

Jörg Kämper, University of Karlsruhe, Institute of Applied Biosciences, Department of Genetics, Hertzstr. 16, D-76187 Karlsruhe; Tel: +49-721-608-5670; E-mail: joerg.kaemper@kit.edu

Running title: *U. maydis* bE/bW controls biotrophic development

Key words: temperature sensitivity, transcription factor, *Ustilago maydis*, secreted effectors, b mating type locus

Summary

Sexual development in fungi is controlled by mating type loci that prevent self-fertilization. In the phytopathogenic fungus *Ustilago maydis*, the b mating type locus encodes two homeodomain proteins, termed bE and bW. After cell fusion, a heterodimeric bE/bW complex is formed, but only if the proteins are derived from different alleles. The bE/bW complex is required and sufficient to initiate pathogenic development as a prerequisite for sexual reproduction; for later stages of pathogenic development, however, its role was unclear. To analyze b function during *in planta* development, we generated a temperature-sensitive bE^{ts} protein with a single amino acid alteration flanking the homeodomain. bE^{ts} strains are stalled in pathogenic development at restrictive temperature *in planta*, and hyphae develop enlarged, bulbous cells at their tips that contain multiple nuclei, indicating a severe defect in cell division. DNA array analysis of bE^{ts} mutant strains *in planta* revealed a b-dependent regulation of genes encoding secreted proteins that were shown to influence fungal virulence. Our data demonstrate that in *U. maydis* the b heterodimer is not only essential to establish the heterodikaryon after mating of two compatible sporidia and to initiate fungal pathogenicity, but also to sustain *in planta* proliferation and ensure sexual reproduction.

2.1.1 Introduction

Mating is an essential step in the life cycle of all sexually reproducing organisms. In fungi, sexual compatibility is controlled by mating-type genes, which function to prevent self-fertilization and ensure the genetic variability of the population. In the Basidiomycete *Ustilago maydis*, the causal agent of the smut disease on maize plants, mating is accompanied with a dramatic change of life style. The haploid cells, called sporidia, grow by budding and are strictly saprophytic. Mating of two of such sporidia leads to the formation of a dikaryon that grows filamentously and requires the plant host for further propagation.

The mating reaction is controlled by two independent mating type loci that are termed *a* and *b* (for review see Kronstad and Staben, 1997). The biallelic *a* locus encodes a pheromone/pheromone receptor system mediating recognition and cell fusion events (Bölker *et al.*, 1992; Spellig *et al.*, 1994a). Subsequently, the *b* mating type locus controls filamentous growth, maintenance of the dikaryon and the initiation of the pathogenic program as a prerequisite for sexual development. *b* encodes two homeodomain proteins, bE and bW, that show no homology to each other, with the exception of the conserved homeodomain DNA binding domain. However, since for both bE and bW proteins the allelic differences cluster within the N-terminal region, the proteins share a similar structure with a variable, N-terminal domain and a highly conserved C-terminal region. These variable dimerization domains facilitate the formation of a transcriptional active bW/bE complex, but only if the proteins are derived from different alleles (Schulz *et al.*, 1990; Gillissen *et al.*, 1992; Kämper *et al.*, 1995). The active b heterodimer is necessary and sufficient to initiate the pathogenic life style of *U. maydis*, as shown by means of a haploid strain that carries compatible *bE* and *bW* alleles (Bölker *et al.*, 1995). This solopathogenic strain infects the plant without a compatible mating partner.

The homeodomains of the b heterodimer have been shown to bind to a specific DNA sequence (b-binding site) in the promoter regions of b-responsive genes (Romeis *et al.*, 2000; Brachmann *et al.*, 2001). Such b-responsive genes have been identified in several attempts (Bohlmann *et al.*, 1994; Schauwecker *et al.*, 1995; Wösten *et al.*, 1996; Urban *et al.*, 1996; Brachmann *et al.*, 2001; Brachmann *et al.*, 2003), but with the exception of *kpp6* (involved in appressoria formation; Brachmann *et al.*, 2003) none of them has been linked to pathogenic development.

Recently, about 350 b-regulated genes have been identified by monitoring the expression profiles of *U. maydis* genes during a 12 hours time course after *b*

induction using DNA microarray analysis (M. Scherer and J. Kämper, unpublished data). Within these data sets three genes have been identified, which are expressed in presence of an active bE/bW heterodimer and which have an impact on filament formation or pathogenic development. *clp1* encodes a protein with unknown function that is involved in cell cycle progression and cell division after plant penetration (Scherer *et al.*, 2006). *rbf1* encodes a zinc-finger transcription factor that is required for the regulation of the majority of b-dependent genes (Scherer *et al.*, 2006; M. Scherer and J. Kämper, unpublished data). The third gene, *biz1*, encodes a zinc finger transcription factor that was shown to be involved in appressoria formation and cell cycle arrest (Flor-Parra *et al.*, 2006). In addition, several b-regulated genes functioning in cell cycle control, mitosis or DNA replication were identified, consistent with the observation that *b* induction leads to a cell cycle arrest, which is released after plant penetration (García-Muse *et al.*, 2003; Scherer *et al.*, 2006; Cánovas and Pérez-Martín, 2009).

The expression of a compatible b heterodimer is required for the initiation of pathogenic development. However, it is unclear whether this central regulator is also required at the developmental stages succeeding plant penetration. It is known that the *bE* and *bW* genes are expressed during biotrophic development of the fungus (Quadbeck-Seeger *et al.*, 2000), but it is unclear which genes are expressed in a b-responsive manner during *in planta* development. To get insights into the function of bE/bW during *in planta* development of *U. maydis*, we generated temperature-sensitive *b* alleles via random PCR mutagenesis.

The temperature-sensitive *bE* allele (*bE^{ts}*) prevents fungal proliferation *in planta* at restrictive temperature, while fungal development is not altered at permissive temperature. At restrictive conditions *in planta*, fungal tip cells are enlarged and contain multiple nuclei, demonstrating the requirement of *b* for cell division. *In planta* DNA microarray expression analysis comparing the *b_{on}* and the *b_{off}* state revealed a b-dependent transcription network important for the expression of secreted proteins previously shown to influence pathogenicity (Kämper *et al.*, 2006). Our data demonstrate that the b heterodimer is essential during *in planta* development of *U. maydis*, affecting fungal proliferation and the biotrophic interaction with the host plant.

2.1.2 Results

Generation of Temperature-sensitive b Alleles

In order to generate temperature sensitive (ts) mutant alleles encoding bE and bW, we applied *in vitro* mutagenesis to alter DNA fragments encompassing the N-terminal dimerization domain of bW and the N-terminal dimerization domain and homeodomain of bE, respectively (Figure 2.1-1A; see Experimental Procedures). Alterations in the dimerization domains could possibly interfere with protein-protein interactions of bW and bE, resulting in an instable complex at higher temperatures unable to accomplish its regulatory function. Mutations within the homeodomain could effect or prevent DNA binding.

The mutagenized fragments were cloned into autonomously replicating *U. maydis* plasmids to restore the complete open reading frames (ORFs) under control of the native promoter regions. Mutant libraries of *bW1*- and *bE2*-plasmids were transformed into *U. maydis* strain FBD11-21 (*a1a2/b2b2*) or FBD12-3 (*a1a2/b1b1*), respectively. Strains harboring the *bW1* or *bE2* plasmids express an active bW1/bE2 complex, which is indicative through the induction of filamentous growth on charcoal containing media plates (PDC, see Experimental Procedures). A total of approximately 30.000 *bE2*- and 20.000 *bW1* mutants were screened for filamentous growth at 22 °C and budding growth at 31 °C by means of replica plating.

Two strains with mutant *bE2* alleles (FBD12-3 + pFSbE2ts52 and FBD12-3 + pFSbE2ts98) showing a ts-dependent growth phenotype were identified. In both cases, filamentous growth was induced at permissive temperature, while cells grew by budding at restrictive temperature (Figure 2.1-1B). Sequence analysis of the two mutant *bE2*^{ts} fragments revealed three missense mutations in each of the alleles. Both mutant-alleles shared one mutation leading to an exchange of serine to proline at position 183, located at the border of the third α -helix of the homeodomain of bE2 (Figure 2.1-1C). To test whether this mutation causes the ts-phenotype, directed PCR mutagenesis was performed to alter serine to proline at position 183 in the wild type *bE2* allele. The resulting *bE2*^{ts183P} allele revealed the same temperature sensitivity as observed for the alleles *bE2*^{ts52} and *bE2*^{ts98} (Figure 2.1-1B).

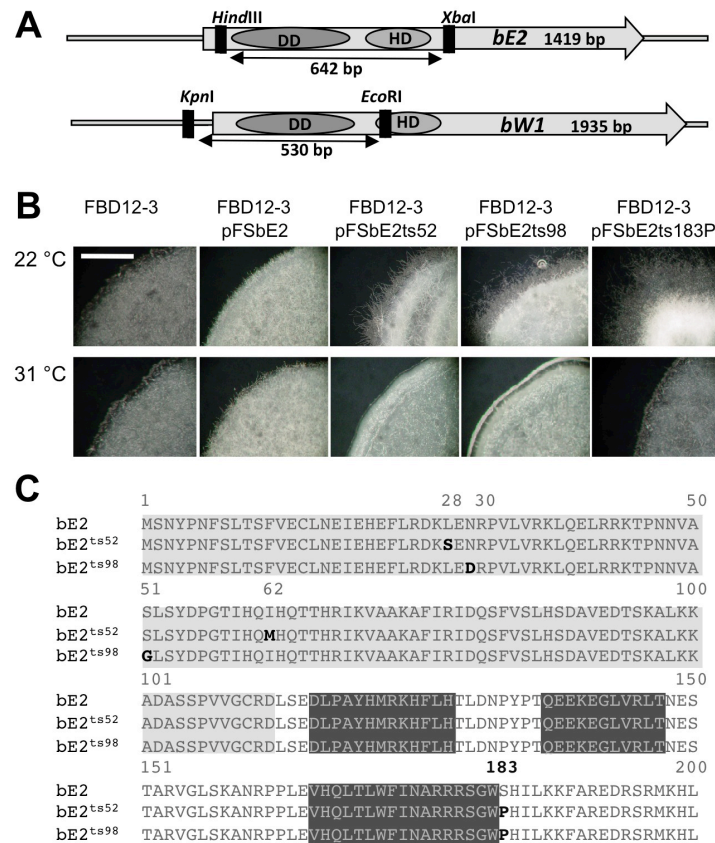


Figure 2.1-1: Temperature-sensitive *b* alleles generated by random PCR mutagenesis. (A) Schematic presentation of the *bE2* and *bW1* genes. Regions chosen for random PCR mutagenesis (flanked by restriction sites) are displayed as bidirectional arrows. Positions of the variable dimerization-domain (DD) and homeodomains (HD) are indicated as ovals. In *bW1* the dimerization domain, and for *bE2* the dimerization- and homeodomain were mutagenized. **(B)** *b*-induced growth on charcoal containing plates at permissive (22°C) and restrictive temperature (31°C). Strain FBD12-3 + pNEBbW1UH harbors a non-compatible *bE1/bW1* combination and grows non-filamentous at both temperatures. Strain FBD12-3 + pFSbE2 harbors an active *bW1/bE2* complex and growth filamentous at both temperatures. Strains carrying plasmids with temperature sensitive *bE2* alleles grow filamentously only at permissive temperature. The single amino acid exchange from serine to proline at position 183 in *bE2*^{tsP183} is sufficient to abolish *b* function in FBD12-3 + pFSbE2tsP183 at 31°C. The white scale bar corresponds to 1mm. **(C)** Alignment of the mutated regions of the temperature sensitive *bE* variants *bE2*^{ts52} and *bE2*^{ts98} with the wild type *bE2*. Dimerization- and homeodomains are indicated in light grey and dark grey boxes, respectively. Position and nature of generated amino acid exchanges are highlighted in black. The exchange of the wild type serine to proline at the border of the third helix of the homeodomain (position 183) leads to the temperature sensitivity of both *bE2*^{ts52} and *bE2*^{ts98}.

The *b* Heterodimer is Essential for Biotrophic Development of *Ustilago maydis*

To test the effects of the *bE2*^{ts183P} allele at restrictive temperature during *in planta* development of *U. maydis*, we introduced the *bE2*^{ts} allele and the wild type *bE2* gene as a control into *U. maydis* strain FB1otef:*pra2* (*a1pra2/b1*). This strain expresses an active pheromone/pheromone receptor system (*mfa1*, *pra2*), which is important to achieve increased virulence (Bölker *et al.*, 1995), and the *bE1* and *bW1* genes of which the latter is needed to form the complex with *bE2*^{ts183P}.

In the obtained strains RAbE2ts and RAbE2, the *bE* genes are expressed at permissive and restrictive temperature to a similar extent, respectively. Expression of *bE* is increased in RAbE2ts compared to RAbE2, due to additional, ectopically integrated copies of the *bE2^{ts}* gene (Figure 2.1-2A,B).

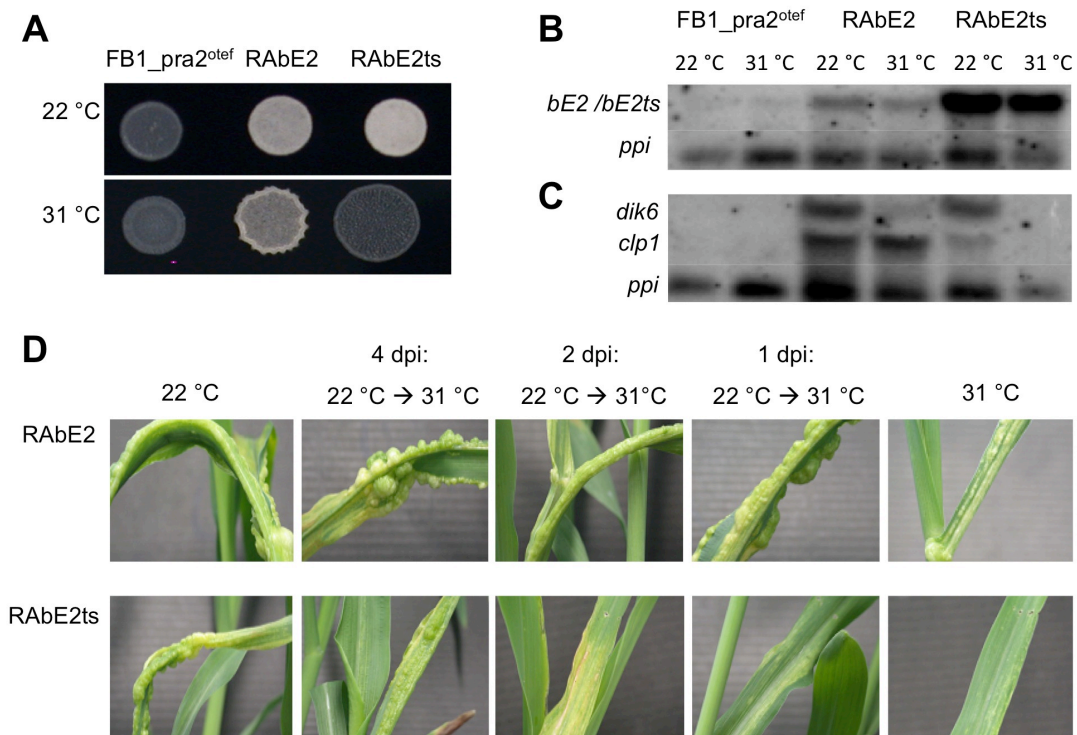


Figure 2.1-2: Temperature inactivation of *bE2^{ts}* disturbs transcriptional activity and abolishes tumour formation. (A) Growth of the solopathogenic strains RAbE2 harboring the wild type *bE2* gene as control and RAbE2ts harboring the temperature-sensitive *bE2^{tsP183}* allele at permissive (22°C) and restrictive temperature (31°C). The progenitor strain FB1*otef:pra2* was used as negative control. (B) Northern Blot analysis of *bE2* and *bE2^{tsP183}* expression at permissive and restrictive temperature. In both strains *bE2* expression is not altered due to the temperature shift; in strain FB1*otef:pra2* used as negative control no *bE2* expression is visible. The constitutively expressed *ppi* gene was used as loading control. (C) Northern blot analysis of b-dependent gene expression at permissive and restrictive temperature. While the control strain RAbE2 expresses the b-dependent genes *clp1* and *dik6* at both temperatures, in RAbE2ts both genes are expressed only at permissive temperature, but not at restrictive temperature. In the negative control strain FB1*otef:pra2* no expression of the b-dependent genes is observed. The constitutively expressed *ppi* gene serves as loading control. (D) Pathogenic development of the temperature-sensitive strain RAbE2ts and its wild type control RAbE2 at permissive and restrictive condition. Plants were infected with both strains, respectively, and either kept constantly at permissive, constantly at restrictive temperature, or were shifted from permissive to restrictive temperature 1, 2, and 4 dpi. Pictures were taken 7 dpi. After infection with RAbE2, tumours develop under all tested conditions, whereas infection with RAbE2ts does not induce tumours when plants are kept or shifted to restrictive conditions. Tumour development of both strains appears normal at permissive temperature.

To address whether *bE2^{tsP183}* alters the function of the bE/bW heterodimer as a transcriptional activator at restrictive temperature, we investigated the expression of the b-dependently expressed genes *dik6* and *clp1*. Both genes have *b*-binding sites

located within their promoter regions and are thought to be regulated directly by the b heterodimer (Bohlmann *et al.*, 1994; Scherer *et al.*, 2006). Transcripts of both genes were detected under permissive and restrictive conditions in the control strain RAbE2. However, in RAbE2ts *dik6* and *clp1* were only expressed under permissive conditions, arguing for an attenuated transcriptional activity of the bW1/bE2^{ts183P} complex at 31 °C (Figure 2.1-2C).

To address the function of the b heterodimer during biotrophic development, maize plants were infected with RAbE2ts and RAbE2 at 22 °C and shifted to restrictive temperature (31 °C) at different time points (0, 1, 2, 4 days post infection, dpi). Tumor development of plants infected with the temperature-sensitive strain was compared to plants infected with the respective wild type control strain at 7 dpi (Figure 2.1-2D). When shifted to restrictive temperature, all plants infected with RAbE2ts developed chlorosis, but no (0 and 1 dpi) or drastically reduced tumor symptoms (2 and 4 dpi), when compared to plants infected with RAbE2. Grown at permissive temperature (22 °C), plants developed symptoms that were indistinguishable in infections with RAbE2ts or RAbE2 (Figure 2.1-2D). These results clearly demonstrate an essential role of the b heterodimer for fungal proliferation during biotrophic development of *U. maydis*.

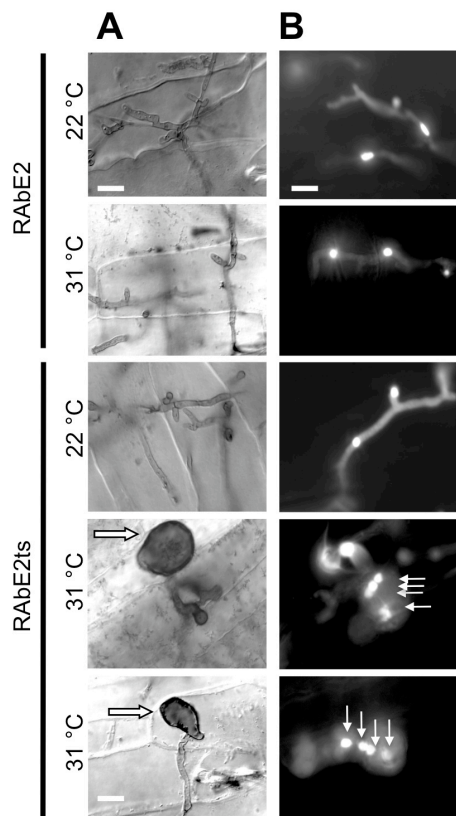


Figure 2.1-3: Temperature-dependent inactivation of b function *in planta* abolishes fungal proliferation. (A) Clorazol Black E staining of RAbE2 and RAbE2ts hyphae *in planta* at restrictive and permissive temperature 3 dpi (kept at 22°C or shifted to 31°C at 2dpi). The control strain RAbE2 shows no differences of hyphal development at both temperatures. Hyphal morphology of RAbE2ts is indistinguishable from that of RAbE2 at permissive temperature, whereas at restrictive temperatures the tip cells of hyphae are severely enlarged (white arrows). **(B)** Visualization of nuclei by expression of a nuclear localized 3xGFP after switching off b activity 2.5 dpi. After 2 dpi, infected plants were shifted from permissive (22°C) to restrictive (31°C) conditions for 12 hours or kept at 22°C as control. Hyphal cells of the haploid strain RAbE2 contain one nucleus at both temperatures; RAbE2ts hyphae resembled the phenotype of RAbE2 at permissive temperatures, whereas at restrictive temperature (31°C) the enlarged hyphal tip cells contain multiple nuclei (white arrows). The white scale bars corresponds to 20 µm.

To study the role of the *b* heterodimer during *in planta* proliferation in more detail, we examined the growth of RAbE2ts-filaments microscopically after infection at permissive and restrictive temperatures. Chlorazol Black E staining of fungal hyphae revealed that proliferation of RAbE2ts under permissive condition was comparable to that of infections with RAbE2 (Figure 2.1-3A). However, at restrictive conditions, the RAbE2ts cells were found to be enlarged, especially the tip cells of proliferating hyphae (Figure 2.1-3A). To visualize nuclei, RAbE2ts was transformed with a triple GFP construct fused to a nuclear localization site (NLS) expressed by the strong plant inducible promoter of the *mig2-5* gene (Zheng *et al.*, 2008). Under permissive conditions, hyphae were composed of cells containing single nuclei as observed previously in the solo-pathogenic strains (Scherer *et al.*, 2006). Under restrictive conditions, enlarged cells were visible that contained multiple nuclei (Figure 2.1-3B), indicating that a dysfunctional *b* heterodimer leads to a cell division defect, while cell cycle and nuclear divisions persist.

The b Heterodimer Affects the Regulation of Pathogenicity Factors in Planta

To investigate the influence of the *b* heterodimer on the *U. maydis* transcriptome during *in planta* proliferation, we performed a DNA array analysis using an Affymetrix *U. maydis* gene chip. After infections with the solopathogenic strain RAbE2ts, fungal biomass in whole leaf samples were insufficient to dissolve the transcriptome of *U. maydis* due to the high background of plant-derived mRNA (data not shown). Therefore, strains RAb1ts (*a1*, *bW1bE1^{ts}*) and RAb2ts (*a2*, *bW2bE2^{ts}*) were constructed. These compatible strains were able to develop an infectious dikaryon harboring the compatible, temperature-sensitive *b* heterodimers *bW1/bE2^{ts}* and *bW2/bE1^{ts}*. At permissive temperature, infections with a mixture of RAb1ts and RAb2ts gave symptoms comparable to that of infections with the compatible wild type strains FB1 (*a1b1*) and FB2 (*a2b2*) (data not shown), yielding fungal biomass sufficient for DNA array analysis. As expected, pathogenic development of the RAb1ts/RAb2ts dikaryon was stalled at restrictive temperature (Figure 2.1-4A).

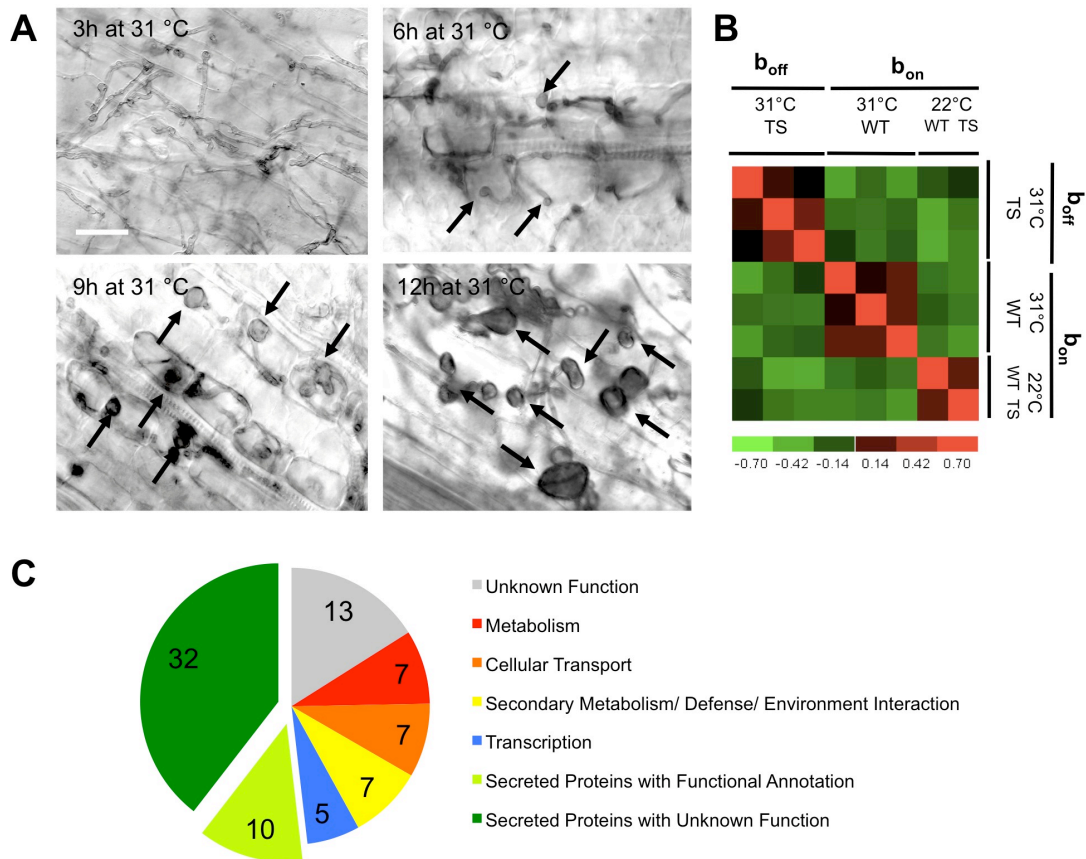


Figure 2.1-4: b inactivation *in planta* alters the expression of genes important for fungal virulence. (A) Time series of enlarged tip cell formation starting 4 dpi after infection with RAb1ts/RAb2ts crossings to determine the time point for expression analysis after b inactivation *in planta*. 3 hours after the temperature shift to 31°C no enlarged tip cells are visible, 6 hours after shift the tip cells start to enlarge (black arrows), and 9 hours after the shift most tip cells are enlarged (black arrows); 12 hours after shift the phenotype was not significantly altered when compared to 9 hours (black arrows). The white scale bar corresponds to 50 μ m. (B) Correlation Matrix of *U. maydis* microarrays performed with RNA from plant tumors obtained from infections with crossings of FB1/FB2 and RAb1ts/RAb2ts; compared are the b_{on} and b_{off} states at permissive and restrictive conditions 5 dpi, respectively. The correlation matrix was calculated with expression values of all genes represented on the DNA chip to display similarities in gene expression of a single array compared to all others. The colour scale bar indicates the similarity of one array compared to another (red=equal, green=different). The first cluster is formed by three experiments of RAbE1ts/RAbE2ts crossings at 31°C indicating that these independent experiments are most similar to each other. The same holds true for the second cluster of the three FB1/FB2 experiments at 31°C. A third cluster is formed by the two experiments with wild type infection FB1/FB2 and the mutant infection RAbE1ts/RAbE2ts performed at permissive conditions. Expression profiles of both strains are similar at permissive conditions, whereas their profiles differ significantly at restrictive conditions. Furthermore, the effect of temperature on gene expression is more significant than the effect of b inactivation, as arrays with plants infected at 31°C are more similar to each other than to those infected at 22°C. Comparison of FB1/FB2 to RAbE1ts/RAbE2ts at 31°C is most suitable to analyze b_{on} and b_{off} states *in planta*. (C) Pie chart of differentially expressed genes after b inactivation comparing b_{on} and b_{off} states at 31°C *in planta*. Categories classifying individual genes are indicated in the Figure legend. Numbers of differentially expressed genes belonging to the individual categories are displayed in the chart. The number of genes within the two subgroups of secreted proteins (green) is significantly enriched (p -Value of 7.6×10^{-12} ; only probe sets identified by Target-P were considered (34); see Experimental Procedures).

For DNA array expression analysis, plants were infected with either a mixture of RAb1ts and RAb2ts or of FB1 and FB2. Array analysis of the two infection experiments 5 dpi (120 hours) at permissive temperature (22 °C) revealed comparable transcription profiles (Figure 2.1-4B). The effect of b-dependent regulation during biotrophic proliferation was addressed by shifting the temperature of FB1/FB2 and RAb1ts/RAb2ts infections from 22 °C to 31 °C after 111 hours past infection for a period of 9 hours. This period was sufficient to stall proliferation for the majority of RAb1ts/RAb2ts hyphae (Figure 2.1-4A).

A total of 81 genes appeared to be differentially expressed after switching off the function of the bE/bW heterodimer (for filter criteria see Experimental Procedures, Table 2.1-S1). We did not observe a significant alteration of specific functional categories among the deregulated genes. However, a group of 42 genes (52 %) coding for predicted secreted proteins was significantly enriched, including the most down-regulated gene *um05027* (Figure 2.1-4C, Table 2.1-S2, criteria for prediction of secreted proteins see Experimental Procedures). 12 of these genes have been described previously as part of *in planta* induced gene clusters for secreted proteins, several of which were shown to be important for full fungal virulence (Table 2.1-S2; Kämper *et al.*, 2006). 10 of the genes organized in the clusters 2A (2 genes - increased virulence), 6A (2 genes - reduced virulence), 9A (1 gene - unaffected) and 19A (5 genes - markedly reduced virulence) were down-regulated, whereas only 2 genes affecting cluster 2B (unaltered virulence) were induced (Kämper *et al.*, 2006; Table 2.1-S2). Only 10 of the 42 genes coding for potentially secreted proteins have a functional annotation, three of which encoding for cell wall degrading enzymes (endoglucanase, *um06332*; endochitinase, *um06190*; pectine lyase, *um10671*; Tables 2.1-S1, S2).

Of the 350 b-dependently regulated genes recently identified by DNA microarray analysis monitoring b induction in axenic culture (M. Scherer and J. Kämper, unpublished data), only 14 were found to be differentially expressed after temperature restriction of b activity *in planta* (Table 2.1-S3). One of these genes is *clp1*, a direct target gene of the b heterodimer (Scherer *et al.*, 2006) and the third most down-regulated gene (10-fold) after switching off b activity *in planta*. Furthermore, we observed an induction of the pheromone and the pheromone receptor genes (*mfa1*, *mfa2*, *pra1* and *pra2*; Table 2.1-S3) known to be down-regulated by an active b complex in axenic culture (Urban *et al.*, 1996). In accordance, 18 pheromone-dependent genes were also up-regulated (Table 2.1-S3; Urban *et al.*, 1996; Zarnack *et al.*, 2008).

2.1.3 Discussion

A Serine/Proline Exchange at the Border of the Third Helix of the bE Homeodomain Leads to Temperature Sensitivity of the bE/bW Heterodimer

bE2^{ts183P}, a temperature-sensitive allele of bE2, harbors a single mutation, leading to an amino acid exchange at the border of the third α -helix of the homeodomain. Helices I and II of homeodomains have structural and stabilizing functions, while helix III is involved in direct target sequence recognition by contacting base residues within the major groove of the DNA (Wolberger *et al.*, 1991). 3D structure analysis of the homeodomains of Antennapedia from *Drosophila melanogaster* and MATa1 from *Saccharomyces cerevisiae* revealed that the positions corresponding to proline 183 in bE are part of the last loop of the DNA binding α -helices (Figure 2.1-S1A, B). The α -ammonium group of proline is covalently bound to the δ -carbon atom; therefore, the amino acid is sterically rather constricted, which often leads to the “breaking” of a helix. Thus, the observed temperature sensitivity of *bE2^{ts183P}* is most likely caused by a helix destabilizing effect, leading to a non-functional DNA recognition helix. The thermo-instability observed for the mutant helix III in bE is apparently not a general effect, as the introduction of proline at the respective position of the bW1 homeodomain did not lead to temperature sensitivity (data not shown). However, the bW and bE homeodomains belong to different subclasses (Schlesinger *et al.*, 1997). The bE domain belongs to an atypical homeodomain class with less similarity to the consensus and additional spacer sequence between helix II and III. The bW domain belongs to the group of “classical” homeodomains with strong conservation throughout the whole domain. It would be worthwhile to test for temperature sensitivity in other atypical homeodomain proteins as the *S. cerevisiae* MAT α 2 protein.

Temperature Inactivation of the b Heterodimer during in Planta Development of U. maydis Blocks Fungal Proliferation

We could show that the b heterodimer is not only essential to establish the heterodikaryon after mating of two compatible sporidia and to initiate fungal pathogenicity, but also to sustain *in planta* proliferation and ensure sexual reproduction. Shutting off the activity of the b heterodimer during *in planta* development of the fungus leads to an enlargement of fungal tip cells that contain multiple nuclei, indicating a defect in cell division. One of the previously described

functions of the b heterodimer is the control of the mitotic cell cycle. In axenic culture, induced expression of an active bE/bW heterodimer leads to a G2 cell cycle arrest, reminiscent to the G2 arrest observed after fusion of two sporidia in the resulting dikaryon (Snetselaar and Mims, 1992; García-Muse *et al.*, 2003; Scherer *et al.*, 2006; Cánovas and Pérez-Martín, 2009). However, after plant penetration, the cell cycle arrest must be released to allow hyphal proliferation. bE/bW expression can be detected during the entire biotrophic phase (Quadbeck-Seeger *et al.*, 2000; M. Vranes and J. Kämper, unpublished data). It is thought that the function of the heterodimer is modulated by action of Clp1, a protein that was shown to counteract b function (Scherer *et al.*, 2006). Clp1 is expressed within the nucleus at the time point of cell cycle release upon plant penetration; however, the “plant signal” triggering this event is still unknown (Scherer *et al.*, 2006). Clp1 was also found to be essential for the formation of clamps, a specialized structure necessary for the distribution of nuclei and cell division *in planta*, and subsequently for cell division of the dikaryotic hyphae *in planta* (Scherer *et al.*, 2006). It is well possible that the loss of b function in the *bEts*-strains (controlling cell cycle) and of the b-dependently regulated gene *clp1* (controlling b function and cell division) leads to an uncoupling of cell cycle and cytokinesis, which would account for the multinucleated, enlarged tip cells formed after inactivation of b.

Pheromone-dependent Genes are De-repressed Due to b Inactivation in Planta

We observed the up-regulation of a total of 23 genes upon b-inactivation that were previously shown to be induced via the pheromone pathway (Table 2.1-S3; Hartmann *et al.*, 1996; Urban *et al.*, 1996; Zarnack *et al.*, 2008). It has been shown that formation of an active b heterodimer leads to the repression of the pheromone and pheromone-receptor genes (Urban *et al.*, 1996; Hartmann *et al.*, 1999). Since the infectious dikaryon harbors a compatible combination of both pheromone- (*mfa1* and *mfa2*) and both receptor-genes (*pra1* and *pra2*) it is conceivable that, upon b-inactivation, the de-repression of the pheromone/receptor genes leads to an activation of a-dependent genes. One of the a-dependently induced genes upregulated upon b-inactivation is *rbf1* (Zarnack *et al.*, 2008). Rbf1 encodes a transcription factor that serves as a central node in the b-regulatory cascade, involved in the regulation of the majority of b-dependently regulated genes (M. Scherer and J. Kämper, unpublished data; Scherer *et al.*, 2006). Thus, the

derepression of the a-pathway maintains the expression of *rbf1*, resulting in expression of b-regulated genes even after b-inactivation.

The b Heterodimer is Necessary for the Regulation of Secreted Proteins Important for Fungal Virulence during Pathogenic Development

Secreted proteins of plant pathogenic bacteria, oomycetes and fungi have been shown to play crucial roles for the establishment of the different pathogenic lifestyles (Kämper *et al.*, 2006; Chisholm *et al.*, 2006; Kamoun, 2006; O'Connell and Panstruga, 2006; Birch *et al.*, 2006; Catanzariti *et al.*, 2006; Ridout *et al.*, 2006; Kamoun, 2007; Morgan and Kamoun, 2007). For *U. maydis*, up to 750 proteins have been predicted to be secreted, dependent on the stringency of the method used for secretion signal prediction (MUMDB; Müller *et al.*, 2008; Kämper *et al.*, 2006). Recently, we have shown that several of these predicted proteins were (1) specifically expressed during *in planta* development and (2) organized as clusters within the *U. maydis* genome (Kämper *et al.*, 2006). In total 12 of these clusters of *U. maydis*-specific secreted proteins have been identified, of which 5 were found to be crucial for pathogenic development (Kämper *et al.*, 2006).

52 % (42) of the genes differentially expressed in the *bEts* strains encode proteins with a bioinformatic prediction to be secreted. We identified 12 genes organized in 5 of the described secreted clusters, among these 5 of the 26 genes of the largest identified "cluster 19" (Table 2.1-S2). Since not all genes were affected by the b heterodimer within these 5 clusters, we have to assume additional regulatory circuits that lead to the *in planta* expression of the entire cluster (Table 2.1-S2). Intriguingly, b inactivation affects 3 out of the 5 clusters that were shown to be crucial for pathogenic development of *U. maydis* (clusters 2A, 6A and 19; Table 2.1-S2; Kämper *et al.*, 2006). Although it is currently not known which of the genes in the clusters are responsive for the observed pathogenicity phenotypes, our finding clearly indicates that the b heterodimer plays an essential role for the regulation of secreted proteins important for fungal virulence.

Most of the genes differentially regulated by b *in planta*, including the genes coding for secreted proteins, are not expressed after b induction in axenic culture (M. Scherer and J. Kämper, unpublished data), indicating that additional plant-specific signals and regulators modify b-mediated transcription. We have identified three genes coding for putative transcription factors (*um06257*, *um10500*, *um01523*) as

down-regulated after b inactivation during biotrophic growth (Table 2.1-S1). It is well possible that these regulators integrate additional environmental cues into the b-dependent regulatory cascade to adapt the fungus to changing environmental conditions as the plant surface or different plant tissues.

Our results support the function of the b mating type locus as the determinant for pathogenic development. The b heterodimer can be positioned as master regulator within a transcriptional network for the spatial and temporal control of cell cycle and cell division, but, as we show now, also for genes required to establish and maintain the biotrophic interaction with its host plant.

2.1.4 Experimental Procedures

Strains and Growth Conditions

Escherichia coli strain TOP10 (Invitrogen) was used for cloning purposes. *Ustilago maydis* cells were grown at 28°C in YEPS (Tsukuda *et al.*, 1988) as pre-cultures for mating assays and plant infections. Mating assays were performed at 22°C (permissive) or 31°C (restrictive) temperature as described by Gillissen *et al.* (1992) on 1% charcoal containing potato dextrose (PDC) medium (Difco) or complete medium (Holliday, 1974). For screening of the plasmid library used for bE or bW mutagenesis all *U. maydis* strains harboring plasmids were grown in Hygromycin-containing media (200 µg/ml). *U. maydis* strains used in this study are listed in Table 2.1-1.

Table 2.1-1: Strains used in this work

Strain	Relevant Genotype	Reference
FBD11-21	a1a2/b2b2	Banuett and Herskowitz, 1989
FBD11-21 + pNEBbW1UH	a1a2/b2b2 + bW1	This work
FBD11-21 + pNEBbW1UH mut. lib.	a1a2/b2b2 + bW1mut	This work
FBD12-3	a1a2/b1b1	Banuett and Herskowitz, 1989
FBD12-3 + pNEBbW1UH	a1a2/b1b1 + bW1	This work
FBD12-3 + pFSbE2	a1a2/b1b1 + bE2mut	This work
FBD12-3 + pFSbE2 mutant library	a1a2/b1b1 + bE2	This work
FBD12-3 + pFSbE2ts52	a1a2/b1b1 + bE2ts52	This work
FBD12-3 + pFSbE2ts98	a1a2/b1b1 + bE2ts98	This work
FBD12-3 + pFSbE2tsP183	a1a2/b1b1 + bE2tsP183	This work
FB1otef:pra2	a1pra2/b1	Müller unpublished
RAbE2	a1pra2/b1bE2	This work
RAbE2_nls3gfp	a1pra2/b1bE2; Pmig2-5: NLS-3xeGFP	This work
RAbE2ts	a1pra2/b1bE2ts	This work
RAbE2ts_nls3gfp	a1pra2/b1bE2ts; Pmig2-5: NLS-3xeGFP	This work
FB1	a1/b1	Banuett and Herskowitz, 1989
FB2	a2/b2	Banuett and Herskowitz, 1989
JB1	a1/Δb1	Scherer <i>et al.</i> , 2006
JB2	a2/Δb2	This work
RAb1ts	a1/bW1bE1ts	This work
RAb2ts	a2/bW2bE2ts	This work

Plasmid and Strain Constructions

Plasmid pCR-Blunt-II-TOPO (Invitrogen) was used for cloning, subcloning, and sequencing of genomic fragments and fragments generated by PCR. Plasmid pFSbE2 (Kämper *et al.*, 1995) was used to construct the *bE2* mutant libraries and the plasmids pFSbE2ts52, -ts98 and -tsP183, in all cases a 642 bp HindIII-XbaI *bE2* fragment was cloned into the vector backbone (primer pairs: RW11 5'-CAC TCC CAC CTT TAG CCT CTA ACA-3' and RW12 5'-CGC CAT ACT TGA TCC AGC TGA TC-3'). Plasmid pNEBUH (Weinzierl, 2001) was used for cloning of the *bW1* gene including a 439 bp 5'-region upstream the open reading frame. The *bW1* gene was amplified from pbW1-pcx (Kämper *et al.*, 1995) in three individual reactions to insert the restriction sites needed for random PCR mutagenesis (359 bp KasI-KpnI fragment, primer pairs RW1 5'-AGG CGC CTT TGC TGG ATC GTT TCG-3' and RW2 5'-GGG GAG ACA AAA GGG GTA CCT GAG-3'; 530 bp KpnI-EcoRI fragment, primer pairs RW3 5'-CAT CCT CAG GTA CCC CTT TTG TCT-3' and RW4 5'-GCC TGC TCC AGA ATTCGG ACT GCT-3'; 1661 bp EcoRI-SphI fragment, primer pairs RW5 5'-AGC AGT CCG AAT TCT GGA GCA GG-3' and RW6 5'-GGC ATG CGA GAA TTG TGA AAA GTA-3'). The three fragments were introduced into pNEBUH to yield plasmid pNEBbW1UH which was used to construct the *bW1* mutant libraries; for this purpose, the 530 bp KpnI-EcoRI fragment was mutagenized by misincorporation-PCR (primer pairs bW1rPCR1 5'-GGC GCA AGG AAA TGA ATG TGT GTG-3' and bW1rPCR2 5'-TGC TTT GGC TTG AGT CCA GTG ACC-3'). The respective *bE2* and *bW1* plasmids were transformed in FB11-21 and FB12-3 for screening purposes (Banuett and Herskowitz, 1989). The strains RAbE2 and RAbE2ts were constructed by stable, ectopic integration of SspI-linearized plasmids pFSbE2 and pFSbE2P183 in the genome of FB1*otef:pra2*, respectively. FB1*otef:pra2* is an FB1 derivative (Banuett and Herskowitz, 1989) in which the *otef:pra2* construct was integrated into the *ip*-locus (Loubradou *et al.*, 2001); Müller, unpublished data). Plasmid pUThsp (Brachmann *et al.*, 2001) was used as backbone to clone the 3376 bp NotI Pmig2-5:NLS-3xeGFP fragment from pMS76 (Scherer *et al.*, 2006). The resulting plasmid pRWnlsGfp was linearized with SspI and ectopically integrated in RAbE2 and RAbE2ts, respectively. For the construction of pUmbE/bW, an *FseI*-linker was introduced into the *StuI* site of pSL1180 (Pharmacia); subsequently, a 1533 bp NotI-*XhoI* *bW2* fragment and a 1398 bp *FseI*/*EcoRI* fragment of *bE2* were integrated into the respective sites. The *EcoRI* site is located 607 bp 3' of the open reading frame of

bE2, the *XhoI* site was generated close to a *HaeIII* site 573 bp 3' of *bW2*. Recombinant PCR was used to integrate synonymous mutations to generate the *FseI* and *NotI* sites at amino acid position 234 to 235 in *bE2* and at position 338 to 339 in *bW2*, respectively. Subsequently, the carboxin-resistance gene was inserted as *EcoRV/SmaI* fragment from pCBX122 (Keon *et al.*, 1991), allowing targeted integration into the *ip*-locus of *U. maydis* (Loubradou *et al.*, 2001). The resulting plasmid, pUmbE/bW, harbors the constant regions of *bE2* and *bW2* with unique *NotI* and *FseI* sites. 2.2 kb fragments of the *b1* and *b2* locus comprising the N-terminal regions of *bE* (from amino acid 236) and *bW* (from amino acid 339) as well as the promoter region were amplified using primer pairs W2Not339 (5'-GCA CGC GGC CGC ATG TAA TCA AAG-3') and E2Fse235 (5'-GAG TGG CCG GCC GAG GTT GTC TG-3'), generating synonymous mutations that introduce an *FseI* site at amino acid position 235/236 in *bE* and a *NotI* site at amino acid position 338/339 in *bW*. Digestion of the PCR products with *NotI* and *FseI* allows cloning into plasmid pUmbE/bW to reconstitute functional *b* alleles, resulting in the plasmids pTHEA2 (*bW1bE1*) and pTHEB5 (*bW2bE2*). Plasmids pTHEA2 and pTHEB5 were used for construction of *bW1bE1^{ts}* and *bW2bE2^{ts}* constructs, respectively. The *bE2^{ts}* mutation was integrated by cloning a 182 bp *XhoI/XbaI* fragment from pFSbE2tsP183 containing the *bE2^{ts}*-mutation and parts of the homeodomain. The resulting plasmids pRAb1ts and pRAb2ts were linearized with *AgeI* for integration into the *ip*-locus (Loubradou *et al.*, 2001) of strains JB1 (*a1Δb1*; Scherer *et al.*, 2006) and JB2 (*a2Δb2*; FB2 derivative, in which the *b2* locus was substituted as described for JB1 by Scherer *et al.*, 2006). The resulting strains were named RAb1ts and RAb2ts, respectively. Sequence analysis of fragments generated by PCR was performed with an automated sequencer (ABI 373A; Applied Biosystems) and standard bioinformatic tools.

DNA and RNA Procedures

Molecular methods followed described protocols (Sambrook *et al.*, 1989). Random PCR mutagenesis was performed following the protocol from Spee *et al.*, 1993. Transformation of *U. maydis* protoplasts with the indicated plasmids was performed as described previously (Tsukuda *et al.*, 1988). DNA isolation from *U. maydis* and transformation procedures were performed as described (Schulz *et al.*, 1990). Homologous recombination into the *ip*-locus was verified by DNA gel blot analysis (Loubradou *et al.*, 2001). For Northern analysis, RNA isolation from charcoal plates

was performed as described (Schmitt *et al.*, 1990). RNA gel blot analysis was performed as described previously (Garrido *et al.*, 2004). ³²P-labeled probes used for detection: *bE2* (PCR product of primers RW11, RW12), *clp1* (Scherer *et al.*, 2006), *dik6* and *ppi* as loading control (Brachmann *et al.*, 2001). Detection of radioactive signals was performed with a STORM 840 PhosphorImager and ImageQuant 5.2 software (Molecular Dynamics).

Microscopy

Microscopic analysis was performed using a Zeiss Axioplan 2 microscope. Photomicrographs were obtained with an AxioCam HrM camera, and the images were processed with Axiovision (Zeiss) and Photoshop (Adobe). Chlorazole Black E staining of fungal cells *in planta* was performed as described (Brachmann *et al.*, 2003). GFP was observed by fluorescence microscopy (excitation/emission for eGFP: 450-490 nm/515-565 nm)

RNA Isolation for DNA Array Expression Analysis

U. maydis infected maize plants (Early Golden Bantam) were grown in a phytochamber in a 15 h/9 h light-dark cycle; light period started/ended with 1h ramping of light intensity. Prior to infection with *U. maydis* temperature was 28°C (light) and 20°C (dark). Plantlets were individually sown in pots with potting soil (Fruhstorfer Pikiererde) and infected 7 days after sowing, 1 h before end of the light period, as described (Brachmann *et al.*, 2001). After infection the plants were kept at 22°C (permissive temperature) or 31°C (restrictive temperature) depending on the requirements. Samples used for RNA preparation were collected 1 h before the end of the light period and directly frozen in liquid nitrogen for three independently replicates. For each experiment, 10 plants were sampled. Total RNA was extracted using Trizol reagent (Invitrogen) according to the manufacturer's instructions. RNA samples to be used for microarray analyses or real-time RT-PCR were further column purified (RNeasy; Qiagen) and the quality checked using a Bioanalyzer with an RNA 6000 Nano LabChip kit (Agilent).

DNA Microarray

Affymetrix Gene Chip^R *Ustilago* genome arrays were done in three biological replicates, using standard Affymetrix protocols (staining: EukGe2V4 protocol on GeneChip Fluidics Station 400; scanning on Affymetrix GSC3000). Expression data were submitted to GeneExpressionOmnibus (<http://www.ncbi.nlm.nih.gov/geo/>), Accession GSE16501. Data analysis was performed using Affymetrix Micro Array Suite 5.1, the R bioconductor package (<http://www.bioconductor.org/>) and dChip1.3 (<http://biosun1.harvard.edu/complab/dchip/>), as described by Eichhorn *et al.* (2006). Probe sets present in at least two of the replicates were defined as “expressed”, resulting in 48 % (3263 out of 6795) present calls in both wild type and temperature sensitive strains. We considered changes >2-fold with a difference between expression values >50 and a corrected p-value <0.01 as significant. For genes displayed by more than one probe set, the probe set giving the strongest signal intensity was chosen. Functional enrichment analyses were performed with the functional distribution tool integrated in the *Ustilago maydis* genome database (<http://mips.gsf.de/cgi-bin/proj/funcatDB/>). Enrichment analysis of secreted proteins was performed calculating the total number of secreted proteins expressed in the wild type background 5 dpi (only considering the 754 genes containing Target-P signals, see below). 395 probe sets (about 12 % of the expressed probe sets) representing secreted proteins were identified to be present under these conditions. Hypergeometrical distribution analysis was performed and p-Values below 0.01 were considered to be significant.

Quantitative Real-Time PCR Analysis

For cDNA synthesis, the SuperScript III first-strand synthesis SuperMix assay (Invitrogen) was employed, using 1 µg of total RNA. qRT-PCR was performed on a Bio-Rad iCycler using the Platinum SYBR Green qPCR SuperMix-UDG (Invitrogen). Cycling conditions were 2 min 95°C, followed by 45 cycles of 30 sec 95°C/ 30 sec 65°C / 30 sec 72°C. *rbf1* expression was analyzed in the RNA probes used for the DNA-array analysis. The *U. maydis actin* (um11232) and *eIF2B* (um04869) genes were used as references. Primer sequences of *rbf1* are described by (Scherer *et al.*, 2006). Primer sequences were rt-eIF-2B-F (5'-ATC CCG AAC AGC CCA AAC-3') and rt-eIF-2B-R (5' ATC GTC AAC CGC AAC CAC-3') for *eIF2B*, rt-actin-F (5'-CAT GTA CGC CGG TAT CTC G-3') and rt-actin-R (5'-CTC GGG AGG AGC AAC AAT C-3') for the *actin* gene.

Prediction of Secreted Proteins

Classical secretion signals (TP) were predicted with Target-P (<http://www.cbs.dtu.dk/services/TargetP/>). RC-values indicate the reliability classes (1 - 5), with class 1 having the highest probability to be secreted (Table 2.1-S2; Emanuelsson *et al.*, 2000). RC=3 was used as cut-off. A complete list of 754 *Ustilago maydis* proteins that encompass this criterion can be obtained at the MIPS *Ustilago maydis* Database (<http://mips.gsf.de/genre/proj/ustilago/Search/listTargetP.html?target=Secretory%20pathway>). Non-classical secretion (SP) was predicted with Secretome-P (<http://www.cbs.dtu.dk/services/SecretomeP/>). Obtained NN-scores indicate the prediction reliability (0-1), with 1 having the highest probability to be secreted (Table 2.1-S2; Bendtsen *et al.*, 2004). A NN-score >0.5 was used as cut-off.

2.1.5 Supplementary Information

A file containing the Supplementary Material of section 2.1 is available on data-CD deposited in section 5 of this thesis. The file includes Figure 2.1-S1 and Tables 2.3-S1 to S3.

Figure 2.1-S1: Mutation from serine to proline at amino acid position 183 in the bE protein most likely affects the structure of DNA-binding helix III of the homeodomain.

Table 2.1-S1: *U. maydis* genes differentially expressed in response to b inactivation *in planta*.

Table 2.1-S2: *U. maydis* genes differentially expressed in response to b inactivation *in planta*: genes encoding proteins predicted to be secreted.

Table 2.1-S3: *U. maydis* genes differentially expressed in response to b inactivation *in planta*: genes that are pheromone- and/or b-dependent *in axenic* culture.

Acknowledgments

We thank Philipp Müller and Regine Kahmann (MPI for terrestrial Microbiology, Germany, Marburg) for the strain FB1otef:pra2, Volker Vincon (MPI for terrestrial Microbiology, Germany, Marburg) for technical assistance and Miroslav Vranes, Kai Heimel and Alexander Zahiri (Institute for Applied Biosciences, University of Karlsruhe, Germany) for critical comments on the manuscript. This work was supported by a grant from the International Graduate School GRK767, from the Research Group FOR666, both funded by the German Research Foundation, and by grants from the German Ministry of Science and Education for the *U. maydis* DNA array setup.

2.2 Reprogramming a Maize Plant: Transcriptional and Metabolic Changes Induced by the Fungal Biotroph *Ustilago maydis*

Gunther Doehlemann^{1*}, Ramon Wahl^{1*}, Robin J. Horst², Lars M. Voll², Björn Usadel³, Fabien Poree³, Mark Stitt³, Jörn Pons-Kühnemann⁴, Uwe Sonnewald², Regine Kahmann^{1#} and Jörg Kämper^{1,5#}

*These authors contributed equally

¹Max Planck Institute for Terrestrial Microbiology, D-35043 Marburg, Germany, ²Friedrich-Alexander University Erlangen-Nuremberg, Department of Biochemistry, 91058 Erlangen, Germany; ³Max Planck Institute for Plant Physiology, D-14476 Potsdam - Golm, Germany; ⁴Justus-Liebig University Giessen, Biometry and Population Genetics, D-35392 Giessen; ⁵current address: University of Karlsruhe, Institute of Applied Biosciences, Department of Genetics, 76187 Karlsruhe, Germany

To whom correspondence should be send:

Regine Kahmann, MPI for terrestrial Microbiology, Karl-von-Frisch-Strasse, D-35043 Marburg; Tel +49-6421-178-501; Fax +49-6421-178-509; Email: kahmann@mpi-marburg.mpg.de

and Jörg Kämper, University of Karlsruhe, Institute of Applied Biosciences, Department of Genetics, Hertzstr. 16, D-76187 Karlsruhe; Tel +49-721-608-4632; Fax +49-721-608-4509; Email: joerg.kaemper@kit.edu

Key words: Microarray, Biotrophy, *Zea mays*, *Ustilago maydis*, Metabolite profiling, Defence signalling

Running title: Plant response to *U. maydis* infection

Summary

The fungal pathogen *Ustilago maydis* establishes a biotrophic relationship with its host plant maize. Hallmarks of the disease are large plant tumours in which fungal proliferation occurs. Previous studies suggested that classical defence pathways are not activated. Confocal microscopy, global expression profiling and metabolic profiling now shows that *U. maydis* is recognized early and triggers defence responses. Many of these early response genes are down-regulated at later time points whereas several genes associated with cell death suppression are induced. The interplay between fungus and host involves changes in hormone signalling, induction of antioxidant and secondary metabolism, as well as the prevention of source leaf establishment. Our data provide novel insights into the complexity of a biotrophic interaction.

2.2.1 Introduction

Plant pathogenic fungi have developed different strategies to cope with the plant environment. While necrotrophic fungi kill plant cells rapidly after infection to feed on the dead tissue, biotrophic fungi acquire nutrients from living plant tissue. The biotrophic relationship requires a highly specialized adaptation of the pathogen to the host plant. Hyphae of biotrophic fungi can grow intercellularly as well as intracellularly, thereby being ensheathed by the plasma membrane of the host cell. Many biotrophic pathogens like rusts and powdery mildew fungi form specialized feeding structures, called haustoria (Hahn and Mendgen, 2001; Voegelé *et al.*, 2001). In these structures, a carbohydrate- and protein-containing interface is developed in between the hyphal cell wall and the plant plasma membrane that facilitates the exchange of signals and nutrients between fungus and host (Hahn and Mendgen, 2001; Perfect *et al.*, 1999; Mendgen and Hahn, 2002).

Plants have developed multifaceted defence systems, many of which are induced only upon pathogen attack. These responses include induction of pathogenesis related (PR) genes, production of secondary metabolites as well as the reinforcement of cell walls. Associated with these responses are the production of reactive oxygen species (ROS) and the induction of localized cell death (hypersensitive response, HR).

Induction of the basal plant defence machinery occurs upon the recognition of conserved molecules which are commonly found in a variety of microbial species, but are absent in the host. These pathogen associated molecular patterns (PAMPs) include for example fungal chitin, β -glucans and ergosterol. Specific virulence factors of the pathogen can be recognized by corresponding R (resistance) genes of the host plant. R gene-mediated resistance is associated with the activation of a salicylic acid (SA)-dependent signalling pathway that leads to expression of defence-related genes like PR1, the production of ROS, and programmed cell death. Other phytohormones involved in pathogen responses are ethylene (ET) and jasmonates (JA). For biotrophs, R gene-mediated defence responses and SA signalling are thought to result in resistance by restricting fungal growth in infected cells that have undergone hypersensitive cell death. Conversely, programmed cell death supports growth of necrotroph pathogens. Thus, plant defence responses appear specifically adapted to the attacking pathogen, with SA-dependent defences acting against biotrophs, and JA- and ET-dependent responses acting against necrotrophs (Greenberg and Yao, 2004; Glazebrook, 2005; Jones and Dangl, 2006; O'Connell and Panstruga, 2006).

One of the best studied biotrophic pathogens is the smut fungus *Ustilago maydis*, that induces plant tumours on all aerial parts of its host plants maize and teosinte. The biotrophic stage of *U. maydis* is initiated after fusion of two haploid sporidia that form the infectious dikaryotic hyphae. Upon formation of a specialized infection structure, the appressorium, penetration of the host cell is most likely facilitated by plant cell wall degrading enzymes. During the early infection stage invading hyphae are surrounded by the host plasma membrane. At later stages, hyphae grow both intra- as well as intercellularly. Tumour development is associated with both plant cell enlargement and increased cell divisions (Callow and Ling, 1973; Banuett and Herskowitz, 1996; Doehlemann *et al.*, 2008b); however, it is currently unknown how this is triggered by the fungus. Finally, within the tumour tissue the diploid teliospores are formed (Banuett, 1995; Martinez-Espinoza *et al.*, 2002; Feldbrügge *et al.*, 2004).

In a previous study, a set of 12 maize genes differentially regulated upon *U. maydis* infection has been identified. From the nature of these genes it was inferred that *U. maydis* triggers a discrete plant defence program and interferes with the differentiation of plant tissue (Basse, 2005). We have studied the responses of maize to *U. maydis* infection by extensive transcriptional and metabolic profiling. Using the MapMan tool (Thimm *et al.*, 2004) specifically adapted to maize, we visualized expressional changes of distinct biological pathways. These studies have revealed a complex interplay of *U. maydis* with its host plant resulting in massive changes in primary and secondary metabolism.

2.2.2 Results

U. maydis is Recognized by Its Host during the Early Infection Phase

To determine the most appropriate time points to perform the array analysis, we used confocal imaging to follow the course of infection using the *U. maydis* strain SG200 which is able to infect plants without a mating partner (Kämper *et al.*, 2006). The different stages of disease progression chosen for our study are depicted schematically in Figure 2.2-1A.

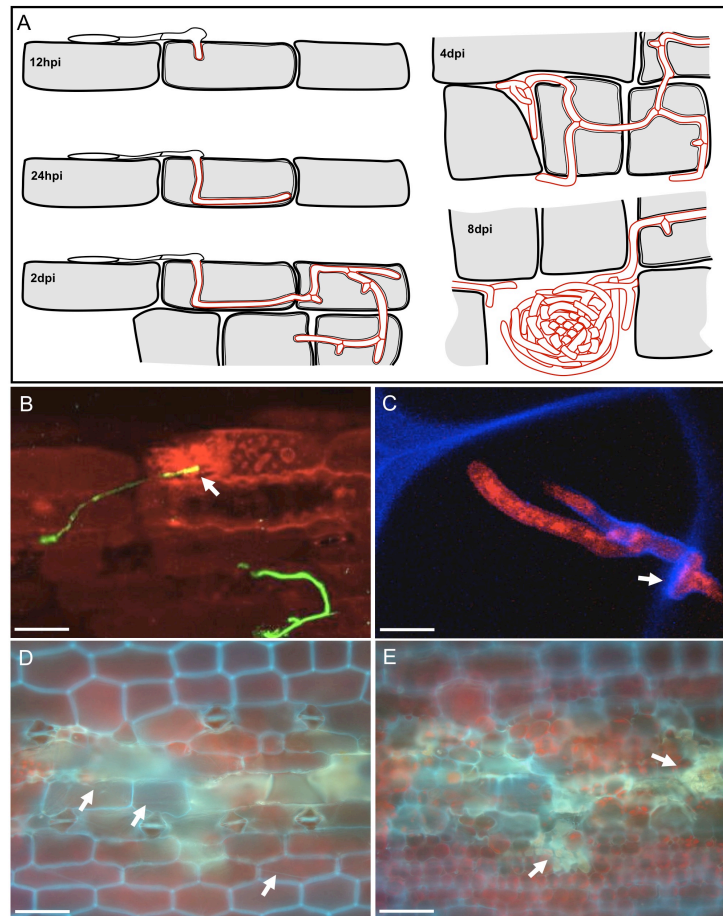


Figure 2.2-1: Pathogenic development of *U. maydis*. (A) Schematic illustration of *U. maydis* development in maize: 12 hpi: Filaments form appressoria penetrating the epidermis. 24 hpi: Invading hyphae in the epidermal layer are surrounded by the plant plasma membrane. 2 dpi: Hyphae proliferate intracellularly within epidermis and mesophyll. 4 dpi: Beginning of tumour induction. Fungi grow both inter- and intra-cellularly. 8 dpi: Tumour formation. Hyphae form huge aggregates in the intercellular space. (B) Infection structure of *U. maydis* (arrow) 12hpi. The attacked maize epidermis cell is collapsing, indicated by disintegration of membrane structures. Hyphae and plant membranes were stained with WGA-AF488 (green) and FM4-64 (red), respectively. Bar: 25µm. (C) Cell-to-cell passage of SG200 Potef::2xRFP hyphae (red:cytoplasmic RFP fluorescence) in the epidermis is accompanied by locally increased cell wall autofluorescence (blue, see arrow). Bar: 5µm. (D, E) Plant cell wall autofluorescence in *U. maydis* colonized leaf tissue 4 dpi; arrows in (D) indicate intracellular hyphae. Collapsed mesophyll cells in (E), (arrows), show bright autofluorescence and are devoid of chlorophyll. (D) and (E) represent focal planes at the epidermal cell layer and in the mesophyll, respectively. Bars: 50µm

12 hours post infection (hpi) the majority of SG200 cells had formed filaments and appressoria. During this initial stage, we observed a small fraction of epidermal cells undergoing cell death, indicating that not all hyphae were able to establish a biotrophic interaction (Figure 2.2-1B). 24 hpi hyphae were found in the epidermal cell layer. This intracellular stage persisted at 2 dpi (days post infection) but was now associated with hyphal branching. Fungal cell-to-cell passage was associated with hyphal tip swelling (Figure 2.2-1C) reminiscent of appressoria. Except for the growing tips, hyphae were surrounded by autofluorescent material accumulating at sites of cell-to-cell passage and around older parts of the hyphae (Figure 2.2-1C), suggesting the elicitation of plant defences.

4 dpi tumour development had commenced and hyphae had colonized meristematic tissue, growing both intra- and intercellularly (Figure 2.2-1A; Doehlemann *et al.*, 2008b). In colonized areas, strong autofluorescence and occasionally small areas with clusters of dead cells were detected (Figures 2.2-1D, E). 8 dpi tumours had increased in size and contained clusters of sporogenic hyphae. At this time point, anthocyanin accumulation was observed and autofluorescence persisted. Our analysis demonstrates that the infection by *U. maydis* elicits visible plant defence reactions throughout the various stages of biotrophic development. As the time points used in this microscopic study provided a comprehensive view of distinct steps in fungal development as well as the plant response, we have chosen the same stages for our subsequent studies.

Changes in Host Gene Expression after U. maydis Infection

For a comprehensive analysis of host cell responses, we have performed transcript profiling using the Affymetrix maize genome array. On this array, 13,339 genes are represented by 17,555 probsets. Under our experimental conditions, significant signals were obtained for 70.8% of the probe sets in at least one of the experiments; 53.0% were present in all experiments. Plants were infected with SG200 and leaf samples were taken 12 and 24 hpi, as well as 2, 4 and 8 dpi in three independent experiments. Changes in gene expression were calculated relative to control plants inoculated with water. Statistical analysis revealed that 2891 genes were differentially regulated at least in one of the time points analyzed.

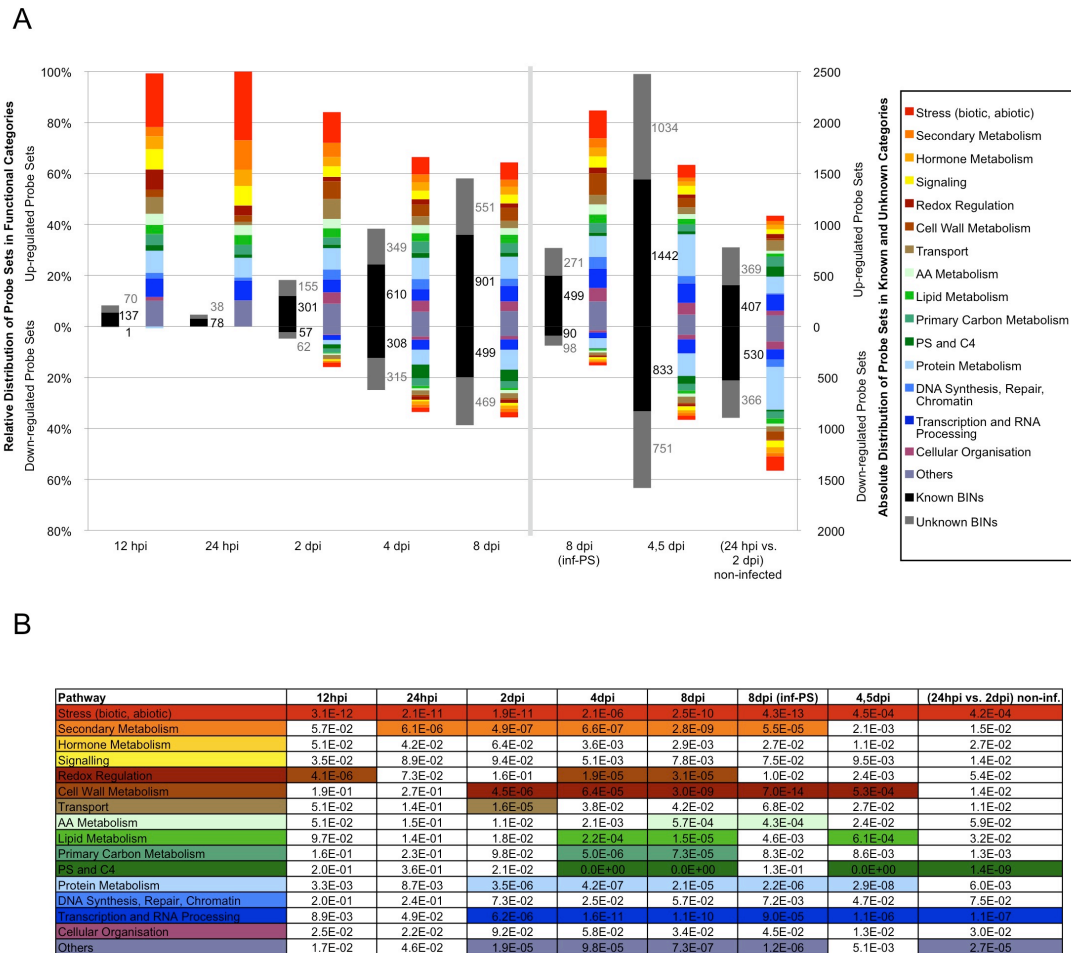


Figure 2.2-2: Functional categories of maize genes regulated upon *U. maydis* infection. (A) Bars in black and grey represent numbers of regulated genes relative to non-infected control leaves; grey and black bars indicate the number of genes with unknown and annotated function, respectively. Coloured bars give the relative distribution of genes within the BINs, as indicated on the right ordinate. The absolute numbers of genes within the different functional categories (BINs) are given in Table 2.2-S1. "8 dpi (inf -PS)" delineates differentially regulated genes in infected leaves compared to those in masked leaves. "24 hpi vs 2 dpi non-infected" delineates transcriptional changes in non-infected leaves at these time points. **(B)** Significant enrichment of genes of the indicated functional categories. BINs with an overrepresentation of regulated genes (Hypergeometric distribution, P-value < 0.001) are indicated in colour. Numbers represent the respective p-values.

12 hpi, 208 genes were differentially regulated in infected leaves, of which 138 were functionally annotated. Of these, genes with a presumed function in stress response and redox regulation, including defence related genes, were significantly enriched (Figure 2.2-2, Table 2.2-S2). 24 hpi, the number of genes with significantly altered transcript levels in infected leaves decreased to 116 (Figure 2.2-2A), which reflects mostly the variation around the threshold level of 2-fold used as cut-off. Nevertheless, 37 of the genes that were induced 12 hpi were significantly down-regulated 24 hpi,

and this down-regulation was in most cases maintained 2 dpi (Figure 2.2-3 and see below).

The number of stress-associated genes remained significantly high 24 hpi, and genes involved in redox regulation became less prominent. Furthermore, an increased number of genes related to secondary metabolism were differentially regulated in infected leaves 24 hpi compared to 12 hpi (Figure 2.2-2B). 2 dpi, the number of differentially regulated genes increased to 575, of which 358 could be functionally annotated (Figure 2.2-2A, Table 2.2-S2). Besides genes of the functional categories "stress" and "secondary metabolism" that were already enriched during the earlier time points, genes associated with "cell wall metabolism" were over-represented (Figure 2.2-2B). Furthermore, genes of the categories "protein metabolism", "transcription and RNA processing", as well as "transport" were significantly enriched 2 dpi (Figure 2.2-2B), indicating the onset of a broad metabolic reprogramming in infected tissue. We also observed a slight, but not yet significant enrichment of genes involved in photosynthesis.

4 and 8 dpi, the number of differentially regulated genes increased to 1582 and 2420, respectively (Table 2.2-S2). The number of defence related genes as well as genes involved in redox regulation increased further (Figure 2.2-2B). The major changes concerned the functional categories "PS and C4", "primary carbon metabolism", "protein metabolism" and "transcription and RNA-processing". Transcriptional changes were visualized by the MapMan tool adapted to maize, which allows an assignment to cellular processes (Figure 2.2-4). In the following we will discuss the most prominent processes that are subject to differential regulation.

Plant Defence Responses to U. maydis Infection

12 hpi, stress related genes were significantly overrepresented in infected plant tissue (Figure 2.2-2B). A rather unspecific defence reaction was elicited as several genes known to be induced by abiotic stresses like temperature, osmolarity and wounding were up-regulated. However, the majority of induced genes encode PR-like proteins (van Loon *et al.*, 2006; Tables 2.2-S2, S3) at a time point when fungal hyphae had just started to penetrate the epidermis. This shows that *U. maydis* cells were recognized.

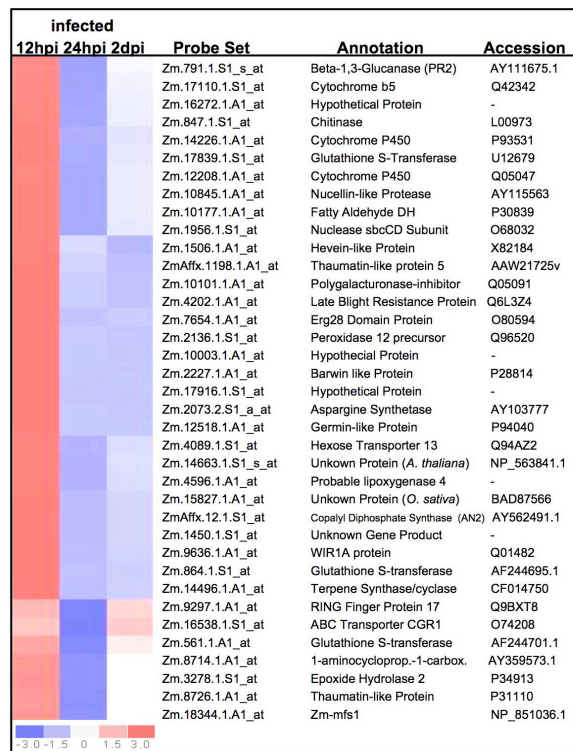


Figure 2.2-3: Down-regulation of early defence response to *U. maydis*. Hierarchical clustering of genes that are least two-fold down-regulated 24 hpi when compared to 12 hpi. Colours represent expression levels for each gene which are either above (red) or below (blue) the mean expression level (white) at the three time points given, according to the dChip 1.3 manual (<http://biosun1.harvard.edu/complab/dchip/manual.htm>).

From a total of 184 PR-like genes identified on the array, 34 genes representing most PR-gene classes were found to be induced (Table 2.2-S3). Furthermore two LRR genes were up-regulated (Zm.10830.1 and Zm.8200.1) as well as Zm.12900.1, encoding a protein similar to a receptor like kinase induced after rust infection of wheat (Feuillet *et al.*, 2003). The four most induced genes (200- to 700-fold) encode a terpene synthase (involved in isoprenoid synthesis; Zm.14496.1), endochitinase B (PR3- like; Zm.1595.1), a barwin-like protein (PR4-like; Zm.2227.1) and an 1,3 beta-glucanase (PR2-like; Zm.791.1) (Table 2.2-S2). The *Zm-mfs1* gene (major facilitator superfamily; Zm.18344.1), which is induced upon infection with the necrotrophic pathogen *Cochliobolus carbonum* (Simmons *et al.*, 2003) was 26-fold induced 12 hpi as well. *Zm-mfs2* (Zm.12717.1) expression was altered neither upon *C. carbonum* infection nor upon infection by *U. maydis*. The *an2* gene (ZmAfx.12.1), which is up-regulated after infection with *Fusarium graminearum* (Harris *et al.*, 2005), was also induced by *U. maydis* 12 hpi, while *an1* (Zm.228.1) expression was not altered. The corresponding rice orthologs encode ent-copalyl diphosphate synthases. *an1* is involved in GA synthesis and *an2* is required for phytoalexin synthesis (Prisic *et al.*, 2004). Both *Zm-mfs1* and *an2* expression decreased significantly 24 hpi.

Further inspection of the genes induced 12 hpi revealed that 37 of these genes were down-regulated at least 2-fold in infected tissue at the 24 hr time point. Most of these

were defence related genes including three of the four most highly induced transcripts (Figure 2.2-3). This indicates that the primary plant response is attenuated when *U. maydis* starts colonizing epidermal cells.

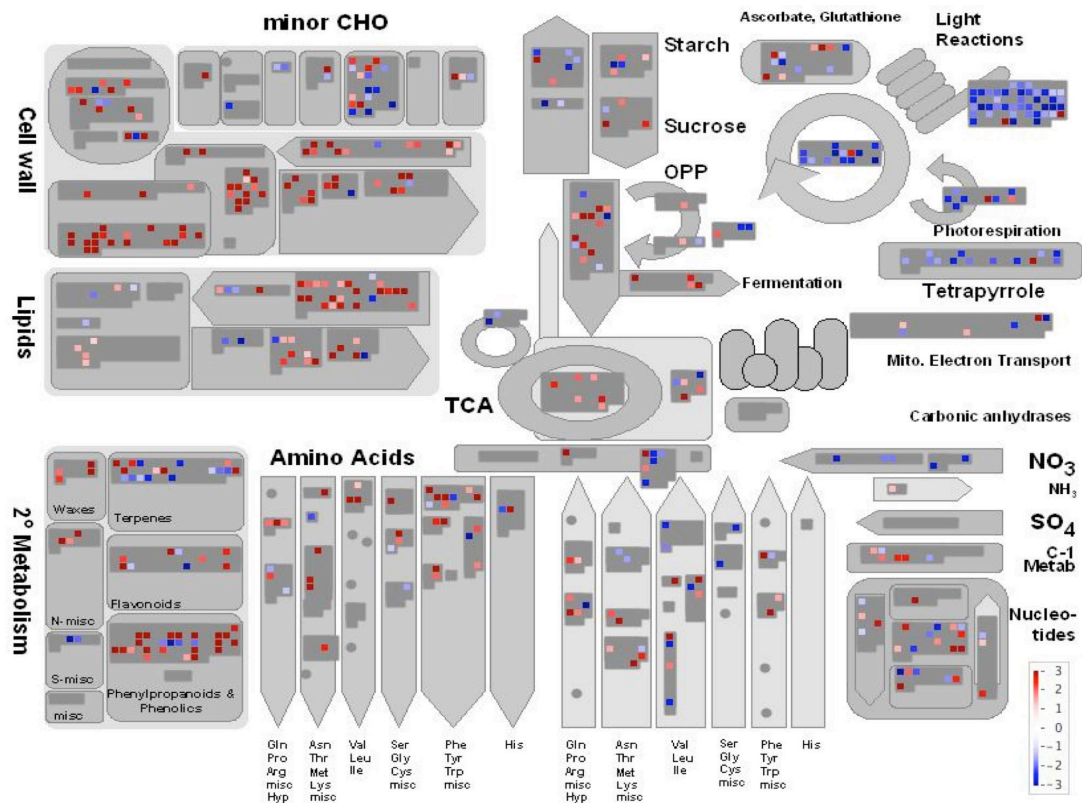


Figure 2.2-4: Overview of metabolic changes in infected leaves 8 dpi, visualized by MapMan. Genes significantly up- and down-regulated in infected tissues relative to non-infected tissue are indicated in red and blue, respectively. Scale bars display log fold changes.

Interestingly, 12 hpi genes for Bax-inhibitor 1 (Zm.12293.1) and a cystatin (Zm.8113.1;), both involved in cell death suppression, were induced (Table 2.2-S4). This induction persisted at 2 to 8 dpi, and additionally two more cystatin genes (Zm.14795.1; Zm.14272.5) were induced in infected tissue. Conversely, one of the two metacaspases present on the array (Zm.18453) was significantly down-regulated at these time points (Table 2.2-S4). Taken together, these data suggest that *U. maydis* infection is accompanied by an inhibition of the plant cell death program.

U. maydis Induced Changes in Hormone Signalling

Of 25 genes annotated as being involved in jasmonate biosynthesis and responses, nine were significantly induced already 12 hpi, and expression levels were

timepoints, which coincide with the onset of massive cell division and enlargement, genes coding for gibberelin biosynthesis enzymes as well as GA responsive genes were also induced (Figure 2.2-5).

Changes in Antioxidant Levels and Secondary Metabolite Synthesis during U. maydis Infection

Abiotic and biotic stress coincides with changes in oxidation state and content of soluble antioxidants, with glutathione (GSH/GSSG) being the most sensitive component (Ogawa, 2005). Seven glutathione S-transferase (GST) genes were induced already 12 hpi (Table 2.2-S2), including *gst15* (Zm.545.1), a homologue to wheat *gst1a* that is induced upon pathogen attack (Dudler *et al.*, 1991).

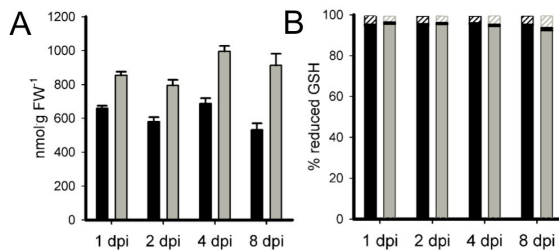


Figure 2.2-6: Changes of antioxidant contents in response to infection with *U. maydis*. (A) Total glutathione contents in *U. maydis*-infected (grey bars) and control leaves (black bars) at the indicated time points post infection. (B) Reduction state of the glutathione pool. The solid areas represent reduced, the hatched areas oxidized glutathione. For all graphs, standard errors are displayed.

To substantiate the transcriptome data, the contents of soluble (glutathione and ascorbic acid) and membrane bound antioxidants (tocopherols) were determined from the same material used for array analysis. Tocopherol and ascorbic acid contents did not change during the infection process (data not shown). Elevated GSH levels were observed 24 hpi and increased further during the infection process, while a high reduction state of the glutathione pool was maintained (Figure 2.2-6A, B). Increased levels of GSH have also been shown to coincide with the induction of PR genes in *A. thaliana* (Senda and Ogawa, 2004). Additionally, GSH plays a major role in secondary metabolite synthesis, mainly by regulating the key enzymes phenylalanin ammonium lyase (PAL) and chalcone synthase (CHS) (Loyall *et al.*, 2000; Gomez *et al.*, 2004).

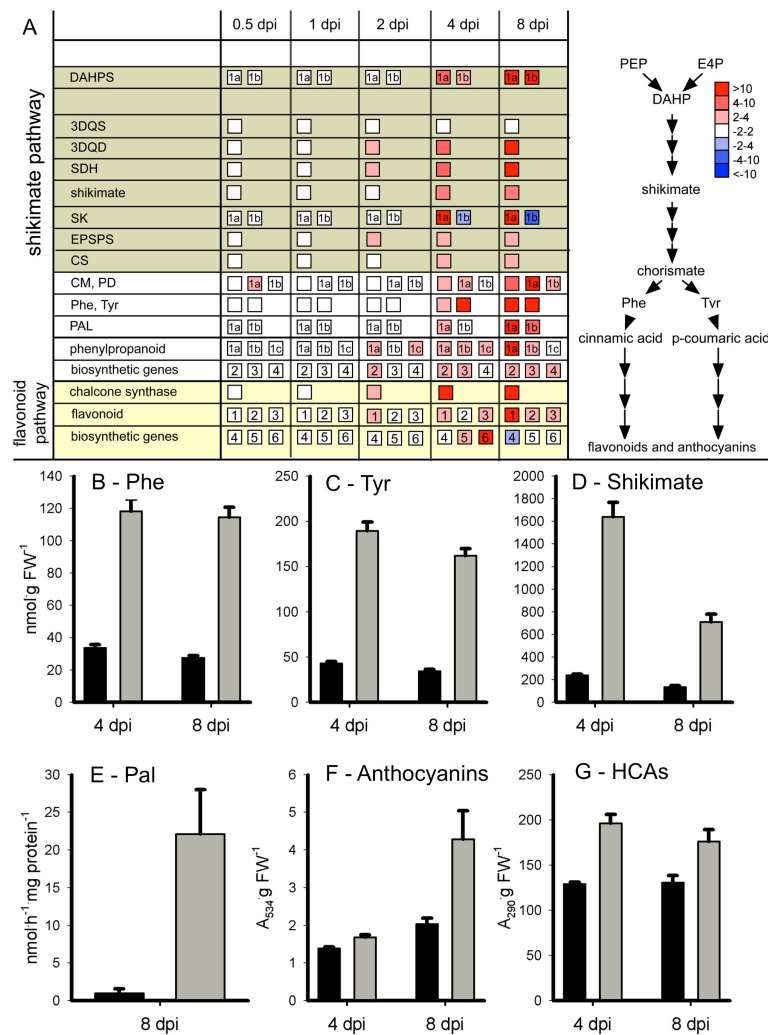


Figure 2.2-7: Transcriptional and metabolic changes in the shikimate and phenylpropanoid pathway. (A) Transcript accumulation for genes involved in the biosynthesis of secondary metabolites. Scale bar indicates up-regulation (red) and down-regulation (blue) in infected compared to non-infected tissue. Isoforms of the same enzyme are marked with a-c, where applicable. Gene annotations and abbreviations of the phenylpropanoid and flavonoid pathway are summarized in Table 2.2-S8 (B – D) Contents of phenylalanine, tyrosine and shikimate at 4 and 8 dpi. (E) Activity of PAL at 8 dpi. (F – G) Total contents of anthocyanins (A_{534}) and hydroxycinnamic acid derivatives (A_{290}) at 4 and 8 dpi. Grey bars represent *U. maydis* infected leaves, black bars represent control leaves. Standard errors are displayed.

Consistently, both PAL enzyme activity and transcript level were strongly increased in tumour tissue 8 dpi (Figure 2.2-7A, E). The substrates for PAL, phenylalanine and tyrosine, accumulated about 4- and 5-fold, respectively, 8 dpi in infected tissue (Figure 2.2-7B, C). Accumulation of these two amino acids was significantly higher than the average increase of most other amino acids, which was in the range of 2-3 fold (data not shown). Consistently, many genes from the shikimate pathway were found to be induced in infected tissue starting 2 dpi (Figure 2.2-7A). Shikimate, an abundant key metabolite upstream of phenylalanine and tyrosine, increased about 8-fold in tumour tissue compared to uninfected leaves 4 and 8 dpi (Figure 2.2-7D).

The major phenylpropanoid products downstream of PAL are hydroxycinnamic acid derivatives predominantly serving as building blocks of lignin and flavonoids, which represent potential phytoalexins, anthocyanins and UV protectants. Anthocyanins accumulated strongly in infected maize tissue (Figure 2.2-7F), which was also evident by visual inspection of infected tissue. Similarly, the overall content of hydroxycinnamic acid derivatives was increased in tumour tissue (Figure 2.2-7G), while the total content of flavonoids was not changed significantly 8 dpi (infected tissue: 114.45 ± 9.81 A310/g FW; control tissue: 121.2 ± 6.9 A310/g FW) 8 dpi. The gene for leucoanthocyanidin dioxygenase (Zm.62.1), a key enzyme for anthocyanin synthesis, was induced about 15-fold at late infection stages (Table 2.2-S2).

Induction of genes involved in lignin biosynthesis was observed already 12 hpi and increased further during the infection process. In tumour tissue (8 dpi) transcript levels for genes involved in almost all steps of lignin biosynthesis were significantly induced (Figure 2.2-S1). The enhanced synthesis of phenolic compounds, such as lignin, flavonoids and phenylpropanoids (Figure 2.2-7A) is reflected by the enhanced cell wall autofluorescence observed in *U. maydis* infected tissue (Figure 2.2-1C-E).

Changes in Plant Primary Metabolism

The experimental conditions used in our experiments resulted predominantly in the infection of the third leaf, which was initially still contained within the leaf whorl. One to two days later, when exposed to light, the onset of photosynthesis was expected to lead to a decrease in free hexose content, which in sink tissues is known to originate from cleavage of imported sucrose (Horst *et al.*, 2008).

Table 2.2-1: Carbohydrate contents in *U. maydis* infected and uninfected leaves.

Contents*	24 hpi		4 dpi		8 dpi	
	control	infected	control	infected	control	infected
hexoses	25.1 ± 0.7	23.2 ± 0.5	1.8 ± 0.3	5.0 ± 0.4	1.1 ± 0.5	26.6 ± 3.0
sucrose	27.7 ± 1.5	23.2 ± 0.7	24.5 ± 2.0	30.4 ± 2.0	22.6 ± 1.1	29.6 ± 2.7
hexoses / sucrose	0.9 ± 0.04	1.01 ± 0.04	0.07 ± 0.01	0.16 ± 0.01	0.05 ± 0.02	0.94 ± 0.11
starch	3.3 ± 0.4	6.95 ± 0.9	75.8 ± 4.9	113.6 ± 7.6	63.3 ± 6.5	69.2 ± 6.1

*Concentrations are given in $\mu\text{mol/g FW}$ for sugars and $\mu\text{mol Glc units/g FW}$ for starch. Standard errors are indicated.

To determine the influence of *U. maydis* on the sink-to-source transition, we measured free hexose and sucrose contents in infected and non-infected leaves (Table 2.2-1). Hexose content in infected and non-infected leaves decreased 4 dpi, reflecting the onset of photosynthetic activity. Whereas hexose levels remained low in control leaves after 8 days, they increased more than 20-fold in infected leaves at this time point (Table 2.2-1); sucrose contents were not altered by *U. maydis* infection. Consequently, this resulted in an increased hexose/sucrose ratio in tumour tissue (Table 2.2-1).

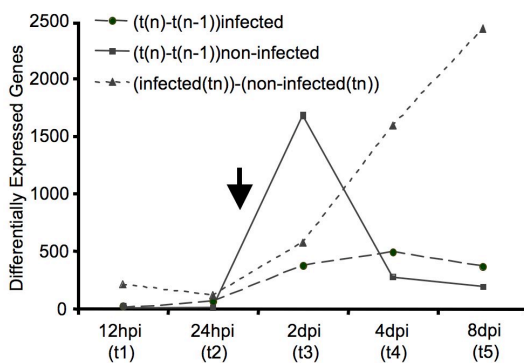


Figure 2.2-8: Transcriptional changes in infected and non-infected tissue during maize leaf development. The total number of differentially expressed genes comparing two consecutive time points in non-infected (square) and infected (circle) leaves is plotted on the ordinate; triangles display the total number of differentially expressed genes comparing infected and non-infected leaves. Arrow indicates the time point when leaves become exposed to light.

To follow the influence of *U. maydis* on normal leaf development, we determined transcriptional alterations in infected and non-infected leaves at 5 consecutive time points. In non-infected leaves the most dramatic changes (1678 genes) occurred at the onset of photosynthesis (equivalent to one and two days post infection), affecting mostly genes involved in protein and RNA synthesis, primary metabolism and photosynthesis (Figures 2.2-2, 2.2-8; Table 2.2-S6; Figure 2.2-S2A). In comparison, expression of only 376 genes was changed in infected leaves (Table 2.2-S6; Figure 2.2-2). Notably, induction of photosynthesis-associated genes was strongly reduced in infected compared to non-infected leaves (Figures 2.2-S2A, B), indicating that normal development from sink to source tissue is impaired. At the same time, we observed significant changes in energy metabolism; both glycolysis and lipid metabolism were induced in tumours (Figure 2.2-4).

To elucidate which of the observed effects resulted from the absence of photosynthesis and which were caused by an active metabolic reprogramming induced by *U. maydis*, we compared transcript profiles of infected, non-infected and masked leaves (shielded from light for 6 days) of the same age (8 dpi).

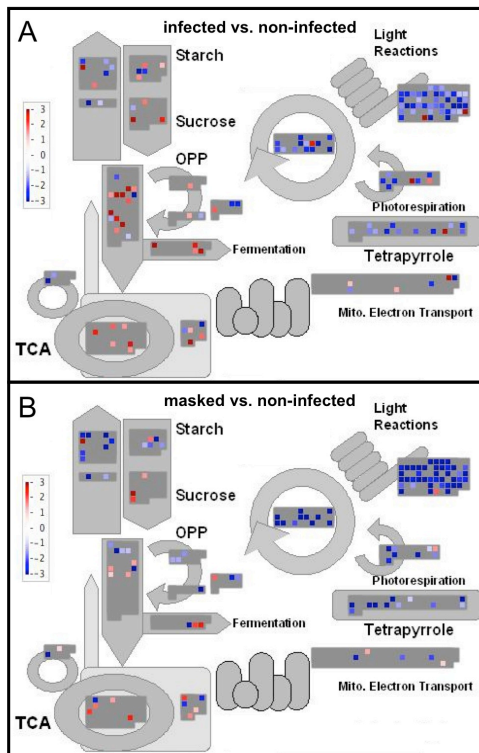


Figure 9: Transcriptional changes of genes related to primary metabolism in infected and masked leaves. Genes significantly up- and down-regulated are indicated in red and blue, respectively. Scale bars display log fold changes. (A) Differentially expressed genes involved in primary metabolism in tumour tissue 8 dpi compared to non-infected leaves. (B) Differentially expressed genes involved in primary metabolism in leaf tissue covered with aluminium foil for 6 days compared to non-infected leaves; time point corresponds to 8 dpi.

Induction of photosynthetic genes was absent in masked leaves when compared to non-infected leaves. Similarly, primary metabolism was down-regulated, with the exception of sucrose degradation that was found to be induced (Table 2.2-S7; Figure 2.2-9B). A comparable induction of sucrose degradation was observed in infected leaves (Figure 2.2-9A), which in addition showed transcriptional induction of glycolysis and TCA cycle (Figure 2.2-9A, Table 2.2-S2). Induction of genes for hexose degradation was significantly less pronounced in masked leaves compared to tumour tissue, indicating higher energy consumption in the infected cells (Figure 2.2-9).

Comparison of genes differentially regulated in masked leaves to genes differentially regulated in tumour tissue identified 958 genes as exclusively regulated upon *U. maydis* infection (Table 2.2-S7). Although the functional distribution within this group did not change dramatically when compared to all differentially expressed genes (Figure 2.2-2A), a significant enrichment of defence related genes was observed among the genes induced more than 100 fold at 8 dpi (34 of 67; Table 2.2-S7).

2.2.3 Discussion

We have analyzed changes in the maize transcriptome and metabolic changes in response to infection with the biotrophic pathogen *U. maydis*. We have focused on changes in distinct cellular processes, which were visualized by a novel version of the MapMan tool adapted to maize. We infer from our data that *U. maydis* is initially recognized and elicits plant defence reactions. With establishment of the biotrophic interaction, these initial responses are attenuated. Additionally, our data indicate that *U. maydis* interferes with normal leaf development and prevents the transition from sink to source leaves.

U. maydis Induced Defence Responses and Cell Death Suppression in Maize

The transient up-regulation of defence-associated genes in infected tissue suggests that *U. maydis* is recognized by the plant via conserved molecular patterns. The currently known PAMP receptors are LRR receptor kinases and receptor-like proteins with an extracellular LRR domain lacking a kinase domain. It has recently been shown that these PAMP receptors are transcriptionally up-regulated after elicitation (Zipfel *et al.*, 2004; Zipfel *et al.*, 2006). During the early phase of host colonization by *U. maydis*, we observed the up-regulation of two putative membrane bound LRR-like receptor kinases. The ortholog of one of them (Zm.10830.1) is induced in *Sorghum bicolor* after infection with the hemibiotrophic fungus *Colletotrichum graminicola* (Hipskind *et al.*, 1996). The second gene (Zm.8200.1) encodes a SER kinase and thus belongs to a group that includes BAK1, which has recently been shown to act as a positive regulator in infection-induced cell death signalling (Chinchilla *et al.*, 2007; Kemmerling *et al.*, 2007). We also observed an induction of Zm.12900.1, encoding a protein similar to a receptor like kinase from wheat, which is induced after infection with the rust fungus *Puccinia triticina* (Feuillet *et al.*, 2003). In analogy to these pathosystems, it is conceivable that the identified maize genes are involved in PAMP perception.

With the onset of biotrophy 24 hpi, defence responses were attenuated and concomitantly, we observed a transcriptional induction of JA signalling components. The observed induction of genes encoding cell death suppressors such as cystatins (Solomon *et al.*, 1999; Belenghi *et al.*, 2003) and Bax-inhibitor 1 (Eichmann *et al.*, 2004) as well as the repression of caspases suggest an interference of *U. maydis* with cell death regulation.

The phytopathogenic bacterium *P. syringae* interferes with programmed cell death by translocation of the effector-protein AvrPtoB into host cells (Rosebrock *et al.*, 2007). Similarly, several fungal Avr proteins have been shown to interact with their cognate R gene products in the cytoplasm of host cells (Jia *et al.*, 2000; Dodds *et al.*, 2006). Whether a similar mechanism is employed by *U. maydis* remains to be shown. In *U. maydis* novel secreted effectors have recently been shown to be important for virulence (Kämper *et al.*, 2006). However, it is currently unknown whether these effectors target apoplastic or cytoplasmic plant targets.

U. maydis Induced Changes in Hormone Signalling

Plant hormone signalling is dramatically changed in response to pathogen attack. In compatible interactions with necrotrophic pathogens, JA signalling plays a minor role, and instead, SA-dependent cell death responses and the expression of a large set of defence genes including PR1 are observed (Seo *et al.*, 2001). Biotrophic pathogens, on the other hand, induce JA and ethylene responses during compatible interactions. These responses do not lead to cell death and are associated with induction of tryptophan biosynthesis, the accumulation of secondary metabolites and the induction of plant genes encoding defensins (Brader *et al.*, 2001; Glazebrook, 2005; Wasternack, 2007). Consistently, after *U. maydis* infection, PR1 expression was undetectable at early time points. At later time points, low expression of PR1 was detected, which likely reflects a mixed response caused by a small fraction of infected plant cells undergoing necrosis.

Induction of JA signalling which antagonizes the SA pathway (Glazebrook, 2005) is detected immediately after infection. At the same time, activation of typical JA-responsive defence genes such as defensins, hevein-like proteins and chitinases is observed (Penninckx *et al.*, 1998; Thomma *et al.*, 1998; Glazebrook *et al.*, 2003). JA synthesis does not depend on the expression level of its biosynthetic genes, but on substrate availability of stored precursors (Wasternack, 2007). In line with this, we do not observe an induction of Zm.13677.1, a homologue to the *OPR7* gene from rice that has been shown to be essential for JA synthesis (Tani *et al.*, 2008).

U. maydis-induced tumours contain elevated auxin levels (Turian and Hamilton, 1960). Recently, it has been shown that auxin produced by *U. maydis* is unlikely to be important for tumour formation (Reineke *et al.*, 2008). We now demonstrate transcriptional induction of both auxin synthesis and -responsive genes during tumour

development, suggesting that cell enlargement observed in *U. maydis* induced tumours is caused by elevated levels of auxin produced by the plant. Recent studies in *A. thaliana* demonstrated repression of auxin signalling by SA (Wang *et al.*, 2007). SA-mediated repression of auxin levels leads to plant resistance, while inhibition of SA signalling allows auxin signalling, which, in turn, would promote fungal growth and host susceptibility. This is in agreement with the minor role of SA signalling in the maize/*U. maydis* interaction.

Antioxidants and Secondary Metabolites

The induction of GSTs by pathogens has been shown previously (Greenberg *et al.*, 1994; Hahn and Strittmatter, 1994; Levine *et al.*, 1994; Marrs, 1996) and has been reported to occur very rapidly, preceding the induction of PR genes (Mauch and Dudler, 1993; Alvarez *et al.*, 1998). Seven glutathione S-transferase genes (GSTs) were induced already 12 hpi. The antioxidative activity of GSTs has been proposed to reduce damage caused by pathogens, and to restrict cell death during HR (Mauch and Dudler, 1993). It is conceivable that some of the induced GSTs could be involved in scavenging oxygen radicals which result also from respiratory processes of the plant cell. Because it is not possible to implicate function or substrate specificity from the primary protein sequence (Wagner *et al.*, 2002), the specific functions of the GSTs regulated during the infection process has to remain speculative.

Although genes involved in glutathione synthesis (Glutathione synthetase, *gsh1*, Zm.3618.2 and glutamate-cysteine ligase, *gsh2*, Zm.9043.1) were not significantly regulated, glutathione contents were increased throughout infection. This could reflect the requirement for a higher antioxidative capacity in infected tissue, once the integrity of the photosynthetic apparatus is impaired in tumours. In addition, the enhanced glutathione levels could serve as a signal for defence gene induction, as it has been described for *A. thaliana* (Senda and Ogawa, 2004).

Our data revealed that genes involved in secondary metabolism are significantly enriched at all time points analyzed. In particular, we observed an induction of genes of the shikimate pathway, as well as a 20-fold increase in PAL activity and an accumulation of the primary pathway products phenylalanine and tyrosine. PAL catalyzes the committed step in the biosynthesis of phenolic secondary metabolites of the phenylpropanoid class (comprising hydroxycinnamic acid derivatives (HCAs),

lignans and flavonoids). In accordance, we detected an accumulation of HCA derivatives and anthocyanins.

HCA derivatives can serve as building blocks for lignin biosynthesis, and consistently, also genes involved in lignin and lignan synthesis were significantly induced during the late infection stages of *U. maydis*. This induction is likely to reflect the increased cell wall synthesis resulting from enhanced cell division and cell expansion within tumour tissue. In addition, *U. maydis* infected cells show enhanced cell wall epifluorescence, indicative of deposition of lignin and/or other phenolic compounds. Reinforcement of cell walls by phenolics has been shown to be part of a defence reaction against pathogens (Bruce and West, 1989; Nicholson and Epstein, 1991; Lange *et al.*, 1995; Huang and Hartman, 1998; Egea *et al.*, 2001). We hypothesize that this late response is also part of the mixed response discussed above where some cells elicit defence reactions while others do not.

In parallel to HCAs, we observe an accumulation of anthocyanins in tissues infected with *U. maydis*, coinciding with the induction of leucoanthocyanidin dioxygenase gene expression. Anthocyanin accumulation is part of the response towards a variety of biotic and abiotic stress situations such as pathogen attack, waterlogging, high light, salinity or cold stress, etc. (Chalker-Scott, 1999). Considering that *U. maydis* as a biotroph does not get in direct contact with the anthocyanins localized in the vacuole, it is likely that the accumulation is an indirect stress response caused by the fungus.

The induction of phenylpropanoid biosynthesis at late infection stages might reflect the increasing activity of the SA pathway at these time points and it is possible that some not yet described phenolic phytoalexins are produced along with then abundant phenolics. For instance, the hydroxamic acid DIMBOA, a derivative of the aromatic amino acid tryptophan and one of the known defence compounds in maize, has been described to be induced upon *U. maydis* infection, consistent with an increased expression of the gene for the initial biosynthesis step, Bx1 (Basse, 2005).

Likewise, isoprenoids serve as phytoalexins, which exhibit antimicrobial properties and are synthesized in response to pathogen attack (VanEtten *et al.*, 1994). Maize has probably a much smaller set of phytoalexins, when compared to other cereals as rice (Walton, 2001). Mining of public databases did not reveal any evidence for the key-enzymes for synthesis of polycyclic diterpenes, which is the major group of phytoalexins in rice. Nevertheless, induction of an ortholog of the *an2* gene indicates that *U. maydis* triggers phytoalexin synthesis throughout the entire infection process.

Photosynthesis and Primary Metabolism

U. maydis is known to infect young meristematic maize tissue, but is unable to infect differentiated source leaves (Wenzler and Meins, 1987). Between 1 and 2 dpi we observed a global induction of genes involved in light reaction, Calvin cycle, photorespiration, tetrapyrrole synthesis as well as sucrose and starch synthesis in non-infected leaves, which was not observed in infected leaves of the same age. This indicates that the transition from a juvenile sink tissue to a mature, photosynthetically active source tissue is blocked in infected leaves. This block is consistent with the recently described observation that *U. maydis* infected leaves are not able to establish C₄ metabolism, but continue to perform C₃ photosynthesis usually only observed in immature maize leaves (Horst *et al.*, 2008). In addition, *U. maydis* infection is associated with pronounced chlorosis, and, concomitantly, with a decline in chlorophyll content and reduced CO₂ assimilation rates of infected leaf tissue (Horst *et al.*, 2008).

In infected leaves, about 60% of the differentially expressed genes can be attributed to the down-regulation of the photosynthetic apparatus, as shown by comparison to masked leaves. Induction of sucrose degradation and reduction of sucrose synthesis was observed in infected and masked tissues, indicating that both rely on sucrose import from photosynthetic-active source tissues. Alterations specific for infected tissue comprise the induction of glycolysis and TCA cycle, which might indicate either an elevated flux of carbon skeletons into amino acid biosynthesis or an increased respiration of infected maize cells.

The increase in free hexose content found in tumours is typical for a sink tissue. It is likely that the developing tumour itself generates a sink through active proliferation. The free hexoses within tumour cells then could be used by *U. maydis* as easily accessible carbon source. This strategy is in strict contrast to powdery mildew infections, where leaves remain source tissues (Scholes *et al.*, 1994; Walters and McRoberts, 2006). In this case, the fungus acquires nutrients via haustoria from single epidermis cells, leaving the physiological state of the entire leaf largely unaltered. Based on the presented results, the key questions are how nutrients are partitioned between *U. maydis* and host cells and to which extent the host metabolism is actively reprogrammed by fungal effectors. For a more comprehensive understanding of these processes, detailed analysis of single, *U. maydis* infected cells instead of complex infected tissues will be one of the major challenges for future research.

2.2.4 Experimental Procedures

Fungal strains and Growth Conditions

U. maydis SG200 (Kämper *et al.*, 2006) and its derivative SG200 Potef::2xRFP expressing cytoplasmic RFP (Fuchs *et al.*, 2006) were grown at 28°C in YEPS light medium (Tsukuda *et al.*, 1988) and used in plant infections as described (Gillissen *et al.*, 1992).

Microscopy

U. maydis hyphae were stained with WGA-AF 488 (Molecular Probes, Karlsruhe, Germany). Plant membranes were visualized using FM4-64 (Invitrogen, Karlsruhe, Germany): Samples were incubated in staining solution (4µg/ml FM4-64, 10µg/ml WGA-AF 488; 0.02% Tween20) for 30 min and washed in 1x PBS (pH 7.4). Confocal images were recorded on a TCS-SP5 confocal microscope (Leica, Bensheim, Germany); FM4-64: excitation: 561-nm and detection at 600-700 nm; WGA-AF 488: excitation 488 nm and detection at 500-540 nm. Autofluorescence of cell wall material was excited at 405 nm and detected at 415-460 nm. For RFP fluorescence of hyphae in maize tissue, an excitation of 561 nm and detection at 580-630 nm was used.

Plant Material and RNA Preparation

For *U. maydis* infections, maize plants (Early Golden Bantam) were grown in a phytochamber in a 15 h/9 h light-dark cycle; light period started/ended with 1h ramping of light intensity. Temperature was 28°C and 20°C, relative humidity 40% and 60% during light and dark periods, respectively, with 1 h ramping for both values. Plantlets were individually sown in pots with potting soil (Fruhstorfer Pikiererde, Lauterbach, Germany) and infected 7 days after sowing 1 h before end of the light period, as described (Brachmann *et al.*, 2001); plants for 12 hpi samples were infected during the beginning of the light period. For three independently conducted experiments (biological replicates), samples used for both RNA preparation and metabolite measurements were collected 1 h before the end of the light period and directly frozen in liquid nitrogen. For each experiment, 30 plants were sampled and divided for the 12 hpi to 48 hpi samples into 3 subsets, for all other samples into 4 subsets, respectively. Metabolite analysis was carried out independently for all these

subsets, i.e. technical replicates. For RNA isolation, material from the subsets was pooled and ground in liquid nitrogen. RNA was extracted with Trizol (Invitrogen, Karlsruhe, Germany) and purified using an RNeasy kit (Qiagen, Hilden, Germany).

DNA Microarray and Verification by Quantitative Real-Time PCR

Affymetrix Gene chip^R maize genome arrays were done in three biological replicates, using standard Affymetrix protocols (Midi_Euk2V3 protocol on GeneChip Fluidics Station 400; scanning on Affymetrix GSC3000). Expression data were submitted to GeneExpressionOmnibus (<http://www.ncbi.nlm.nih.gov/geo/>), Accession Number GSE10023. Data analysis was performed using Affymetrix Micro Array Suite 5.1, bioconductor (<http://www.bioconductor.org/>) and dChip1.3 (<http://biosun1.harvard.edu/complab/dchip/>), as described (Eichhorn *et al.*, 2006). We considered changes >2-fold with a difference between expression values >100 and a corrected p-value <0.001 as significant. For pathway analysis we used the MapMan tool optimized for maize. Expression changes in Mapman pathways were filtered by a p-value <0.001.

To verify microarray results, selected genes were analyzed by qRT-PCR (Table 2.2-S9). For cDNA synthesis, the SuperScript III first-strand synthesis SuperMix assay (Invitrogen, Karlsruhe, Germany) was employed, using 1 µg of total RNA. qRT-PCR was performed on a Bio-Rad iCycler using the Platinum SYBR Green qPCR SuperMix-UDG (Invitrogen, Karlsruhe, Germany). Cycling conditions were 2 min 95°C, followed by 45 cycles of 30 sec 95°C / 30 sec 61°C / 30 sec 72°C. Primer sequences are listed in Table 2.2-S10.

Metabolite Analysis

Amino acids were extracted in 80% ethanol and determined by HPLC after derivatization with 6-aminoquinolyl-N-hydroxysuccinimidyl carbamate as described in Cohen and Michaud (1993). Soluble carbohydrates and starch were determined from the same extract by coupled enzymatic assays as described (Bergmeyer; Cohen and Michaud, 1993; Voll *et al.*, 2003). Small thiols were extracted with 0.1 M HCl and quantified after derivatization with monobromobimane by HPLC (Summit Series, Dionex Corp., Sunnyvale, USA; equipped with a Luna 5u C18(2) column, Phenomenex Ltd., Aschaffenburg, Germany and a Dionex RF2000 fluorescence

detector). Separation of thiols was achieved with an isocratic mixture of 89% 100 mM potassium acetate, pH 5.5 and 11% methanol; detection was performed at 380 nm after excitation at 480 nm. Shikimate was extracted with perchloric acid (Häusler *et al.*, 2000) and isolated by ion exchange chromatography using a Dionex IonPac AG11-HC (2 x 50mm) precolumn and two Dionex IonPac AS11-HC (2 x 250mm) columns on a Dionex ICS3000 system using a KOH step gradient (0 to 100 mM). The eluate was passed on to a mass spectrometer (API3200 Q-trap tandem MS, Applied Biosystems, Foster City, USA) and shikimate was detected and quantified by the transition $m/z = 173$ to $m/z = 93$ in the negative ion mode relative to standards.

To determine the total content of phenolics, A_{534} , A_{310} and A_{290} were measured spectrophotometrically in perchloric acid extracts (see above) and in 80% methanol extracts of the perchloric acid insoluble material to account for water soluble and water insoluble derivatives, respectively. The absorptions of both extracts were normalized to fresh weight and added to yield total content of phenolics.

PAL Activity

Leaf material was homogenized in extraction buffer (100 mM borate, pH 8.8, 0.1 mM PefaBloc, 5 mM β -mercaptoethanol, insoluble PVP) and incubated for 30 min on ice. After sonification for 30 s, the soluble fraction was desalted using Sephadex G25 columns, and protein content was determined (Zor and Selinger, 1996) for normalization of activity. PAL activity was assayed in a buffer containing 240 μ L of a 100 mM L-phenylalanine solution, 80 μ L extract and 80 μ L 0.2 M borate buffer, pH 8.8. The increase in released *trans*-cinnamic acid was monitored for 1 h at 290 nm and quantified using a standard curve.

2.2.5 Supplementary Information

Files containing the Supplementary Material of section 2.2 are available on data-CD deposited in section 5 of this thesis. The files include Figures 2.2-S1 and S2 and Tables 2.2-S1 to S10.

Figure 2.2-S1: MapMan: Lignin biosynthesis 8 dpi.

Figure 2.2-S2: MapMan: Genes regulated during sink to source transition.

Table 2.2-S1: Functional categories of maize genes regulated upon *U. maydis* infection

Table 2.2-S2: Maize-genes with significant changes in expression in response to *U. maydis* infection.

Table 2.2-S3: PR-like genes on the Affymetrix maize gene chip.

Table 2.2-S4: Regulated genes involved in cell death regulation.

Table 2.2-S5: Regulated genes associated to "hormone metabolism".

Table 2.2-S6: Genes regulated during sink to source transition.

Table 2.2-S7: Influence of photosynthesis on gene regulation in *U. maydis* infected leaves.

Table 2.2-S8: Genes involved in the shikimate pathway depicted in Figure 7.

Table 2.2-S9: Verification of microarray results by qRT-PCR.

Table 2.2-S10: Primers used for qRT-PCR.

Acknowledgements

We are grateful to the Bioanalytics Group, Department of Biochemistry, FAU Erlangen-Nuremberg for the assistance in IC-MS analysis. We thank Dr. Olga Levai (Leica Microsystems GmbH, Wetzlar, Germany) for expert technical advice with confocal microscopy. This work was supported by the DFG priority program FOR666.

2.3 A Novel High Affinity Sucrose Transporter is Required for Fungal Virulence and Avoids Extracellular Glucose Signaling in Biotrophic Interactions

Ramon Wahl,^{1,2+} Kathrin Wippel,³⁺ Jörg Kämper,^{1,2*} and Norbert Sauer^{3*}

¹ University of Karlsruhe, Institute of Applied Biosciences, Department of Genetics, Hertzstrasse 16, D-76187 Karlsruhe, Germany.

² Max Planck Institute for terrestrial Microbiology, Karl von Frisch Straße, D-35043 Marburg, Germany

³ Friedrich-Alexander-University Erlangen-Nürnberg, Molekulare Pflanzenphysiologie, Staudtstrasse 5, D-91058 Erlangen, Germany.

+ These authors contributed equally to this work.

* To whom correspondence should be addressed.

E-mails: nsauer@biologie.uni-erlangen.de (N.S.) and joerg.kaemper@kit.edu (J.K.).

Running Head: Sucrose transport and fungal biotrophy

Keywords: biotrophic fungus, major facilitator superfamily, Srt1, sucrose transport, *Ustilago maydis*

Summary

Plant pathogenic fungi cause massive yield losses and affect both quality and safety of food and feed produced from infected plants. The main objective of plant pathogenic fungi is to get access to the organic carbon sources of their carbon-autotrophic hosts. However, the chemical nature of the carbon source(s) and the mode of uptake are largely unknown. Here we present a novel, plasma membrane-localized sucrose transporter (Srt1) from the corn smut fungus *Ustilago maydis* and its characterization as a fungal virulence factor. Srt1 has an unusually high substrate affinity, is absolutely sucrose-specific, and allows the direct utilization of sucrose at the plant/fungal interface without extracellular hydrolysis; thus, without the production of extracellular monosaccharides known to elicit plant immune responses. *srt1* is expressed exclusively during infection, and its deletion strongly reduces fungal virulence. This emphasizes the central role of Srt1 both for efficient carbon supply and for avoidance of apoplastic signals potentially recognized by the host.

2.3.1 Introduction

Plant pathogenic fungi cause major yield losses and affect the quality and safety of food and feed produced from infected plant material. Different fungi have developed different strategies to deal with their hosts. Infected plants are either kept alive to ensure a prolonged supply of organic carbon and other compounds to the pathogen (biotrophic fungi), or they are destroyed and the pathogen feeds on dead or dying plant tissue (necrotrophic fungi). Other fungi start their infections as biotrophs and switch to necrotrophic behavior at later stages of infection or under certain environmental conditions (hemi-biotrophic fungi). Recognition of such pathogens by infected plants typically results in the production of reactive oxygen species (ROS) and in hypersensitive cell death (HR) (Glazebrook, 2005). Obviously, plant defense responses resulting in HR are very effective against biotrophic fungi, whereas necrotrophic pathogens might even benefit from host cell death. Therefore, plants use different defense responses for biotrophic or necrotrophic fungi (Glazebrook, 2005; Kliebenstein and Rowe, 2008). The most important challenge for all pathogens is the development of strategies allowing the avoidance of signals potentially recognized by the host.

The basidiomycete *Ustilago maydis* is a ubiquitous pathogen of maize (*Zea mays*), one of the world's most important cereal crops (Martinez-Espinoza *et al.*, 2002). As a biotrophic fungus, *U. maydis* depends on living plant tissue and, therefore, does not use aggressive virulence strategies (Mendgen and Hahn, 2002). During the infection process, fungal hyphae traverse plant cells without eliciting apparent host defense responses, a prerequisite for successful infection and the persistent growth and development of a biotroph on its living host. *U. maydis* hyphae invaginate the plasma membranes of invaded plant cells, resulting in narrow contact zones that are perfectly suited for the uptake of organic carbon by the fungus (Bauer *et al.*, 1997). Infections with *U. maydis* lead to the formation of tumors that consist of proliferating plant cells and of fungal hyphae (Figures 2.3-1A and 1B). Comparisons of transcript and metabolite levels in *U. maydis*-infected with none-infected maize leaves revealed an inhibition or delay in the sink-to-source transition of infected leaves (Horst *et al.*, 2008; Doehlemann *et al.*, 2008b), which is in line with the increased carbon demand of the forming tumor.

So far all transport proteins identified in symbiotic or pathogenic fungus/plant interactions are specific for monosaccharides (Voegelé *et al.*, 2001; Schüssler *et al.*, 2006; Polidori *et al.*, 2007) and catalyze the uptake of glucose or fructose and, to a

lesser extent, of other hexoses. It was speculated that these hexose transporters act in combination with fungal and/or plant-derived cell wall invertases to supply the pathogen with carbohydrates derived from extracellular sucrose hydrolysis. The impact of these transporters on the development of fungal pathogens within the host plant has never been proven. However, plants have evolved mechanisms to sense extracellular (apoplastic) changes in glucose concentrations, e.g. produced from extracellular sucrose hydrolysis, and to respond to these changes with the induction of defense responses (Herbers *et al.*, 1996b; Ehness *et al.*, 1997; Schaarschmidt *et al.*, 2007; Kocal *et al.*, 2008). Thus, feeding strategies avoiding invertase-derived glucose production in the apoplast might be advantageous especially for biotrophic fungi.

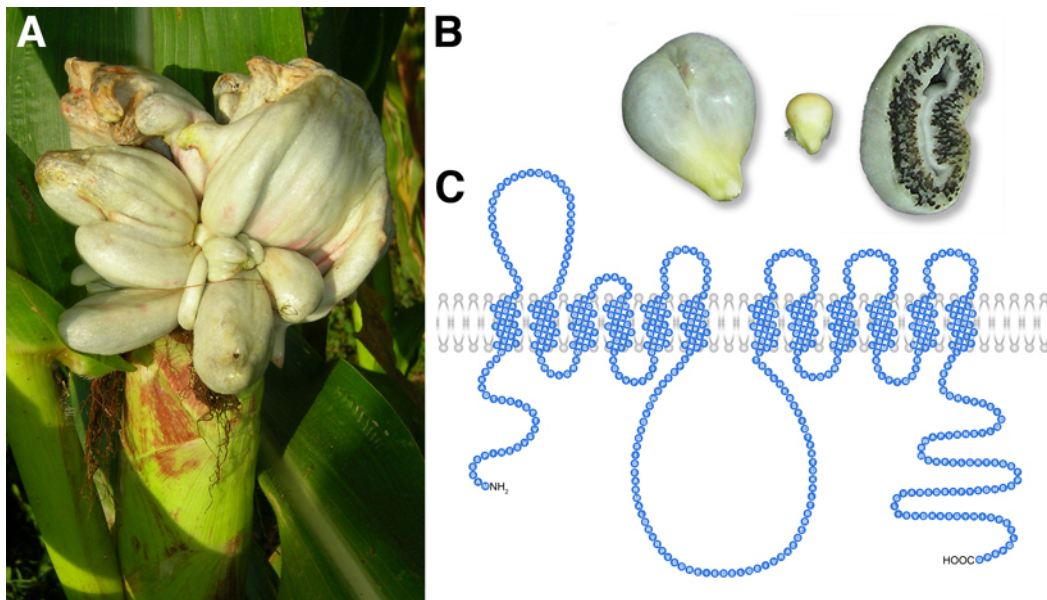


Figure 2.3-1: *U. maydis*-induced tumor formation in maize and predicted structure of Srt1. (A) Ear tumors of a maize plant infected with *U. maydis* that caused tumor induction. (B) Uninfected (left) and *U. maydis*-infected, tumorous (middle) maize kernels, plus a tumor section (right) showing layers of black fungal teliospores. (C) Putative topology of Srt1.

Here we present the identification and functional characterization of Srt1, a novel high affinity, sucrose-specific transporter from the biotroph *U. maydis*. We show that Srt1 represents a virulence factor essential for successful development of the fungus within its host, as infection of maize with $\Delta srt1$ strains results in strongly reduced disease symptoms. The successful infection of maize by *U. maydis* without inducing defense responses is likely to result from efficient competition for apoplastic sucrose by the *U. maydis* Srt1 protein with the low-affinity plant sucrose transporters, and from the avoidance of apoplastic glucose signaling.

2.3.2 Results

To address the relevance of sugar transporters for biotrophic development in *U. maydis*, we generated strains deleted for individual hexose transporters or hexose transporter-like proteins and assayed them for symptom development after syringe inoculation into young corn seedlings. Out of a total of 19 genes encoding hexose transporter-like proteins in the *U. maydis* genome (Figure 2.3-S1; Kämper *et al.*, 2006), two were identified to influence the virulence of *U. maydis*. Here we report the characterization of one of these genes (*um02374*, MIPS *Ustilago maydis* database, <http://mips.gsf.de/genre/proj/ustilago/>) that was named *srt1* after functional characterization of the encoded protein (Figure 2.3-1C) as sucrose transporter.

Deletion of srt1 Reduces Virulence of U. maydis, but Does Not Affect Plant Colonization or Fungal Growth on Axenic Media

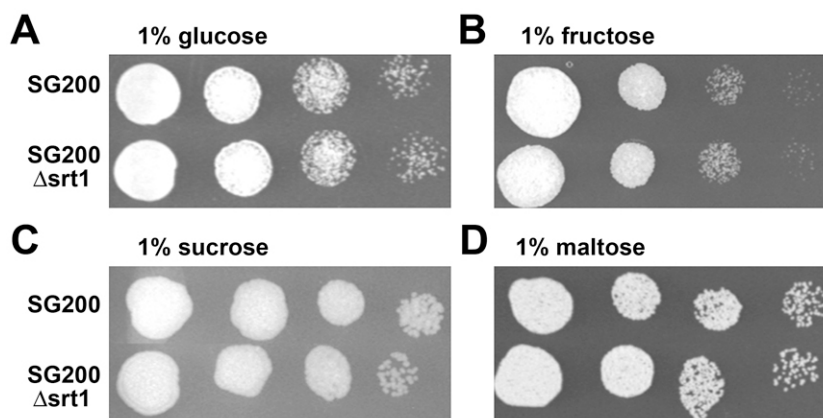


Figure 2.3-2: *srt1* deletion does not affect *U. maydis* growth in axenic culture. Growth of SG200 Δ *srt1* on glutamine minimal media containing the monosaccharides (A) glucose or (B) fructose or the disaccharides (C) sucrose or (D) maltose is not reduced compared to the wild type strain SG200. Cultures from liquid glutamine minimal medium (1% glucose) were spotted in a series of 10-fold dilutions on the media indicated.

Compared to the progenitor strain SG200, a solopathogenic strain that can infect corn plants without a mating partner (Kämper *et al.*, 2006), *U. maydis* strains deleted for *srt1* (SG200 Δ *srt1*) did not show altered growth on agar media supplemented with different carbon sources (Figure 2.3-2A to 2D). This is in line with the observation that *srt1* is not expressed under these conditions (Figure 2.3-3D). Moreover, *srt1* expression is not induced on medium without any carbon source, demonstrating that it is not regulated by catabolite repression. In contrast, growth of wild type *U. maydis* *in planta* results in a rapid and strong expression of *srt1* (Figure 2.3-3D). Expression

peaks at 4 days post infection (dpi) when most hyphae have reached the vascular bundles to spread inside the plant and when tumor formation is initiated. During earlier stages of infection only weak expression of *srt1* was observed (Figure 2.3-3D). This suggests that plant-derived signals are needed for *srt1* expression.

Plant infection experiments with SG200 and SG200 Δ *srt1* revealed major differences. While infections with SG200 caused massive tumor formation (Figures 2.3-3A and 3C), infection with SG200 Δ *srt1* resulted only in marginal disease symptoms. In most cases, infected plants showed no or only minute tumors (Figures 2.3-3B and 3C). With respect to tissue colonization, SG200 Δ *srt1* hyphae did not differ from SG200 hyphae at the different developmental stages during disease progression (Figure 2.3-S2).

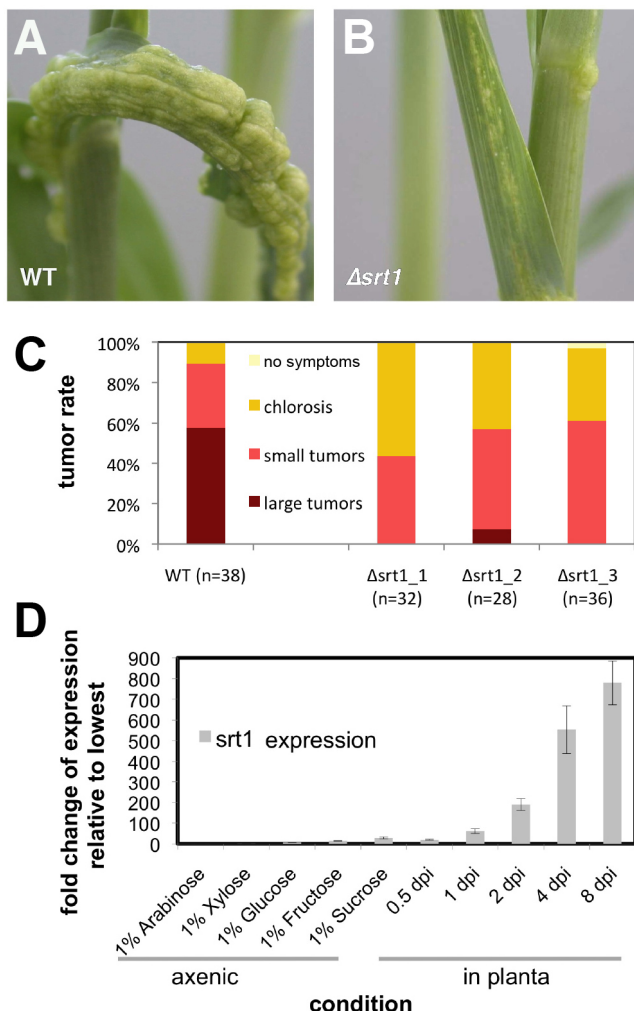


Figure 2.3-3: Srt1 is necessary for pathogenic development of *U. maydis*.

(A) Tumor development on maize leaves infected with fungal wild type strain SG200 at 7 dpi. (B) Symptom development on maize leaves infected with SG200 Δ *srt1* at 7 dpi. (C) Disease rating of plants infected with the wild type strain SG200 and three independent SG200 Δ *srt1* deletion mutants at 7 dpi. Percentage of plants showing large tumors, small tumors, or only chlorosis are color-coded (n = total number of plants analyzed). (D) Expression profile (real time PCR) of *srt1* in SG200 grown on agar media supplemented with different carbon sources (left) or on plant tissue at different time points after infection. Gene expression was normalized to the expression of the constitutively expressed genes *actin* and *eIF2B*. Changes in *srt1* expression are displayed relative to the lowest expression value (dpi = days post infection). Error bars indicate the standard deviations of mean expression values.

Srt1 is an Energy-dependent, Sucrose-specific Transporter of the Fungal Plasma Membrane

The intron-less *srt1* gene encodes for a protein of 546 amino acids. Srt1 has 12 predicted transmembrane domains (TMDs; Sonnhammer *et al.*, 1998) and a large extracellular loop between TMD1 and TMD2 (Figure 2.3-1C), a typical structural feature of previously characterized fungal and plant hexose transporters (Schüssler *et al.*, 2006; Büttner and Sauer, 2000). Sequence comparison revealed a moderate similarity (less than 30% identity) of Srt1 to a large group of transport proteins (Figure 2.3-S3) that includes numerous well-characterized high-affinity monosaccharide transporters from plants and fungi as well as some low-affinity maltose transporters from *Saccharomyces cerevisiae* (Cheng and Michels, 1991; Stambuk *et al.*, 1999; Alves *et al.*, 2008), *Pichia angusta* (synonym: *Hansenula polymorpha*; Viigand *et al.*, 2005) or *Schizosaccharomyces pombe* (Reinders and Ward, 2001). Phylogenetic analyses revealed that Srt1 is most closely related to a small group of so far uncharacterized proteins (Figure 2.3-S3). This group contains uncharacterized transporters from different *Aspergillus* species (up to 47% identity) and from two biotrophic relatives of *U. maydis*, *Sporisorium reilianum* (88% identity) and *Ustilago hordei* (81% identity).

To functionally characterize Srt1, the gene was expressed in the monosaccharide transport-deficient *S. cerevisiae* strain EBY.VW4000 (Wieczorke *et al.*, 1999), and uptake was analyzed with radiolabeled putative substrates (D-glucose, D-fructose, D-ribose, D-xylose, D-galactose, mannitol, sorbitol, xylitol, *myo*-inositol). As Srt1 did not catalyze the uptake of any of these compounds, additional tests were performed with ¹⁴C-sucrose and ¹⁴C-maltose. However, as yeast strain EBY.VW4000 encodes an extracellular invertase that slowly hydrolyzes extracellular sucrose, these Srt1 studies had to be performed in the invertase-deficient yeast strain SEY2102 (Emr *et al.*, 1983). In fact, transport activity could be measured with ¹⁴C-sucrose (Figure 2.3-4A), but no uptake was observed for ¹⁴C-maltose (Figure 2.3-S4).

In competition analyses with an excess of unlabeled maltose (an alternative substrate of plant sucrose transporters), trehalose (an alternative substrate of yeast maltose transporters), raffinose (an alternative substrate of the sucrose-hydrolyzing enzyme invertase), or sucrose (as positive control), raffinose was the only alternative compound that caused a minor inhibition of sucrose uptake (Figure 2.3-4B). No transporter described so far, not even the very well characterized sucrose

transporters from higher plants (Sauer, 2007), showed such an extreme specificity for the disaccharide sucrose.

In fungi, sucrose transport activities were so far only described as side activities of maltose or maltotriose transporters with broad specificity and low affinity (Reinders and Ward, 2001; Stambuk *et al.*, 2000). In uptake analyses in *S. cerevisiae* and with wide range of different sucrose concentrations, the K_M of Srt1 for sucrose was found to be $\sim 25 \mu\text{M}$ (Figure 2.3-4C). Thus, the affinity of Srt1 for sucrose is several hundred-fold to several thousand-fold higher than that of fungal maltose/maltotriose transporters (Reinders and Ward, 2001; Stambuk *et al.*, 2000). Moreover, its affinity is also much higher than that of higher plant sucrose transporters (50-fold to 100-fold), which catalyze sucrose uptake with K_M -values in the millimolar range (Viigand *et al.*, 2005).

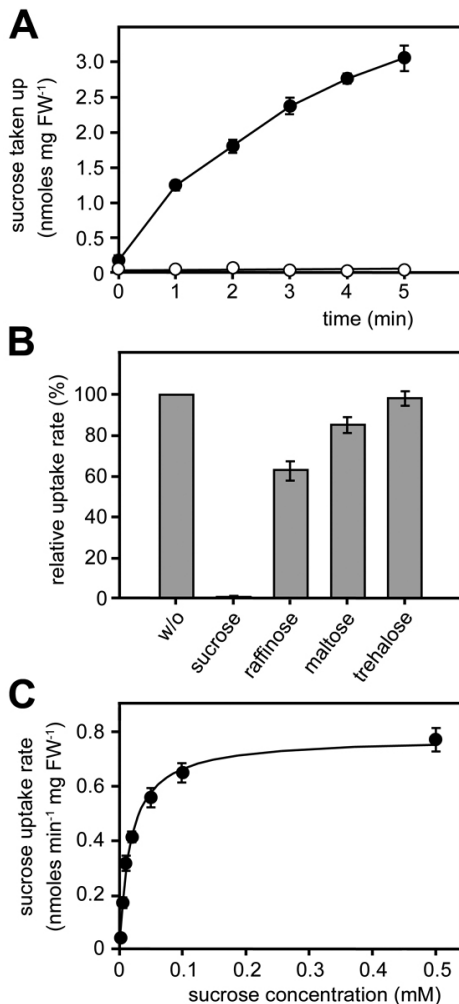


Figure 2.3-4: Srt1-dependent ¹⁴C-sucrose uptake in *S. cerevisiae*. (A) Uptake of ¹⁴C-sucrose by *srt1*-expressing (closed circles) and control cells (open circles). (B) Competition analysis (0.1-mM ¹⁴C-sucrose) with different potential substrates added at 100-fold molar excess. (C) Michaelis-Menten kinetics of sucrose uptake rates (pH 5.0) indicate a K_M of $\sim 25 \mu\text{M}$. Error bars represent standard error ($n = 3$).

For the yeast strain SEY2102, D-glucose represents the primary carbon source that can be both imported and metabolized. In contrast, sucrose can be imported when *srt1* is expressed, but it cannot be hydrolyzed, as the strain is invertase deficient (Emr *et al.*, 1983). If, however, sucrose uptake by Srt1 is energy-dependent, the available energy might be limiting and the determined sucrose transport rates might be sub-maximal. The simultaneous presence of ^{14}C -sucrose and glucose as metabolizable energy source strongly enhanced sucrose uptake (Figure 2.3-5A), which is indicative for an energy-dependent transport. In addition to this glucose-enhanced sucrose uptake, both the clear optimum of Srt1-driven sucrose transport at acidic pH values (Figure 2.3-5B) as well as the sensitivity to the protonophore carbonylcyanide *m*-chlorophenylhydrazone (CCCP; Figure 2.3-5C) underline that Srt1 is an active, energy-dependent H^+ -symporter.

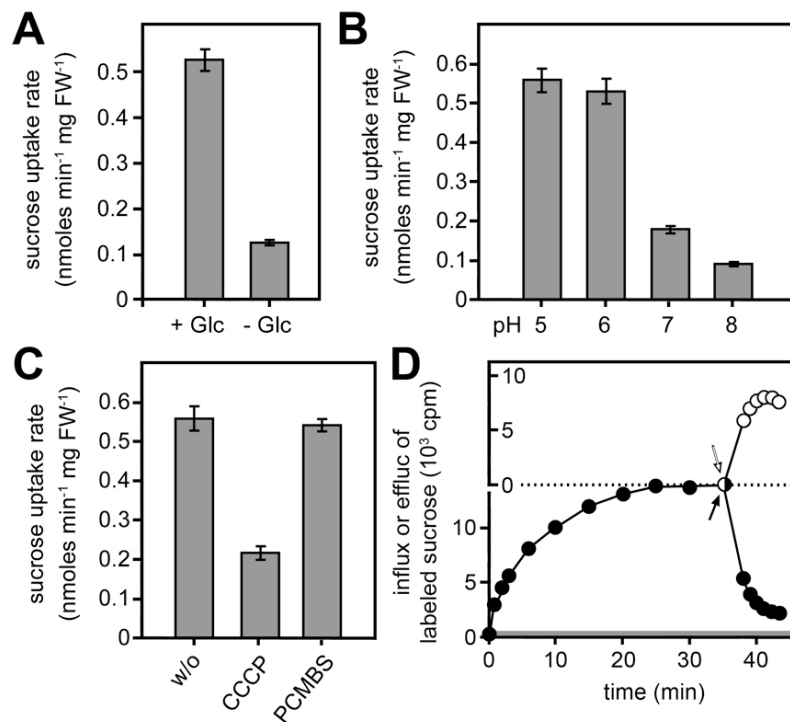


Figure 2.3-5: Transport characteristics of Srt1. (A) Transport is activated in the presence of the metabolizable carbon source glucose. (B) The pH-optimum for sucrose uptake by Srt1 is in the acidic pH range. (C) Sucrose uptake is sensitive to the protonophore CCCP, but not to the SH-group inhibitor PCMBs. (D) The plateau of sucrose accumulation in baker's yeast results from an equilibrium of influx and efflux. Black symbols show the uptake of ^{14}C -labeled sucrose and the onset of an immediate efflux, after replacement of labeled extracellular sucrose by unlabeled sucrose (black arrow). The grey region at the bottom of the graph shows the amount of sucrose that was sufficient to reach a concentration equilibrium of ^{14}C -sucrose between the medium and the cell interior. White symbols show the onset of an immediate influx of ^{14}C -labeled sucrose in an identical experiment that was started with unlabeled sucrose. The white arrow indicates the replacement of unlabeled extracellular sucrose by ^{14}C -labeled sucrose. One of three experiments with identical results is presented. Error bars in (A) to (C) represent standard error ($n = 3$).

Expression of *srt1* in a yeast strain (DBY2617) that possesses a cytoplasmatic but no secreted invertase (Carlson *et al.*, 1981) enabled this strain not only to import ^{14}C -sucrose, but also to grow efficiently on sucrose as sole carbon source (Figure 2.3-S5). This proves that Srt1 activity alone is sufficient to meet the carbon import requirements of these cells. Thus, Srt1 is a high affinity, high capacity transporter that catalyzes the uptake of sufficient sucrose to fuel the growth of fungal cells.

Additional analyses of the subcellular localization in *S. cerevisiae* with a functional Srt1::GFP fusion protein demonstrated that, as expected from the transport tests (Figures 2.3-4 and 5) and complementation analysis (Figure 2.3-S5), Srt1::GFP localizes exclusively to the plasma membrane (Figure 2.3-6).

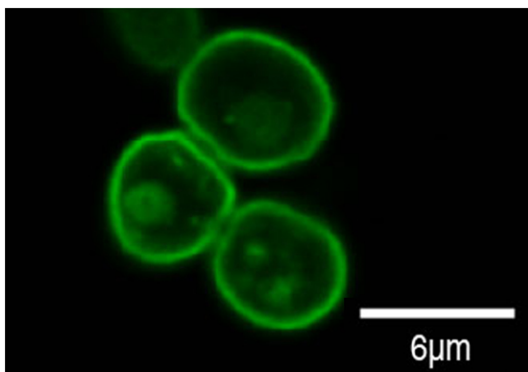


Figure 2.3-6: Subcellular localization of Srt1 in *S. cerevisiae*. A functional Srt1::GFP fusion protein expressed in *S. cerevisiae* cells is localized specifically in plasma membranes (see Experimental Procedures).

Srt1 Differs from Plant Sucrose Transporters in Two Functional Aspects

The primary physiological functions of plant sucrose transporters are the loading of sucrose into the phloem or the loading of sucrose into storage vacuoles, two processes that depend on the accumulation of high sucrose concentrations on one side of the respective membrane (Sauer, 2007). Uptake beyond a certain maximum is subject to feed back inhibition and total inactivation of sucrose transport. These activities of plant sucrose transporters can be inhibited very specifically by the SH-group inhibitor *p*-chloro-mercuribenzenesulfonate (PCMBS) that does not affect plant hexose transporters (M'batchi and Delrot, 1984). The specificity of this inhibitor is so high that sucrose fluxes and phloem loading can be inhibited by PCMBS in whole plant or in intact plant tissues (Turgeon and Gowan, 1990).

In contrast, Srt1 is a transporter that imports sucrose for immediate consumption, thus high intracellular concentrations of sucrose in *U. maydis* are unlikely to occur. In invertase-deficient *srt1*-expressing *S. cerevisiae* cells, however, imported sucrose is not hydrolyzed, and Srt1 accumulates sucrose to concentrations higher than in the extracellular medium (more than 60-fold higher in Figure 2.3-5D). In contrast to plant

sucrose transporters, the resulting plateau does not result from feed back (“shut-off”) inhibition of sucrose uptake, but rather from an equilibrium of sucrose influx and sucrose efflux, a typical property of transporters that do not accumulate their substrates under physiological conditions (Komor *et al.*, 1972; Eddy, 1982).

Finally, in accordance with its closer phylogenetic similarity to plant and fungal hexose transporters, and unlike to sucrose transporters described in numerous plant species, Srt1 is also insensitive to PCMBS (Figure 2.3-5C). In summary, Srt1 appears to be the prototype of a novel sucrose transporter that is unique with regards to its high specificity and its high affinity for sucrose, and that differs significantly in its functional behavior from sucrose transporters of higher plants.

2.3.3 Discussion

The basidiomycete *U. maydis* is a biotrophic fungus that feeds on photoassimilated carbohydrates of maize to promote extensive fungal proliferation within the plant (Figure 2.3-1). Deletion analyses of genes encoding sugar transporter-like proteins in *U. maydis* led to the identification of *srt1*. Under axenic growth conditions on different carbon sources, including sucrose (Figure 2.3-3C), this gene is not or only weakly expressed. Infection of maize tissue, however, causes a rapid induction of *srt1* expression (Figure 2.3-3C) that peaks at 4 dpi, when tumor formation is initiated. In agreement with these expression data, deletion of *srt1* neither affects axenic growth (Figure 2.3-2) nor the colonization of infected plants (Figure 2.3-S2), but it results in strongly reduced symptom formation at later stages of biotrophic development (Figures 2.3-3A to 3C).

Functional analyses in different *S. cerevisiae* strains characterized Srt1 as a plasma membrane-localized (Figure 2.3-6), energy-dependent (Figure 2.3-5), high affinity (Figure 2.3-4C) sucrose transporter with unusually narrow substrate specificity (Figures 2.3-4B and S4). *S. cerevisiae* cells expressing *srt1* do grow on sucrose as sole carbon source if they possess a cytoplasmatic invertase (Figure 2.3-S5), or they accumulate sucrose to high intracellular concentrations if this invertase is deleted (Figure 2.3-5D). This demonstrates that Srt1 is also a high capacity transporter that supplies rapidly growing fungal cells with carbon skeletons necessary for energy production and metabolism.

Fungal sucrose transporters with comparable kinetic properties and transport characteristics have so far not been cloned or characterized. *S. cerevisiae* has transporters that accept several α -glucosides, including maltose, trehalose, maltotriose, melezitose, α -methylglucoside and sucrose. However, these transporters have K_M -values for sucrose between 8 and 120 mM (Stambuk *et al.*, 2000). Moreover, transporters with K_M -values in this concentration range have to compete with the yeast extracellular invertase that hydrolyzes sucrose with a K_M that is also in the millimolar range.

In contrast to all of these transporters, Srt1 transports sucrose with high specificity and with an unusually low K_M . The presented data demonstrate that the uptake of sucrose by Srt1 is not a possible side activity of this protein, but rather its only and exclusive function and that Srt1 activity is essential to develop full virulence of *U. maydis*.

Srt1 Enables *U. maydis* to Feed on Apoplastic Sucrose without Extracellular Hydrolysis

The primary long-distance transport and storage form of assimilated carbon in most higher plants, including maize, is sucrose. Apoplastic sucrose concentrations were determined in several dicotyledonous plants and are typically in the low-millimolare range (Nadwodnik and Lohaus, 2008). Thus, a transporter with the properties of *Srt1* represents a perfect tool of a biotrophic fungus that resides the major part of its life cycle in the extracellular space of a living plant. The specificity and extremely high affinity of this transporter enables the pathogen to compete efficiently and successfully with the adjacent host cells for sucrose at the plant/fungus interphase (Figure 2.3-7). *Srt1* is perfectly suited to out-compete both the plants sucrose transporters (SUC or SUT proteins; Sauer, 2007) with their comparatively low substrate affinities as well as the plants invertase (INV)/monosaccharide transporter (STP) system that is used to feed certain plant sink tissues (Figure 2.3-7; Sonnhammer *et al.*, 1998). Like plant sucrose transporters, plant extracellular invertases have K_M -values in the millimolar range (Roitsch and González, 2004).

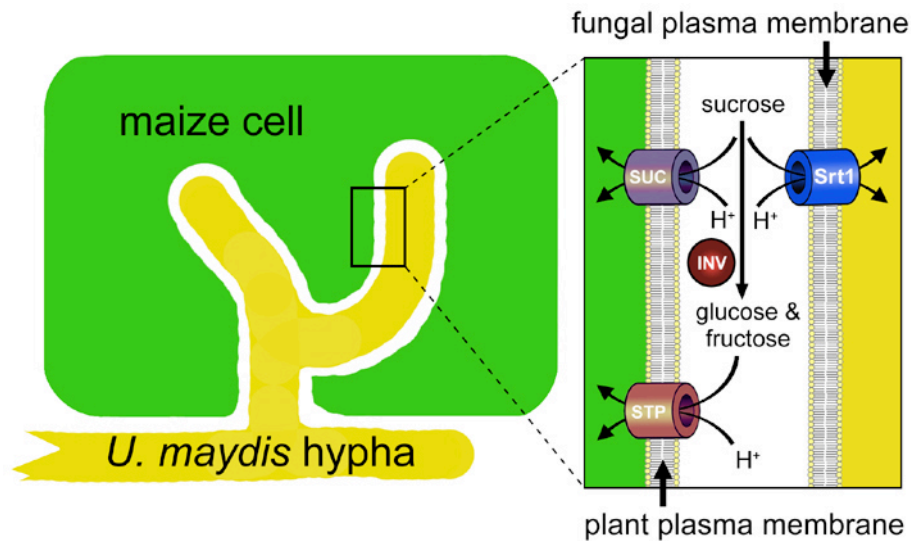


Figure 2.3-7: Model of the bidirectional competition for extracellular sucrose at the plant/fungus interface. Plants are known to use apoplastic sucrose either via plasma membrane-localized sucrose transporters (SUC or SUT proteins) or due to the activity of extracellular invertases (INV) via membrane-localized hexose transporters (STP or MST proteins). *Srt1*, a high-affinity sucrose H^+ -symporter, localizes to the fungal plasma membrane, and with its high substrate specificity and extremely low K_M -value it enables the fungus to efficiently use sucrose from the plant/fungus interface.

Direct uptake of sucrose by a plant pathogenic fungus most likely provides a second, more strategic advantage over the uptake of monosaccharides produced by the activity of a secreted fungal invertase. It was reported repeatedly that invertase-derived monosaccharides in the apoplast act as signaling molecules that trigger reduction of photosynthetic activity and induction of defense genes (Herbers *et al.*, 1996b; Ehness *et al.*, 1997; Schaarschmidt *et al.*, 2007; Kocal *et al.*, 2008; Rolland *et al.*, 2006; Roitsch *et al.*, 2003; Heineke *et al.*, 1992). Both responses are highly unfavorable for a biotrophic pathogen, as the first would reduce carbon availability and the second would harm the pathogen and stop the infection. The use of a sucrose transporter rather than of an invertase/hexose transporter system might, therefore, represent a mechanism of signal avoidance in an environment that is well prepared to sense and destroy potential pathogens.

The exclusive induction of *srt1* expression in tumor tissue implies that the transporter is specifically employed for sucrose uptake at the plant/fungal interface. During saprophytic growth on sucrose containing media the gene is neither expressed, nor needed, since $\Delta srt1$ strains do not show reduced growth rates on media with sucrose as sole carbon source. As the presence of sucrose alone is not sufficient for *srt1* induction (Figure 2.3-3), we must assume additional plant signals triggering the expression.

Srt1 is the first described fungal transporter that allows direct utilization of apoplastic sucrose without prior hydrolysis. During evolution of pathogenicity, especially of biotrophic fungi, this may have been a major step to successfully adapt to the hostile environment in host plants. The extremely high sucrose affinity and -specificity of Srt1 has not only advantages to carbon acquisition of the pathogen, but also to prevent host plant defense responses by avoiding the production of signaling molecules in the plant apoplast.

2.3.4 Experimental Procedures

Strains and Growth Conditions

Escherichia coli strain TOP10 (Invitrogen) was used for cloning purposes. For plant infections, *Ustilago maydis* cells were grown at 28°C in YEPSL (Brachmann *et al.*, 2001). For RNA extraction, *U. maydis* was grown in glutamine minimal medium, which is based on the minimal medium described by Holliday (Holliday, 1974) with 30 mM L-glutamine as nitrogen source. Plant infections with *U. maydis* were performed as described (Gillissen *et al.*, 1992). The *U. maydis* strain used in this study is SG200, a haploid, solopathogenic strain that can infect maize plants without a mating partner (Kämper *et al.*, 2006). *S. cerevisiae* strains used for analyses of Srt1 were EBY.VW4000 (Wieczorke *et al.*, 1999), SEY2102 (Emr *et al.*, 1983), D458-1B (Nikawa *et al.*, 1991) and DBY2617 (Carlson *et al.*, 1981). Cells were grown in minimal medium (0.67 % yeast nitrogen base w/o amino acids plus required amino acids depending on the strain) containing 2% maltose (EBY.VW4000) or glucose (all other strains) at 29 °C.

DNA and RNA Procedures

Molecular methods followed described protocols (Sambrook *et al.*, 1989). DNA isolation from *U. maydis* and transformation procedures were performed as described (Schulz *et al.*, 1990). Homologous integration of constructs was verified by gel blot analyses. Transformation of *S. cerevisiae* followed the protocol given in Gietz *et al.* (1992). Total RNA from *U. maydis* cells grown in axenic culture was extracted using Trizol reagent (Invitrogen) according to the manufacturer's instructions. RNA samples to be used for real-time RT-PCR were further column purified (RNeasy; Qiagen) and the quality checked using a Bioanalyzer with an RNA 6000 Nano LabChip kit (Agilent).

Deletion of srt1

The deletion of *srt1* was performed by a PCR-based approach (Kämper, 2004). The entire *srt1* ORF was replaced by a hygromycin resistance cassette in strain SG200.

Cloning of srt1 and Expression in Yeast

The *srt1* open reading frame (ORF) was amplified from *U. maydis* genomic DNA using the primers 2374_EcoRI_for (5'-CAG AAT TCA AAA ATG GCG TCG TCT TCT CCC ATT CGT-3') and 2374_EcoRI_rev (5'-CAG AAT TCT CGG ACT GCC AAG TCA TTG TGG AC-3'). DNA was sequenced and cloned into the yeast/*E. coli* shuttle vector NEV-E (Sauer and Stolz, 1994) and the resulting plasmid was used for yeast transformation. For the fusion of Srt1 to the N-terminus of GFP, *srt1* ORF was PCR-amplified with primers that removed the stop codon. The resulting *srt1* ORF was cloned upstream of the open reading frame of GFP in the yeast expression plasmid pEX-Tag (Meyer *et al.*, 2000).

Transport Studies with Radiolabeled Substrates

Yeast cells were grown to an $A_{600\text{ nm}}$ of 1.0, harvested, washed twice with water and re-suspended in buffer to an $A_{600\text{ nm}}$ of 10.0. If not otherwise indicated, uptake experiments were performed in 50-mM Na-phosphate buffer pH 5.0 with an initial substrate concentration of 1-mM ^{14}C -labeled sucrose (or another ^{14}C -labeled or ^3H -labeled substrate). Cells were shaken in a rotary shaker at 29°C and transport tests were started by adding labeled substrate. Samples were withdrawn at given intervals, filtered on nitrocellulose filters (0.8 μm pore size) and washed with an excess of distilled H_2O . Incorporation of radioactivity was determined by scintillation counting. Competition analyses were performed with 0.1-mM ^{14}C -sucrose in the presence of 10-mM competitor (100-fold excess). For analyses of the energy-dependence of sucrose transport, D-glucose was added to the yeast cells 2 min before the start of the experiment to a final concentration of 10 mM. For inhibitor analyses CCCP (carbonylcyanide *m*-chlorophenylhydrazone) or PCMBs (*p*-chloromercuribenzene sulfonate) were used at final concentrations of 50 μM .

For influx/efflux analyses in the plateau of sucrose accumulation (Figure 2.3-5D), identical amounts of yeast cells were incubated in two flasks with either 100- μM of ^{14}C -labeled sucrose or with unlabeled sucrose, and sucrose uptake was determined in the flask with the labeled substrate. When the plateau was reached (after 35 min), the cells were quickly pelleted and washed in Na-phosphate buffer (pH. 5.0). Cells from the unlabeled flask were then resuspended to the initial volume with 100- μM ^{14}C -sucrose, cells from the labeled flask with 100- μM unlabeled sucrose, and uptake experiments were continued.

Light Microscopy

Light microscopic analyses were performed using a Zeiss Axioplan 2 microscope. Photomicrographs were obtained with an AxioCam HrM camera, and the images were processed with Axiovision (Zeiss) and Photoshop (Adobe). Chlorazole Black E staining of fungal cells *in planta* was performed as described (Brachmann *et al.*, 2003).

Confocal Microscopy

Subcellular localization of the Srt1::GFP fusion protein in yeast cells was determined by confocal microscopy (Leica TCS SP1I; Leica Microsystems) and processed with the Leica Confocal Software 2.5 (Leica Microsystems). Emitted fluorescence was monitored at detection wavelengths longer than 510 nm.

Quantitative Real Time PCR Analysis

To analyze *srt1* expression on different carbon sources, SG200 was grown in glutamine minimal media supplemented with the indicated amount of the respective carbon source to an OD₆₀₀ of 1.0 for 6 h. Pre-cultures were grown overnight in glutamine minimal medium containing 1% of glucose. RNA samples were frozen in liquid nitrogen for two independently conducted replicates. RNA of maize plants infected with SG200 was prepared as described (Doehlemann *et al.*, 2008a). Samples were taken 0.5, 1, 2, 4 and 8 dpi. For cDNA synthesis, the SuperScript III first-strand synthesis SuperMix assay (Invitrogen) was used on 1 µg of total RNA. qRT-PCR was performed on a Bio-Rad iCycler using the Platinum SYBR Green qPCR SuperMix-UDG (Invitrogen). The *U. maydis actin* (*um11232*) and *eIF2B* (*um04869*) genes were used as references. Primer sequences were rt-eIF-2B-F (5'-ATC CCG AAC AGC CCA AAC-3') and rt-eIF-2B-R (5' ATC GTC AAC CGC AAC CAC-3') for *eIF2B*, rt-actin-F (5'-CAT GTA CGC CGG TAT CTC G-3') and rt-actin-R (5'-CTC GGG AGG AGC AAC AAT C-3') for the *actin* gene, and 2374_rt_for (5'-AGA CGC GTG GAA GGA CTT TCT TCG-3') and 2374_rt_rev (5'-CCT AGC TCG AAC TTT GAC CAC CGC-3') for *srt1*.

Phylogenetic Analysis

For the phylogenetic analysis of the *U. maydis* Major Facilitator Superfamily (MFS) and for the identification of the 19 members of the *U. maydis* sugar transporter superfamily, 86 amino acid sequences of putative MFS members were obtained at MUMDB (<http://mips.gsf.de/genre/proj/ustilago/>) (IPR007114 Major facilitator superfamily; <http://mips.gsf.de/genre/proj/ustilago/>). Two sequences of *U. maydis* ammonium transporters were included as out-group (Figure 2.3-S1 and Table 2.3-S1). For comparative phylogenetic analysis of Srt1, the amino acid sequence was aligned with 95 transporter sequences obtained by BLASTP analysis. This includes fungal and plant sequences with the highest similarity to Srt1, fungal and plant sequences with highest homology to *Arabidopsis thaliana* sucrose transporters, as well as fungal and plant ammonium transporter sequences as out-group (Figure 2.3-S3 and Table 2.3-S2). Sequences were aligned with MAFFT version 6 using the global alignment G-INS-i. A phylogenetic tree was calculated using the minimum linkage clustering method (<http://align.bmr.kyushu-u.ac.jp/mafft/online/server/>). TreeIllustrator 1.0.1 was used to visualize the Nexus formats of the MAFFT results.

2.3.5 Supplementary Information

A file containing the Supplementary Material of section 2.3 is available on data-CD deposited in section 5 of this thesis. The file includes Figures 2.3-S1 to S5 and Tables 2.3-S1 and S2.

Figure 2.3-S1: Phylogenetic analyses of the *U. maydis* Major Facilitator Superfamily (MFS).

Figure 2.3-S2: SG200 Δ *srt1* hyphae do not differ with respect to leaf colonization from SG200 hyphae at 4 and 7 dpi during disease progression.

Figure 2.3-S3: Comparative phylogenetic analyses of Srt1.

Figure 2.3-S4: ^{14}C -Maltose is not a substrate for Srt1.

Figure 2.3-S5: Srt1 complements the growth defect of *S. cerevisiae* strain DBY2617.

Table 2.3-S1: Accession numbers, gene-numbers [MUMDB (IPR007114 Major facilitator superfamily; <http://mips.gsf.de/genre/proj/ustilago/>)] and predicted functions of the putative transport proteins used to calculate the phylogenetic tree shown in Figure S1.

Table 2.3-S2: Accession numbers, putative or determined functions of the transport proteins used to calculate the phylogenetic tree shown in Figure S3.

Acknowledgements

We thank R. Kahmann for reading the manuscript and for helpful comments, and J. Schirawski, R. Kahmann and G. Backeren for access to unpublished sequence information of *S. reilianum* and *U. hordei*. This work was supported by grants of the Deutsche Forschungsgemeinschaft to J.K. and N.S. (research unit 666 “Mechanisms of compatibility”, grants KA 411/9-1 and SA382/16-1).

2.4 Hxt1, a Monosaccharide Transporter and Sensor Required for Virulence of the Maize Pathogen *Ustilago maydis*

Ramon Wahl^{1,2}, Kathrin Wippel³, Sarah Goos¹, Miroslav Vranes^{1,2}, Norbert Sauer³ and Jörg Kämper^{1,2+}

¹ University of Karlsruhe, Institute of Applied Biosciences, Department of Genetics, Hertzstrasse 16, D-76187 Karlsruhe, Germany.

² Max Planck Institute for terrestrial Microbiology, Karl von Frisch Straße, D-35043 Marburg, Germany

³ Friedrich-Alexander-University Erlangen-Nürnberg, Molekulare Pflanzenphysiologie, Staudtstrasse 5, D-91058 Erlangen, Germany.

+ To whom correspondence should be send:

Jörg Kämper, University of Karlsruhe, Institute of Applied Biosciences, Department of Genetics, Hertzstr. 16, D-76187 Karlsruhe; Tel: +49-721-608-4632; E-mail: joerg.kaemper@kit.edu

Keywords: biotrophic pathogen, Hxt1, monosaccharide transport, monosaccharide sensor, *Ustilago maydis*

Running title: *Ustilago maydis* Transporter/Sensor Hxt1 Required for Pathogenicity

Abstract

Plant pathogenic fungi cause massive crop losses and therefore severe economic deficits. The smut *Ustilago maydis*, a ubiquitous pest of corn, is highly adapted to its host to parasitize on its organic carbon sources. Recently, we have identified the *U. maydis* sucrose transporter Srt1 as crucial for biotrophic development. Here we report the identification of Hxt1, a second member of the *U. maydis* sugar transporter family, which is of importance for full fungal virulence. Hxt1 mainly utilizes the hexoses glucose, fructose and mannose, and with lower affinity also galactose and xylose. Deletion of *hxt1* in *U. maydis* reduces growth on the primary substrates of Hxt1 in contrast growth on its secondary substrates xylose and galactose is enhanced. Expression analysis revealed that monosaccharide-dependent regulation of transcription is hampered in *hxt1* deletion mutants, leading to the expression of genes involved in the metabolism of the secondary substrates of Hxt1. Furthermore, we observed an induction of genes that were shown to be involved in mating and subsequent pathogenic development in *hxt1* deletion mutants. Thus, we propose that Hxt1 has a dual function as monosaccharide-transporter and -sensor. While the sensor function of Hxt1 is most important to aid the initiation of pathogenicity at starvation conditions on the plant surface, its transport function is most important to feed the fungus *in planta*.

2.4.1 Introduction

Phytopathogenic fungi infect their host plants to get access to plant-produced carbohydrates causing substantial yield losses every year. Two main strategies are used by the different fungal pathogens to realize plant infection and subsequent nutrient acquisition. Necrotrophic fungi kill their host plants to live saprophytically on the dead plant tissue. In contrast, biotrophic fungi establish a close relationship with their hosts, while keeping them alive. In biotrophic interactions fungal virulence is strongly dependent on nutrient availability during infection, as it affects the fitness of the pathogen. Thus, biotrophic fungi have to manipulate their hosts to redirect the plants metabolism and feed on its resources.

The biotrophic basidiomycete *Ustilago maydis* is a ubiquitous pest of maize, one of the most cultivated crop plants worldwide. *U. maydis* infection causes the corn smut disease, resulting in the formation of large plant tumors filled with fungal teliospores. Sexual reproduction of *U. maydis* is essentially coupled to plant infection. Therefore, fusion of two sexually compatible sporidia and the formation of the infectious, filamentous dikaryon is controlled by two mating type loci *a* and *b* (Banuett and Herskowitz, 1989; Spellig *et al.*, 1994b). The *a*-locus encodes a pheromone/pheromone receptor system that regulates cell-to-cell recognition and cell fusion (Bölker *et al.*, 1992; Hartmann *et al.*, 1996). The *b*-locus encodes two unrelated homeodomain proteins bE and bW that dimerize, when derived from different alleles, and form an active transcription factor which initiates pathogenic development (Kämper *et al.*, 1995; Romeis *et al.*, 2000; Brachmann *et al.*, 2003).

After establishment of the infectious dikaryon on the plant surface, *U. maydis* penetrates the plant cuticle via specialized appressoria-like infection structures (Snetselaar and Mims, 1992; Snetselaar and Mims, 1993; Banuett and Herskowitz, 1994). *In planta* *U. maydis* hyphae traverse plant cells without eliciting apparent host defense responses, a prerequisite for the establishment of a successful biotrophic interaction. An interaction zone develops between plant and fungal membranes that is thought to be involved in the exchange of signal molecules (Snetselaar and Mims, 1993; Doehlemann *et al.*, 2009). It is conceivable that this interaction zone is also involved in nutrient supply during biotrophic growth, since *U. maydis* does not develop specialized feeding structures as the haustoria observed during infections with rust fungi (Voegelé *et al.*, 2001).

The most prominent sugar in plants is the disaccharide sucrose, which serves as transport and storage molecule. Although it is widely believed that sucrose-derived

hexoses are the most important carbon source for fungal plant pathogens, the true nature of carbohydrates utilized during plant infection remains obscure. In various pathosystems some effort was made to investigate which carbohydrates are utilized by fungal pathogens during infection. A hexose transporter (HXT1p) has been identified in the rust fungus *Uromyces fabae* that is expressed only in haustoria (Voegelé *et al.*, 2001). Heterologous expression of HXT1p in *S. cerevisiae* revealed that the protein functions as a proton co-transporter specific for glucose and fructose. The substrates of HXT1p are thought to result from cleavage of sucrose by the secreted invertase of *U. fabae*, which is also expressed in haustoria (Voegelé *et al.*, 2006). However, as rust fungi are yet not amenable to reverse genetic approaches, the function of transporter and invertase during biotrophic development could not be addressed in the homologous system (Voegelé *et al.*, 2001).

Similarly, in the ectomycorrhizal fungi *Amanita muscaria*, *Tuber borchii*, and *Geosiphon pyriformis* specific hexose transporters were identified as upregulated during symbiosis (Nehls *et al.*, 1998; Schüssler *et al.*, 2006; Polidori *et al.*, 2007) and thus thought to be responsible for symbiotic sugar uptake. However, also in the mycorrhizal systems, a causal relationship between transporters and symbiotic development has not been established yet.

Also in necrotrophic interactions, glucose and fructose are discussed to be the main carbon sources utilized by the pathogen. During infection of sunflower with the necrotrophic fungus *Sclerotinia sclerotiorum* the sucrose content of the plant drops dramatically, as a result of the activity of a fungal invertase. Induction of two hexose transporters, *Sshxt1* and *Sshxt2*, during this stage of fungal proliferation indicates that the fungus predominantly feeds on sucrose cleavage products (Jobic *et al.*, 2007).

The best-studied system for sugar utilization is the yeast *Saccharomyces cerevisiae*. Uptake of glucose is facilitated through 17 closely related hexose transporters (Hxt genes; Ozcan and Johnston, 1999). Glucose, the predominantly utilized carbon source of *S. cerevisiae* is sensed by two glucose receptors Rgt2 and Snf3 (Ozcan *et al.*, 1996; Vagnoli *et al.*, 1998). Both proteins harbor an elongated cytoplasmatic C-terminus, which is involved in signal transduction (for review see Forsberg and Ljungdahl, 2001; Gancedo, 2008). In addition, a cytoplasmatic glucose repression pathway exists that operates via the hexose kinase Hxk2, the protein kinase Snf1 and the transcription factor Mig1 (Ostling and Ronne, 1998; Treitel *et al.*, 1998; Smith *et al.*, 1999; Papamichos-Chronakis *et al.*, 2004).

Reasoned from the paucity of plant cell wall degrading enzymes compared to other fungal pathogens (Doehlemann *et al.*, 2008b), it is unlikely that *U. maydis* feeds on carbohydrates derived from the digestion of plant cell wall material. A comprehensive transcriptome and metabolome analysis of the host plant revealed that *U. maydis* infection leads to a reprogramming of the host metabolism (Doehlemann *et al.*, 2008a). Mature maize leaves invaded by *U. maydis* develop sink, rather than source tissue characteristics. The carbon supply of the infected areas is not mediated by photosynthesis, but by sucrose import (Doehlemann *et al.*, 2008a; Horst *et al.*, 2008). Thus, it is likely that *U. maydis* uses sucrose and/or its cleavage products glucose and fructose as energy source within the plant. Recently, we have identified the *U. maydis* sucrose transporter Srt1 to be essential for full fungal virulence (see 2.3). Here we report the identification of Hxt1, a monosaccharide transporter predominantly for glucose and fructose, which is required for full fungal virulence. In addition to its function as a transporter, Hxt1 functions as a sensor for monosaccharides, as it was found to influence carbohydrate-dependent gene expression.

2.4.2 Results

Hxt1 is a Hexose Transporter with High Affinity to Glucose and Fructose Required for Pathogenic Development of *U. maydis*

In total we identified 19 sugar transporters in the *U. maydis* genome (see 2.3). To investigate their impact on fungal pathogenicity we performed deletion analyses in the haploid, solopathogenic strain SG200, which is infectious without an additional mating partner (Kämper *et al.*, 2006). Deletion mutants of two of the identified transporter genes were reproducibly hampered in pathogenic development, respectively. *srt1* was described previously (see 2.3), the second transporter gene found to influence pathogenicity was *um05023* (MIPS).

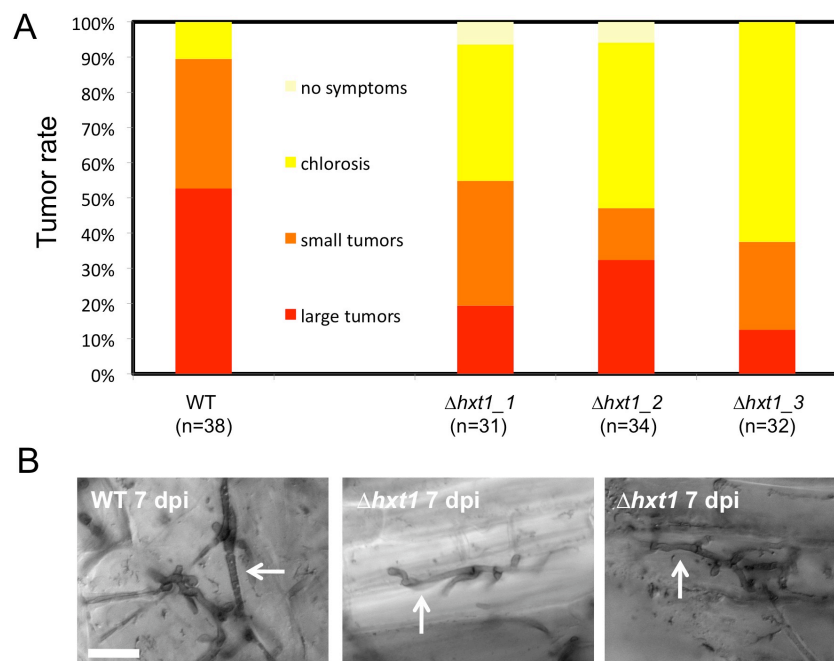


Figure 2.4-1: *U. maydis hxt1* deletion mutants show reduced virulence. (A) Disease rating of plants infected with the wild type strain SG200 (WT) and three independent SG200 $\Delta hxt1$ deletion mutants (7 dpi). Percentage of plants with large tumors, small tumors, or with chlorosis are color-coded (n = total number of plants analyzed; one of three independent experiments giving similar results is displayed). (B) Chlorazole Black E staining of maize leaves infected with SG200 (WT) and SG200 $\Delta hxt1$ at 7 dpi. In both cases hyphae spread within the plant leaf tissue. Arrows indicate fungal hyphae; scale bars: 20 μ m.

Plants were infected with 3 independent SG200 *um05023* deletion mutants and tumor development was compared to SG200 wild type infections after 7 dpi (days post inoculation). The number of infected plants after inoculation with *um05023* deletion strains was decreased to about 60%, compared to 90 % after SG200 wild type infection (Figure 2.4-1A). Chlorazol Black E stainings of infected plant material were performed to visualize fungal hyphae during *in planta* growth 7 dpi. Hyphae of

Δum05023 strains were indistinguishable from SG200 wild type hyphae 7 dpi, revealing no obvious physiological differences during pathogenic development (Figure 2.4-1B).

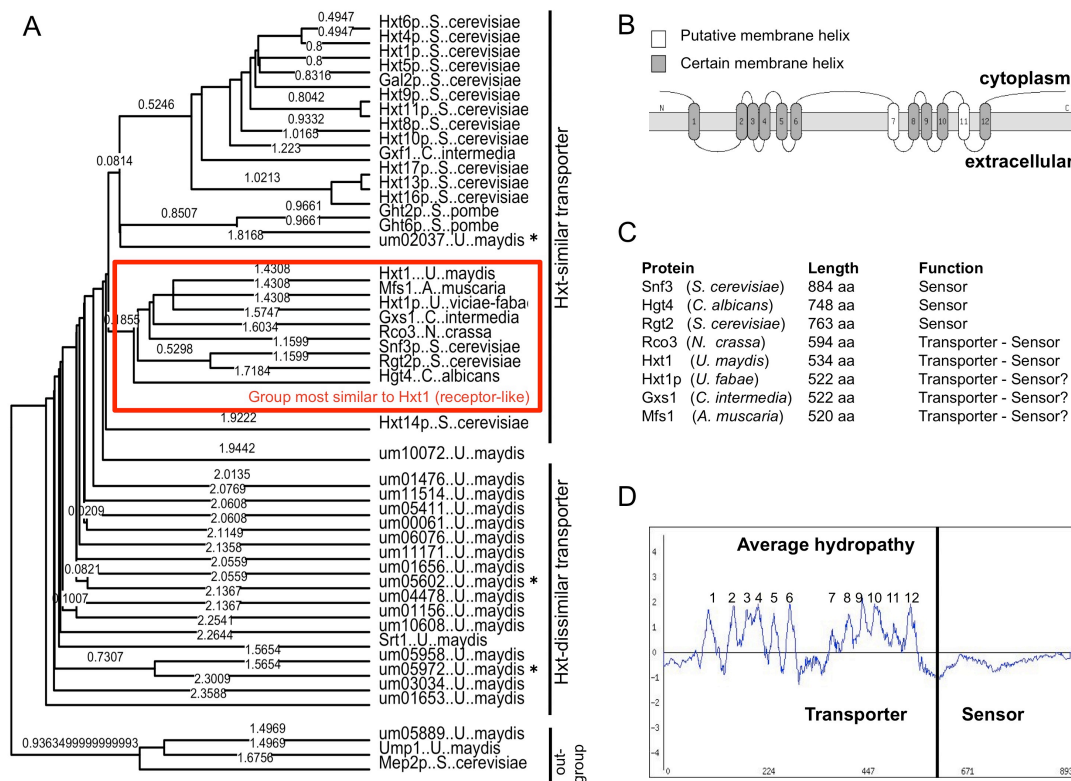


Figure 2.4-2: Hxt1 is related to glucose sensors and hexose transporters involved in biotrophic development of fungi. (A) Comparative phylogenetic analysis of Hxt1 (see Experimental Procedures). The transporters are separated in two major groups, one comprising transporter sequences similar to the yeast hexose transporters (Hxt-similar) and the other one comprising *U. maydis* transporters that are more distantly related to the first group (Hxt-dissimilar). Within the Hxt-similar transporter group, Hxt1 forms a distinct group with receptor-like proteins (red box). Stars indicate proteins not represented as probe set on the *Ustilago* DNA-microarray. Species and gene names are given, for accession numbers see Table 2.4-S1. (B) Putative topology of Hxt1 obtained with the topology prediction program TopPred (<http://mobyle.pasteur.fr/cgi-bin/portal.py?form=toppred>). The Hxt1 prediction corresponds to the typical structure of hexose transporter with 12 transmembrane helices (TM). (C) Protein length and function of Hxt1 and its homologues (D) Average hydropathy plot of the proteins given in (C) obtained with a multiple sequence alignment tool that marks transmembrane helices (<http://www.tcd.org/progs/msaTMS.php>). All sequences contain 12 hydrophobic peaks indicating the TMs. Snf3, Rgt2 and Hgt4 possess a C-terminal extension involved in hexose signaling, which is not found in the *U. maydis* Hxt1 protein.

The Um05023 protein is predicted to contain 12 transmembrane domains (TMDs) with a large extracellular loop between TMD1 and TMD2, which is typical for hexose transporters (Figure 2.4-2B; Sonnhammer *et al.*, 1998; Schüssler *et al.*, 2006). BLAST analysis revealed that the protein is most similar to the high affinity glucose/arabinose transporter Mst1 (53%) from *A. muscari* and to the high affinity glucose/fructose-transporter Hxt1 (49%) from *U. fabae* (Figure 2.4-2A; Voegelé *et al.*,

2001; Nehls *et al.*, 1998). Furthermore, Um05023 shows significant similarities to the glucose sensors Rgt2 and Snf3 from *S. cerevisiae* (42% and 39% identity on amino acid level, respectively) and to Hgt4 from *Candida albicans* (41% identity on amino acid level); however, in contrast to these sensors, neither Um05023 nor one of the other 18 potential sugar transporters from *U. maydis* possess a C-terminal extension that was shown to be involved in signal transduction (Figure 2.4-2A, 2C and 2D; Ozcan and Johnston, 1999; Brown *et al.*, 2006). Because of its similarities to known hexose transporters we named Um05023 as Hxt1.

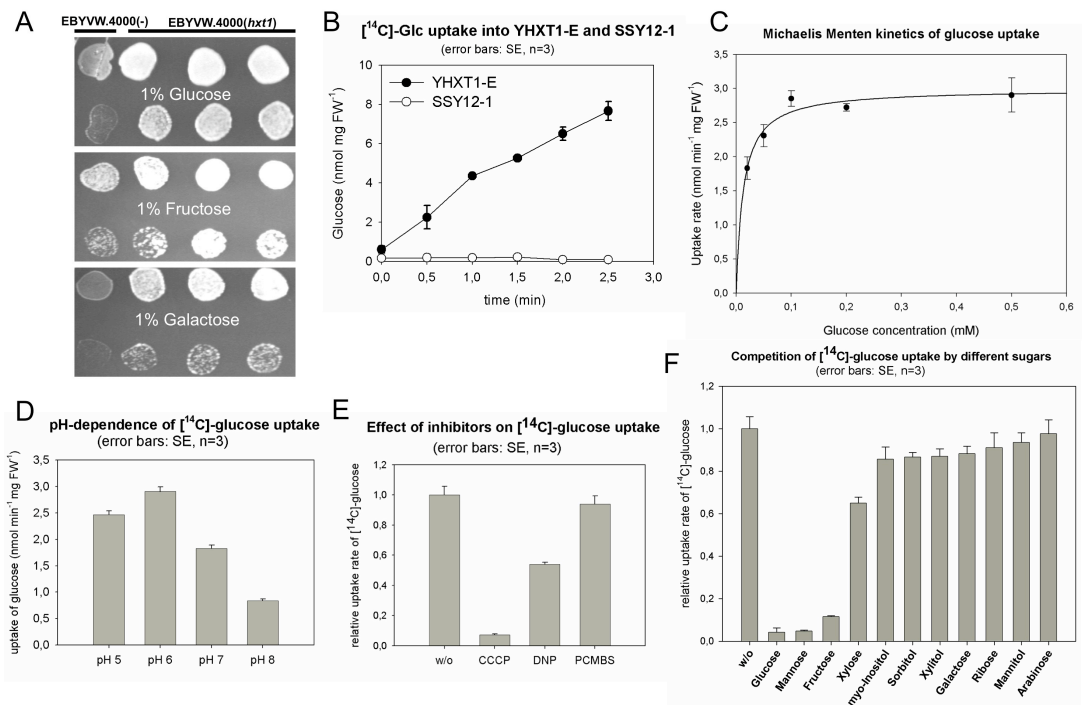


Figure 2.4-3: Hxt1-dependent hexose uptake in *S. cerevisiae*. (A) Growth of *S. cerevisiae* strains EBVW.4000 and EBVW.4000 expressing Hxt1 (B) Uptake of ^{14}C -glucose by *hxt1*-expressing (closed circles) and control cells (open circles). (C) Michaelis-Menten kinetics of glucose uptake rates (pH 6.0) indicate a K_M of $\sim 6.6 \mu\text{M}$. (D) The pH-optimum for glucose uptake by Hxt1 is in the acidic pH range. (E) Glucose uptake is sensitive to the protonophors CCCP and DNP, but not to the SH-group inhibitor PCMBs. (F) Competition analysis (0.1-mM ^{14}C -glucose) with different sugars added at 100-fold molar excess. Error bars represent standard error (n = 3).

To functionally characterize *U. maydis* Hxt1, the protein was expressed in the *S. cerevisiae* strain EBV.WV4000, a deletion mutant of 22 genes encoding hexose-utilizing transporter, which is unable to grow on hexoses (Wieczorke *et al.*, 1999). Expression of Hxt1 in EBV.WV4000 resulted in enhanced growth on medium containing 1% glucose, 1% fructose or 1% galactose (Figure 2.4-3A). To characterize the kinetics of Hxt1, we measured the uptake of ^{14}C -glucose in EBV.WV4000 (Figure 2.4-3B). Hxt1 has a high glucose affinity (K_M of $6.6 \mu\text{M}$), which is about 70- and 50-fold higher than the affinities of the homologous glucose transporters from *A.*

muscaria and *U. fabae*, respectively (Figure 2.4-3C; Nehls *et al.*, 1998; Voegele *et al.*, 2001). The ^{14}C -glucose transport of Hxt1 has an optimum at acidic pH values and was found to be sensitive to the protonophore carbonylcyamide *m*-chlorophenylhydrazone (CCCP) and 2,4-dinitrophenol (DNP), but not to the SH-group inhibitor *p*-chloromercuribencene sulfonate (PCMBs), suggesting that Hxt1 is an energy-dependent H^+ -symporter (Figure 2.4-3D and 3E). Competition assays with different hexoses, pentoses and polyols revealed a high affinity of Hxt1 to the hexoses fructose and mannose, and a lower affinity to the pentose xylose (Figure 2.4-3F).

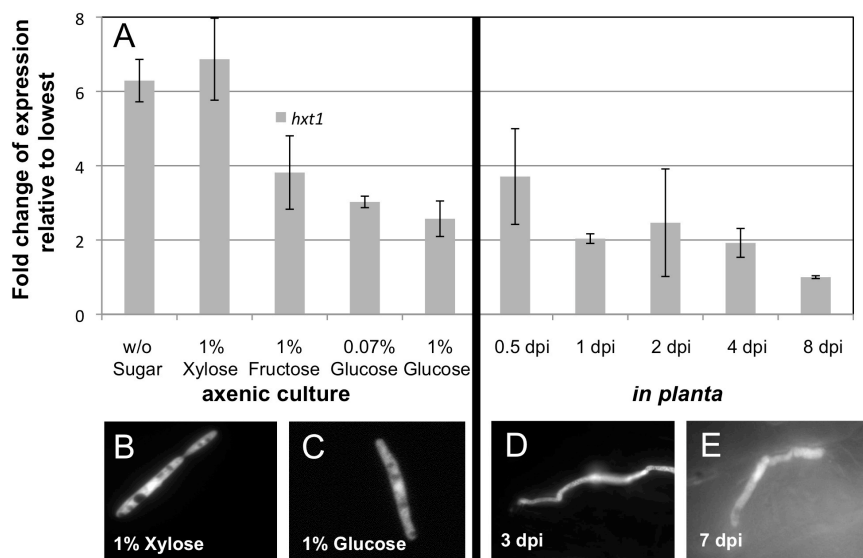


Figure 2.4-4: *hxt1* is constitutively high expressed. (A) *hxt1* expression (quantitative real time PCR) in *U. maydis* SG200 grown in liquid media supplemented with different carbon sources (left) or on plant tissue at different time points after infection. Gene expression was normalized to the expression of the constitutively expressed genes *actin* and *eIF2B* (Experimental Procedures). Changes in *hxt1* expression are displayed relative to the condition with lowest expression (dpi = days post infection). Error bars indicate the standard deviation of mean expression values. (B), (C), (D) and (E) display *hxt1* expression by GFP fluorescence. The *gfp* gene was fused to and expressed by the *hxt1* promoter in SG200 on selected artificial media and during *in planta* development as indicated.

Since the Hxt1-homologs from *U. fabae* and *A. muscari* are specifically expressed during biotrophic development (Nehls *et al.*, 1998; Voegele *et al.*, 2001), we investigated expression of *hxt1* in SG200 by quantitative real time PCR in strains grown in minimal media supplemented with high (1%) or low (0.07%) levels of glucose, 1% fructose, 1% xylose, or without any additional carbon source. In addition, we analyzed *hxt1* expression in SG200 during plant infection at 0.5, 1, 2, 4, and 8 dpi; non-infected plants were used as negative control. *hxt1* was found to be

constitutively expressed, with slightly increased expression in media without sugar or supplemented with the pentose xylose (Figure 2.4-4A). Yet, *hxt1* expression levels were similar during growth on glucose or fructose or during plant infection (Figure 4A). In addition, a transcriptional fusion of the *gfp* gene to the *hxt1* promoter revealed that *hxt1* is highly expressed throughout all tested conditions (Figure 2.4-4B-E).

Hxt1 and *Srt1* Have Additive Effects on the Pathogenicity of *U. maydis*

Srt1, the second *U. maydis* sugar transporter involved in pathogenic development, is specific for the uptake of sucrose, the main soluble carbon source in plants. Since *Hxt1* transports glucose and fructose, both transporters compete for the same substrate, sucrose, either directly, or indirectly after its cleavage by invertases. To address the question whether both transporters have redundant functions, we generated the double deletion in strain SG200. In infections with SG200, 90% of the plants developed disease symptoms, compared to 60 % in SG200 Δ *hxt1* infections and, 30 % in SG200 Δ *srt1* infections (Figure 2.4-5A, B). The infection rate of the double deletion strains was further reduced: only 10 % of the infected plants developed marginal symptoms (Figure 2.4-5A, B).

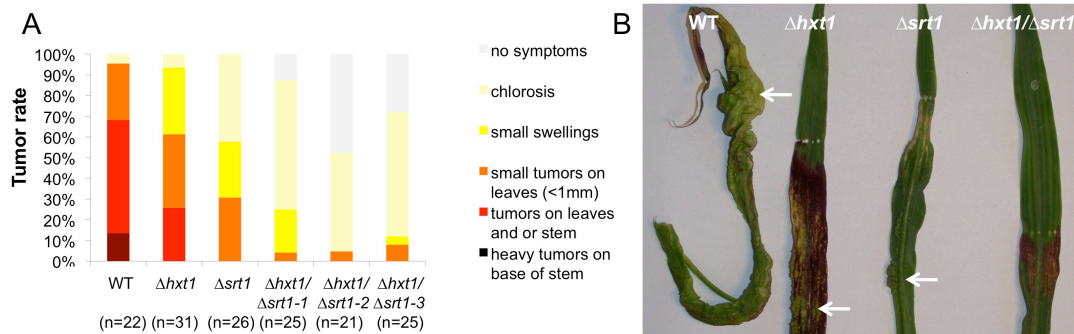


Figure 2.4-5: *Hxt1* and *Srt1* have additive effects during pathogenic development of *U. maydis*. (A) Disease rating of plants infected with the fungal wild type strain SG200 (WT), the transporter single deletion mutants SG200 Δ *hxt1* and SG200 Δ *srt1* as well as three independent double deletion mutants (SG200 Δ *hxt1*/ Δ *srt1*) at 7 dpi. Percentage of plants with different disease symptoms are color-coded (n = total number of plants analyzed; one of three independent experiments giving similar results is displayed). (B) Plant leaves infected with SG200 wild type, Δ *hxt1*, Δ *srt1* and Δ *hxt1*/ Δ *srt1* strains. White arrows mark the development of plant tumors, which are comparably small after infection with both single deletion mutants and not present after infection with double deletion mutants.

Hxt1 Senses Environmental Carbon Sources Independent from the Cytoplasmatic Glucose Repression Pathway

To test whether deletion of *hxt1* influences growth of *U. maydis*, we compared growth of SG200 Δ *hxt1* to SG200 on media supplemented with different sugars as sole carbon source. Growth of *U. maydis* Δ *hxt1*-strains was reduced on glucose, fructose and mannose containing minimal media and also on media containing the disaccharide maltose, whereas growth on arabinose and sucrose was unaffected (Figure 2.4-6A). Interestingly, growth of SG200 Δ *hxt1* on xylose and galactose was enhanced (Figure 2.4-6A). These results indicate that Hxt1 induces growth on its primary substrates, due to its uptake capability. However, in addition Hxt1 represses growth on its secondary substrates, indicating a sensor function, which influences the regulation of gene expression in response to environmental carbon sources.

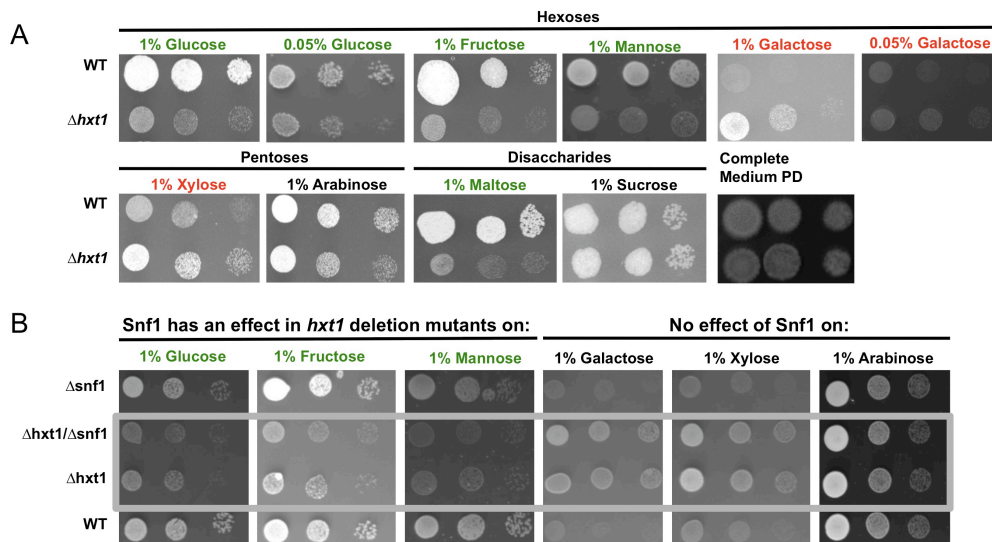


Figure 2.4-6: Growth of *U. maydis* *hxt1* deletion mutants on different carbon sources and the influence of *snf1*. (A) Growth of SG200 Δ *hxt1* on nitrate minimal media containing the indicated carbohydrate sources compared to the SG200 wild type strain. Green, red and black carbon source labels indicate reduced, enhanced and unaltered growth of SG200 Δ *hxt1*, respectively. (B) Growth of SG200 Δ *snf1* and SG200 Δ *hxt1*/ Δ *snf1* on nitrate minimal media containing the indicated carbohydrate sources compared to SG200 and SG200 Δ *hxt1*. Green carbon source labels indicate reduced growth of SG200 Δ *hxt1*/ Δ *snf1* compared to SG200 Δ *hxt1* given in the grey box. Growth of SG200 Δ *snf1* was comparable to SG200 under all conditions tested. For (A) and (B) cultures were grown in liquid complete medium, and spotted in a series of 10-fold dilutions on the media indicated.

In *S. cerevisiae* glucose is sensed by the glucose receptors Rgt2 and Snf3 (Ozcan *et al.*, 1996; Vagnoli *et al.*, 1998). In addition, a cytoplasmatic glucose repression pathway exists that operates via the transcription factor Mig1. Mig1 is inactivated by the kinase Snf1 under glucose-limiting conditions, which leads to a release of glucose repression (Ostling and Ronne, 1998; Treitel *et al.*, 1998; Smith *et al.*, 1999;

Papamichos-Chronakis *et al.*, 2004; Ahuatzki *et al.*, 2007). We were wondering if, similar to *S. cerevisiae*, glucose repression is released by Snf1 in *U. maydis*, and if the release of carbohydrate-mediated repression in *hxt1* deletion strains is caused by Snf1.

An *U. maydis* protein of 841 amino acids, highly similar to Snf1 of *S. cerevisiae* was identified by BLAST analysis (Um11293; 51% identity). Sequence comparison of various fungal Snf1 proteins revealed a high level of conservation in their N-terminal halves (Figure 2.4-S1), which contain the AMP-activation sites of the kinases (Johnson *et al.*, 1996; Cziferszky *et al.*, 2003). In Snf1 of *U. maydis* this activation site is about 94 % identical to the corresponding site of Snf1 in *S. cerevisiae* and also harbors Threonine²⁰⁷ (Figure 2.4-S1), phosphorylation of which is required for activation in *S. cerevisiae* (McCartney and Schmidt, 2001). The C-terminal part of the protein is, with the exception of few conserved aa-stretches, highly diverse. One of these conserved stretches contains Leucine⁵⁶⁴ (Figure 2.4-S1). The respective Leucine of the *S. cerevisiae* Snf1 was shown to be required for interaction with Snf4, the γ -subunit required for activation of the kinase complex (Jiang and Carlson, 1996; Momcilovic *et al.*, 2008). Phylogenetic analysis revealed that the Snf1 proteins from *U. maydis* and from other basidiomycete fungi form a distinct group separated from Snf1 proteins of ascomycete fungi (Figure 2.4-S2). Snf1 of the basidiomycete *Cryptococcus neoformans* was recently described to influence growth on simple carbon sources (Figure 2.4-S2; Hu *et al.*, 2008).

We deleted the *snf1* gene in SG200 and the respective SG200 Δ *hxt1* deletion strain. The resulting strains were grown on different carbon sources and compared to the respective control strains (SG200, SG200 Δ *hxt1*, SG200 Δ *snf1*, SG200 Δ *hxt1* Δ *snf1*). No difference in growth was observed on complete media and on minimal media containing 1% arabinose or 1% sucrose for any of the strains (Figure 2.4-6B). Also growth on 1% xylose or 1% galactose containing minimal media was not altered in *snf1* deletion strains (Figure 2.4-6B). On media supplemented with 1% glucose, 1% fructose or 1% mannose, growth of SG200 Δ *snf1* was comparable to that of SG200; however, growth of SG200 Δ *hxt1* Δ *snf1* was slightly reduced when compared to SG200 Δ *hxt1* (Figure 2.4-6B). Snf1 seems not to be involved in the release of Hxt1-dependent monosaccharide repression in *U. maydis* on secondary carbon sources. However, as deletion of *snf1* reduces growth of SG200 Δ *hxt1*, the *U. maydis* Snf1 kinase has an effect on the response towards primary carbon sources when Hxt1 is inactive.

Glucose Repression is Released in *hxt1* Deletion Strains

To investigate the potential function of Hxt1 in carbohydrate sensing, we performed DNA array expression analyses. The comparison of the expression profiles of SG200 and SG200 $\Delta hxt1$ grown in liquid minimal medium with 1% glucose revealed a total of 165 differentially expressed genes, of which 109 (66%) were induced in SG200 $\Delta hxt1$, and 56 (34%) were repressed (Figure 2.4-7 and Table 2.4-S2A).

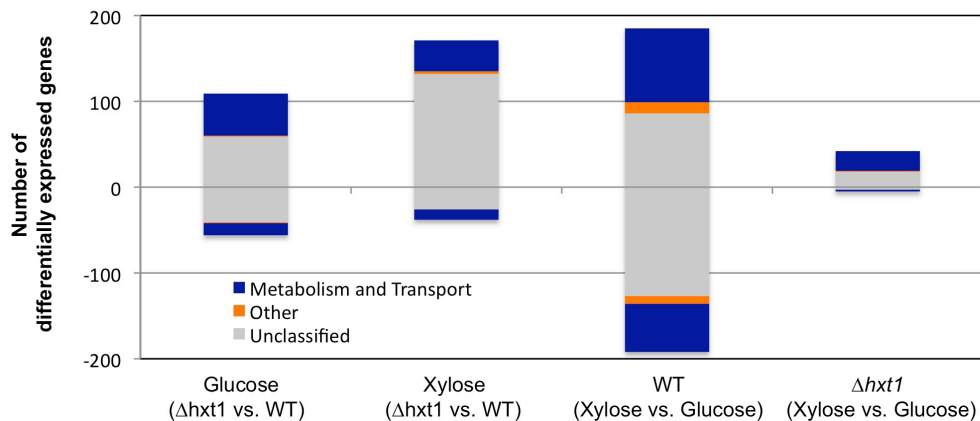


Figure 2.4-7: Hxt1 influences gene expression in response to different carbon sources. Gene expression changes in SG200 and SG200 $\Delta hxt1$ in response to glucose and xylose. The height of each column indicates the number of up- and down-regulated genes in each comparison. Most of the classified genes are involved in metabolism and/or transport (blue; detailed FunCats are given in Table 2.4-S3). Unclassified and classified genes that do not belong to this group are indicated in grey and orange, respectively.

Of genes with a functional annotation, nearly all could be classified within the functional categories (FunCats) “Metabolism” and/or “Cellular Transport” (Figure 2.4-7). Enrichment analyses revealed significant alterations in the categories “Amino Acid-”, “C-compound-”, “Lipid/Fatty Acid-” and “Secondary Metabolism” as well as “Transported Compounds” (Table 2.4-S3), caused by the genes derepressed in SG200 $\Delta hxt1$ (data not shown). Enhanced expression of genes involved in gluconeogenesis is typically regulated via glucose repression (reviewed by Ronne, 1995). We found 5 genes involved in gluconeogenesis to be induced in SG200 $\Delta hxt1$ grown on glucose-containing media, arguing for a release of glucose repression (Table 2.4-S2A; alcohol dehydrogenase (*um01984*; 6.9-fold), acetaldehyde dehydrogenase (*um02508*; 5.6-fold), acetoacetyl-CoA synthetase (*um05131*; 2.6-fold), phosphoenol pyruvate carboxykinase (*um05130*; 2.2-fold) and fructose 1,6 bisphosphatase (*um02703*; 1.9-fold, below cut-off).

Among the 14 down-regulated genes in SG200 Δ *hxt1* with functional annotation (Figure 2.4-7), we identified only one sugar transporter gene. The basal level of the sucrose transporter gene *srt1* was about 3-fold decreased (Table 2.4-S2A). Of the 19 sugar transporters genes present in the *U. maydis* genome, only 16 are represented on the *U. maydis* DNA array. One of the genes not present on the array is *um02037*, which encodes the only Hxt-similar transporter next to Hxt1 in *U. maydis* (Figure 2.4-2A). Real-time analysis revealed no significant alterations of *um02037* gene expression in *hxt1* deletion strains (data not shown). Thus, we can exclude that the reduced growth of SG200 Δ *hxt1* on hexoses is due to an *hxt1*-mediated down-regulation of other transporter genes, as it has been described for Rgt2 and Snf3 in *S. cerevisiae* (Ozcan *et al.*, 1996).

Transcription Profiles of hxt1 Deletion Mutants are Similar on Glucose and Xylose Containing Media

As Hxt1 seems to modulate catabolite-repression not only in response to glucose, but also in response to secondary carbon sources like xylose, deletion of *hxt1* should abolish dramatic changes in gene expression after a shift from glucose to xylose. To test this hypothesis, we performed DNA-array expression analysis of SG200 and SG200 Δ *hxt1* strains grown on 1% xylose and compared the expression profiles to their respective glucose-dependent profiles.

Whereas the expression profile of SG200 changed dramatically after shifting the carbon source from glucose to xylose (377 differentially expressed genes), only 47 genes were differentially expressed in SG200 Δ *hxt1* (Figure 2.4-7, Table 2.4-S2C and S2D). Enrichment analysis of differentially expressed genes in SG200 after shifting the carbon source revealed significant changes within various FunCats (“Amino Acid-“, “Lipid/Fatty Acid-“, “Carbon-“, “Secondary Metabolism”, “Glycolysis”, “Fermentation”, “Cellular Transport” as well as “Cellular Sensing and Response to External Stimuli”), in SG200 Δ *hxt1* only the FunCats “Carbon Metabolism”, “Fermentation” and “Cellular Transport” were significantly affected (Table 2.4-S3).

32 of 42 genes that are up-regulated in SG200 Δ *hxt1* on xylose containing media were also induced by xylose in the SG200 (Figure 2.4-8, Table 2.4-S4). Three of these xylose-induced genes were coding for putative enzymes needed to convert xylose for catabolism via the pentose phosphate pathway (*um11944*, encoding a putative xylose reductase; *um02150*, encoding a putative xylitol dehydrogenase;

um12177, encoding a putative xylulokinase). Since all 3 genes are induced in both SG200 as well as SG200 Δ *hxt1* during growth on xylose, their induction does not explain the enhanced growth rate of SG200 Δ *hxt1* on xylose containing medium (Figure 2.4-8, Table 2.4-S4). This phenotype might be explained by the remaining 10 xylose-induced genes, which are in addition Hxt1-repressed (Figure 2.4-8, Table 2.4-S4). Interestingly, one of these genes encodes a probable monosaccharide transporter (*um10072*). Expression of *um10072* is slightly increased (3-fold) in SG200, but strongly induced (14-fold) in SG200 Δ *hxt1* on xylose. However, as Um10072 is not biochemically characterized yet, its function in xylose transporter remains speculative.

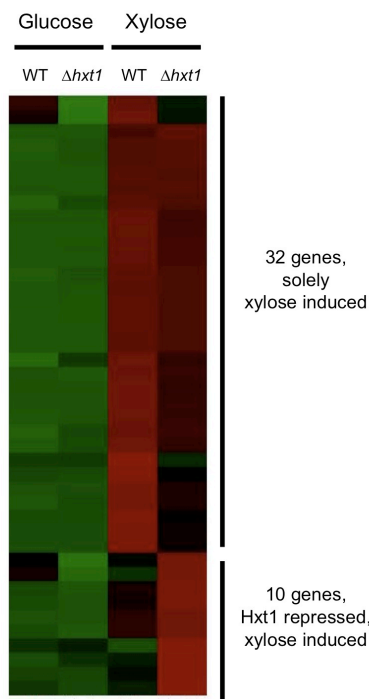


Figure 2.4-8: Xylose-dependent genes that are repressed by Hxt1. Hierarchical clustering of 42 induced genes (>2-fold) in SG200 Δ *hxt1* grown on xylose compared to growth on glucose (column 4 in Figure 2.4-7). Colours represent expression levels for each gene, which are either above (red) or below (green) the mean expression level (black) in the indicated experiment, according to the dChip 1.3 manual (<http://biosun1.harvard.edu/complab/dchip/manual.htm>).

Deletion of hxt1 Mimics Carbohydrate Starvation

To identify genes, which are preferentially expressed in response to Hxt1, we were searching for genes differentially expressed in SG200 Δ *hxt1* compared to SG200 on both glucose and xylose containing media (Table 2.4-S2A, S2B and S5). In total 36 genes were found to be differentially expressed in a similar manner under both conditions (Figure 2.4-9, Table 2.4-S5). Interestingly, two of the 29 genes repressed by Hxt1 were coding for Prf1 (*um02713*; 2.7-fold on glucose and 8 fold on xylose) and the *Magnaporthe grisea* Con7-homolog (*um02717*; 5.2-fold on glucose and 8-fold on xylose), two transcription factors important for the initiation of pathogenic

development (Figure 2.4-9, Table 2.4-S5; Hartmann *et al.*, 1996; Odenbach *et al.*, 2007).

As the observed de-repression of *prf1* and *con7* in SG200 Δ *hxt1* indicates that Hxt1 contributes in the initiation process of pathogenicity, a release of Hxt1 repression should be favoured by the starvation conditions on the plant surface. Therefore we examined the expression levels of the 36 strictly Hxt1-dependent genes on the plant surface and during infection (5; 9 and 13 dpi). About 80 % of the 36 genes, which were up-regulated (down-regulated) upon *hxt1* deletion were also found to be up-regulated (down-regulated) on the plant surface whereas expression was decreased (increased) after plant infection (Figure 2.4-9, Table 2.4-S5). These findings indicate that Hxt1-mediated sensing of the starvation conditions on the plant surface may influence mating and pathogenic development.

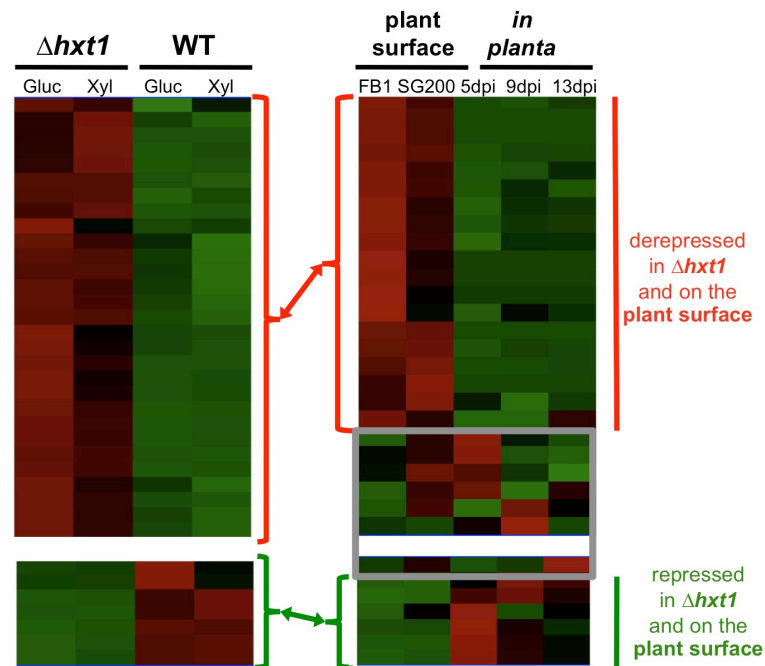


Figure 2.4-9: Strictly Hxt1-repressed genes are expressed on the plant surface. Hierarchical clustering of gene expression in axenic culture (left) and during plant infection (right) displaying genes that are Hxt1-dependently expressed in both glucose and xylose containing media. Gene expression on the plant surface was investigated for strains FB1 (non-infectious; Banuett and Herskowitz, 1989) and SG200 (infectious; Kämper *et al.*, 2006), respectively. Expression changes in SG200 Δ *hxt1* compared to SG200 grown on glucose and xylose containing media, respectively, are at least 2-fold at both conditions. Colours represent expression level for each gene, which are either above (red) or below (green) the mean expression level (black) in the indicated experiment, according to the dChip 1.3 manual (<http://biosun1.harvard.edu/complab/dchip/manual.htm>).

2.4.3 Discussion

Hxt1 Has a Dual Function as Monosaccharide Transporter and Sensor

Glucose and fructose are the most important energy sources for most organisms as they are easy to metabolize via glycolysis. Uptake of these “primary” carbon sources is often preferred over the uptake of “secondary” carbon sources, which are more difficult to metabolize. Therefore, carbohydrate metabolism is tightly regulated. In *U. maydis* Hxt1 plays a central role within this regulatory circuit, not only by the transport of “primary” carbon sources, but also due to the transduction of carbohydrate signals.

It is likely that Hxt1 transduces carbohydrate signals directly during interaction with its substrates, rather than indirectly after transport. The very high affinity of Hxt1 for glucose, fructose and mannose results in increased growth of SG200 on these sugars compared to SG200 Δ *hxt1*; the very low affinity for xylose and galactose, in contrast, triggers reduced growth of SG200. Especially the enhanced growth of *hxt1* deletion strains on xylose and galactose cannot be explained as a result of a cytoplasmatic sensing event subsequent to utilization. Because of its affinity for galactose and xylose, deletion of Hxt1 would reduce cytoplasmatic carbohydrate signals and therefore decrease growth on xylose and galactose, rather than increasing it, as observed in SG200 Δ *hxt1*. Thus, we have to assume that Hxt1 not only utilizes glucose, fructose, mannose and to a lesser extent galactose and xylose, but also triggers a response towards these sugars.

In *S. cerevisiae*, Rgt2 and Snf3, two proteins with high similarities to Hxt1, trigger a signal cascade to adjust expression of the Hxt transporter genes pending on glucose availability via the transcriptional activator Rgt1. Both transporters have lost the ability to transport glucose; they harbor an elongated C-terminal tail involved in signal transduction (Ozcan *et al.*, 1996; Vagnoli *et al.*, 1998; Ozcan and Johnston, 1999). A similar function has also been shown for Hgt4 of *C. albicans*, which in addition binds galactose and triggers a subsequent transcriptional response (Brown *et al.*, 2009). However, in *U. maydis*, both the glucose receptors harboring an elongated C-terminal tail as well as the homologs of the yeast co-repressors Mth1 and Std1 (Schmidt *et al.*, 1999) that interact with these C-termini, are absent.

In addition to the glucose receptors, *S. cerevisiae* harbors a cytoplasmatic glucose repression pathway that operates through the kinase complex Hxk2/Snf1 and the repressor Mig1 (for review see Santangelo, 2006; Zaman *et al.*, 2008; Gancedo, 2008). Snf1 binds to and phosphorylates Mig1 under glucose-limiting conditions,

which in turn releases glucose repression (Ostling and Ronne, 1998; Treitel *et al.*, 1998; Smith *et al.*, 1999; Papamichos-Chronakis *et al.*, 2004; Ahuatzli *et al.*, 2007). A similar glucose repression pathway is described for various Aspergilli, where the transcription factor CreA (homolog of Mig) represses genes in the presence of glucose that are necessary for growth on minor important carbon sources as xylose and galactose (Prathumpai *et al.*, 2004; David *et al.*, 2005). In the pathogenic fungi *Cochliobolus carbonum*, *Fusarium oxysporum*, *Magnaporthe oryzae*, *Cryptococcus neoformans* and *Gibberella zea*, deletion of *snf1* leads to reduced growth on various sugars, suggesting that Snf1 is involved in the release of carbon repression (Tonukari *et al.*, 2000; Ospina-Giraldo *et al.*, 2003; Yi *et al.*, 2008; Hu *et al.*, 2008; Lee *et al.*, 2009).

The *U. maydis* Snf1 was found to enhance growth on hexoses, but only when Hxt1 is inactive, suggesting an involvement in the release of glucose-repressed genes. Yet, the release of catabolite repression in response to secondary carbon sources is independent of Snf1. Thus, carbohydrate signaling in *U. maydis* is clearly different compared to *S. cerevisiae*. Snf1 does not play a central role in carbohydrate signaling, and neither yeast-like glucose receptors nor the interacting co-repressors Mth1 and Std1 exist in *U. maydis*.

Interestingly, it was shown that the elongated C-terminus of the glucose sensor Rgt2 is not required for glucose signaling in *S. cerevisiae* (Moriya and Johnston, 2004). The C-terminal tail only enhances signaling through interaction with Mth1 and Std1, which leads to subsequent degradation of both co-repressors (Moriya and Johnston, 2004). Thus, the presence of a sugar transporter-like protein harboring an elongated C-terminal tail is not obligatory for membrane coupled glucose perception. The Hxt1-homolog, Rco3 of *N. crassa*, was found to influence gene expression and growth in response to glucose without possessing a C-terminal extension (Madi *et al.*, 1997). Since sugar uptake by Rco3 has not been demonstrated yet (Madi *et al.*, 1997), no fungal member of the sugar transporter family has been described to expose two functions as transporter and sensor. However, a putative dual function cannot be excluded for the proteins most similar to Hxt1, Hxt1p of *U. fabae* and Mst1 of *A. muscaria*. Both transporters have only been characterized with respect to their uptake abilities in *S. cerevisiae*, but not to their deletion phenotypes in the homologous systems (Nehls *et al.*, 1998; Voegelé *et al.*, 2001; Leandro *et al.*, 2006).

A dual function as transporter and sensor has been demonstrated for the human Na⁺/glucose symporter GLUT2 (Leturque *et al.*, 2009). The glucose sensing ability of

GLUT2 was found to be dependent on the large, cytoplasmatically localized loop between helix 6 and 7, which was further shown to interact with the nuclear importin karyopherin alpha2 (Guillemain *et al.*, 2000; Guillemain *et al.*, 2002). Similar to GLUT2 of humans, Hxt1 of *U. maydis* functions as monosaccharide facilitator and at the same time influences carbohydrate dependent gene expression. It is likely that also in Hxt1 the cytoplasmatic loop between helix 6 and 7 is involved in transducing a carbohydrate signal. In conclusion, Hxt1 of *U. maydis* is the first fungal member of the sugar transporter family with a dual function in carbohydrate transport and signaling.

Hxt1 Senses Starvation Conditions, Inducing Genes Involved in Mating and Pathogenic Development

Hxt1 responds to various monosaccharides available during fungal development within a maize plant (sucrose-derived: glucose and fructose; cell wall-derived: glucose, xylose, galactose and mannose). Hxt1 activity promotes growth on “primary” carbon sources; however, it negatively influences growth on the “secondary” carbon sources xylose and galactose. Thus, the question arises why Hxt1-mediated repression is maintained even at conditions where it impairs fungal growth? Firstly, the different affinities of Hxt1 towards various monosaccharides enable a fine-tuning of gene expression depending on the environmental carbohydrate conditions. Secondly, Hxt1-mediated sensing of several plant-derived carbon sources ensures that strictly Hxt1-repressed genes are only expressed when no sugar is available, like for example on the plant surface.

Interestingly, we identified two transcription factors, Prf1, and a protein with similarities to the *M. grisea* Con7, as repressed by Hxt1 independent from the provided carbon source. The zinc-finger transcription factor Con7 was shown to be essential for the induction of appressoria formation in *M. grisea* (Shi *et al.*, 1998; Odenbach *et al.*, 2007). Expression analysis of germinating spores on the plant surface has revealed that Con7 is required for induction of genes involved in the rearrangement of fungal cell walls (Odenbach *et al.*, 2007). In *U. maydis* *hxt1* deletion mutants, the *U. maydis* *con7* homolog is induced together with genes involved in remodeling of fungal chitin and glucan cell walls (Table 2.4-S6). Furthermore, 3 of 15 by Müller *et al.* (2008) identified genes that are coding for secreted repetitive proteins were highly induced in *hxt1* deletion strains (Table 2.4-S6). These proteins are thought to localize at the surface of fungal cell walls to mediate cell adhesion for

example to the plant surface (Müller *et al.*, 2008). Thus, the starvation conditions mimicked in *hxt1* deletion strains seem to promote *U. maydis* infection, by preparing the fungal cell surface for the penetration process and subsequent *in planta* development.

The *U. maydis* pheromon response factor Prf1 not only orchestrates pheromone-induced mating and the formation of the b-dependent infectious filament in *U. maydis*, but also integrates environmental signals into these developmental processes (Hartmann *et al.*, 1996; Hartmann *et al.*, 1999). In accordance with the findings by Hartmann *et al.* (1999) we could show that *prf1* expression in *U. maydis* wild type cells is slightly increased on glucose compared to xylose containing media. *prf1* induction is accompanied with the induction of the pheromone and pheromone receptor genes *mfa1* and *pra1*, which were shown to be *prf1*-dependently induced (Table 2.4-S7A and S7B; Hartmann *et al.*, 1996). However, the expression levels of *prf1*, *mfa1*, *pra1*, and of genes involved in pheromone signaling like *gpa3*, *bpp1* and *kpp6*, as well as of several pheromone-dependent genes, increased significantly when *hxt1* is deleted (Table 2.4-S7A and S7B; Regenfelder *et al.*, 1997; Müller *et al.*, 2004; Brachmann *et al.*, 2003). In addition, we observed an induction of the two pheromone-dependent transcription factor genes, *ncp1* and *rbf1* (Table 2.4-S7A and S7B; Hartmann *et al.*, 1999; Zarnack *et al.*, 2008). Ncp1 was shown to modulate Prf1-mediated gene expression in response to environmental carbon sources (Hartmann *et al.*, 1999), and Rbf1 was described as a central regulator of pathogenic development (Scherer *et al.*, 2006).

Our findings indicate that Hxt1 of *U. maydis* negatively influences the initiation of pathogenic development as a monosaccharide sensor. It is well possible that this negative response is released during the starvation conditions on the plant surface, where no substrate of Hxt1 is available to trigger a signaling event. Thus starvation conditions support the initiation of mating and plant infection by rendering Hxt1 inactive. Deletion of *hxt1* may mimic starvation conditions triggering, *prf1* expression to induce mating and pathogenicity, and *con7* expression to induce appressoria formation and prepare the fungal cell surface for *in planta* development.

Hxt1 Supports Biotrophic Growth most likely by Utilizing Hexoses Derived from Plant Sucrose

On the one hand, deletion of *hxt1* leads to an induction of genes that positively influence fungal pathogenicity, on the other hand it reduces fungal virulence. This contradiction is explained by the dual function of Hxt1. As discussed, Hxt1-mediated sensing is expected to be most important on the plant surface, where it is not activated. Under such carbohydrate-limiting conditions, also the transport function of Hxt1 is inactive. Since deletion of *hxt1* mimics these conditions, the deletion does not influence the infection process dramatically.

The situation during biotrophic growth within carbohydrate-rich plant tissues is different. Abolished carbohydrate sensing by Hxt1 does not seem to be responsible for reduced fungal virulence of *hxt1* deletion mutants, indicated by the induced expression of several pathogenicity factors *in axenic* culture. Moreover, none of the genes down-regulated in SG200 Δ *hxt1* could be related to the growth reduction on glucose containing media, which was observed for the mutant strains. Thus, it appears likely that reduced growth of *U. maydis* on glucose observed in *hxt1* deletion strains is caused by the lacking glucose transport activity of Hxt1. Since sucrose and, therefore, also its cleavage product glucose is a prominent carbon source *in planta*, reduced glucose uptake should result in reduced fungal virulence. However, an additional impact of Hxt1-mediated signaling on virulence of *U. maydis* cannot be excluded.

Nevertheless, the extremely high glucose affinity of Hxt1 (K_M of 6.6 μ M) enables *U. maydis* to compete with the most affine plant transporters for glucose utilization. All plant hexose transporters characterized so far (STPs) with sink tissue-specific expression have K_M values ranging between 10 and 100 μ M (Büttner, 2007). Moreover, the glucose affinity of Hxt1 was found to be 50- to 70-fold higher than those of the homologous transporters of *U. fabae* and *A. muscaria*, both of which also compete with the plant transporters for carbohydrates within their host plants (Nehls *et al.*, 1998; Voegelé *et al.*, 2001).

The reduction in virulence of *hxt1* deletion mutants was less severe than the reduction observed for the previously described deletion mutants of the sucrose transporter gene *srt1*. Thus, sucrose uptake by Srt1 seems more important during pathogenic development than hexose uptake by Hxt1. Moreover, the virulence of double deletion mutants of both Hxt1 and Srt1 was further reduced compared to

single deletion mutants. These findings place Hxt1 and Srt1 in two partially redundant carbon uptake systems promoting biotrophic development.

Sucrose was discussed several times to be the main carbon source for plant pathogens. Yet, the uptake of sucrose-derived hexoses, which are produced by fungus or plant invertases, was thought to be most important for pathogenicity (Fotopoulos *et al.*, 2003; Voegelé *et al.*, 2006; Jobic *et al.*, 2007; Schaarschmidt *et al.*, 2007; Horst *et al.*, 2008; Kocal *et al.*, 2008). For *Ustilago maydis*, the direct uptake of sucrose was demonstrated to be essential for biotrophic development (see 2.3). Here we report that also the uptake of sucrose-derived hexoses mediated by Hxt1 is important for successful biotrophic development of *U. maydis*. In contrast to Srt1, Hxt1 is dependent on prior invertase-driven sucrose hydrolysis to make use of the plants sucrose pool. Horst *et al.* (2008) have shown that both expression of the *U. maydis* invertase gene *suc2* as well as the maize cell wall invertase *incw2* is induced during the infection process. Furthermore, they demonstrated that soluble as well as cell wall bound invertase activity is increased during *U. maydis* infection (Horst *et al.*, 2008). Thus, the question arises if Suc2, the only potential secreted fungal invertase present in *U. maydis*, acts in concert with Hxt1 or if increased plant cell wall invertase activity is sufficient to supply Hxt1 with substrate. Since maize plants infected with *suc2* deletion mutants develop similar disease symptoms as plants infected with *U. maydis* wild type strains (R. Wahl and J. Kämper, unpublished data), it appears likely that plant cell wall invertases as Incw2 function to supply Hxt1 with hexoses during pathogenic development of *U. maydis*.

U. maydis seems to be perfectly suited to compete for plant-derived carbon sources, not only with the high affinity sucrose transporter Srt1, but in addition by use of the high affinity hexose transporter Hxt1. This parallel, functionally redundant carbon uptake system of *U. maydis* ensures the most effective carbon uptake for the fungus during biotrophic development.

2.4.4 Experimental Procedures

Strains and Growth Conditions

Escherichia coli strain TOP10 (Invitrogen) was used for cloning purposes. For plant infections, *Ustilago maydis* cells were grown at 28°C in YEPSL (Brachmann *et al.*, 2001). Plant infections with *U. maydis* were performed as described (Gillissen *et al.*, 1992). The *U. maydis* strain used in this study is SG200, a haploid, solopathogenic strain that can infect maize plants without a mating partner (Kämper *et al.*, 2006). For RNA extraction, *U. maydis* was grown in glutamine minimal medium, which is based on the minimal medium described by Holliday (Holliday, 1974) with 30 mM L-glutamine as nitrogen source. Phenotypic analyses of *U. maydis* deletion mutants were performed on glutamine or nitrate minimal medium containing agar plates supplemented with the respective carbon source (see 2.4.2 Results). The *S. cerevisiae* strain used for analyses of Hxt1 was EBY.VW4000 (Wieczorke *et al.*, 1999). EBY.VW4000 was grown in minimal medium (0.67 % yeast nitrogen base w/o amino acids plus required amino acids depending on the strain) containing 2% maltose at 29 °C. Complementation studies in EBY.VW4000 were carried out on minimal medium containing the respective hexose concentrations (see 2.4.2 Results).

DNA and RNA Procedures

Molecular methods followed described protocols (Sambrook *et al.*, 1989). DNA isolation from *U. maydis* and transformation procedures were performed as described (Schulz *et al.*, 1990). Homologous integration of constructs was verified by gel blot analyses. Transformation of *S. cerevisiae* followed the protocol given in Gietz *et al.* (1992). Total RNA from *U. maydis* cells grown in axenic culture was extracted using Trizol reagent (Invitrogen) according to the manufacturer's instructions. RNA samples to be used for real-time RT-PCR and DNA array expression analyses were further column purified (RNeasy; Qiagen) and the quality checked using a Bioanalyzer with an RNA 6000 Nano LabChip kit (Agilent).

Deletion of hxt1 and snf1

The deletions of *hxt1* and *snf1* were performed by a PCR-based approach (Kämper, 2004). For single deletion of *hxt1* and *snf1* in SG200 the respective open reading

frame (ORF) was replaced by the hygromycin resistance cassette. Double deletion mutants of *hxt1* and *snf1* were generated in SG200 Δ *hxt1*, replacing the *snf1* ORF with the CloneNat resistance cassette. Double deletion mutants of *hxt1* and *srt1* were generated in SG200 Δ *srt1* (see 2.3), replacing the *hxt1* ORF with the CloneNat resistance cassette. Primer sequences were 5023_LB1 (5'-GTG AAC AAC CGT GGT CTG CTC ACC-3'), 5023_LB2 (5'-GTT GGC CAT CTA GGC CGC CAT CTT GAA AGA GAG AGA GAG C-3'), 5023_RB1 (5'-CAC GGC CTG AGT GGC CTG CCG TAT GGC AAT GCT TTC TAC C-3') and 5023_RB2 (5'-TTT GCT CAG CGT CGA TTA TTC ACG-3') for the 5'- and 3'-boarders of *hxt1* and 11293_LB1 (5'-TTT TGA GTT GGG TGG GAG CTC ACG-3'), um11293_LB2 (5'-GTT GGC CAT CTA GGC CGG CAG GCA CAG AAA ATC GCT ATG G-3'), um11293_RB1 (5'-GTT GGC CTG AGT GGC CTC GGT CTC GTA CCA AGG AGC TTC G-3') and um11293_RB2 (5'-TAG AGC GAG CTG ACG ATG TTG GGC-3') for the 5'- and 3'-boarders of *snf1*. In the *U. maydis* strain carrying the triple *gfp* gene fused to the *hxt1* promotor, the *hxt1* ORF was replaced with a triple GFP cassette containing the hygromycin resistance gene using the same strategy as for the generation of simple deletion strains (Kämper, 2004; Brachmann *et al.*, 2004). Primer sequences were like indicated above with the exception of 5023_LB2.gfp (5'-GAT GGC CGC GTT GGC CGC CAT CTT GAA AGA GAG AGA GAG C-3') carrying a Sfil site compatible to the fusion cassette.

Cloning of hxt1 and Expression in Yeast

The *hxt1* open reading frame (ORF) was amplified from *U. maydis* genomic DNA using the primers 5023_EcoRI_for (5'-CAG AAT TCA AAA ATG GCT GGA GGT GCT GTT GCC GAT-3') and 5023_EcoRI_rev (5'-CAG AAT TCG CAG AGC TGC TTA GTA CTT TTT CT-3'). DNA was sequenced and cloned into the yeast/*E. coli* shuttle vector NEV-E (Sauer and Stolz, 1994) and the resulting plasmid was used for yeast transformation into EBY.VW4000.

Transport Studies with Radiolabeled Substrates

Yeast cells were grown to an $A_{600\text{ nm}}$ of 1.0, harvested, washed twice with water and re-suspended in buffer to an $A_{600\text{ nm}}$ of 10.0. If not otherwise indicated, uptake experiments were performed in 50-mM Na-phosphate buffer pH 5.0 with an initial substrate concentration of 1-mM ^{14}C -labeled glucose. Cells were shaken in a rotary

shaker at 29°C and transport tests were started by adding labeled substrate. Samples were withdrawn at given intervals, filtered on nitrocellulose filters (0.8 µm pore size) and washed with an excess of distilled H₂O. Incorporation of radioactivity was determined by scintillation counting. Competition analyses were performed with 0.1-mM ¹⁴C-glucose in the presence of 10-mM competitor (100-fold excess). For inhibitor analyses CCCP (carbonylcyanide *m*-chlorophenylhydrazone), DNP (2,4-dinitrophenol) or PCMBS (*p*-chloromercuribenzene sulfonate) were used at final concentrations of 50 µM.

Light Microscopy

Light microscopic analyses were performed using a Zeiss Axioplan 2 microscope. Photomicrographs were obtained with an Axiocam HrM camera, and the images were processed with Axiovision (Zeiss) and Photoshop (Adobe). Chlorazole Black E staining of fungal cells *in planta* was performed as described (Brachmann *et al.*, 2003).

Quantitative Real Time PCR Analysis

To analyze *hxt1* expression on different carbon sources, SG200 was grown in glutamine minimal media supplemented with the indicated amount of the respective carbon source to an OD600 of 1.0 for 6 h. Pre-cultures were grown overnight in glutamine minimal medium containing 1% of glucose. RNA samples were frozen in liquid nitrogen for two independently conducted replicates. RNA of maize plants infected with SG200 was prepared as described (Doehlemann *et al.*, 2008a). Samples were taken 0.5, 1, 2, 4 and 8 dpi. For cDNA synthesis, the SuperScript III first-strand synthesis SuperMix assay (Invitrogen) was used on 1 µg of total RNA. qRT-PCR was performed on a Bio-Rad iCycler using the Platinum SYBR Green qPCR SuperMix-UDG (Invitrogen). The *U. maydis actin* (um11232) and *eIF2B* (um04869) genes were used as references. Primer sequences for *eIF2B*, *actin* and *srt1* were described by Wahl *et al.* 2009. Primer sequences were 5023_rt_for (5'-CTC ATT GTT GCC GTT GTC GGT ACC -3') and 5023_rt_rev (5'-AAA CCG GCA ATG TAG ATG CAG ACG-3') for *hxt1*.

DNA Microarray Expression Analyses

To analyze expression changes of SG200 and SG200 Δ *hxt1* both strains were grown in glutamine minimal array media supplemented with 1% glucose or 1 %xylose to an OD600 of 1.0 for 6 h, respectively (Scherer *et al.*, 2006). Pre-cultures were grown overnight in glutamine minimal medium containing 1% of glucose. RNA samples were frozen in liquid nitrogen for two independently conducted replicates. Isolation and processing of RNA from fungal cells grown in axenic culture, on the plant surface and in tumor material was described previously (Eichhorn *et al.*, 2006; Doehlemann *et al.*, 2008b; Kämper *et al.*, 2006). Affymetrix Gene chip^R *Ustilago* genome arrays were conducted using the following standard Affymetrix protocols (staining: EukGe2V4 protocol on GeneChip Fluidics Station 400; scanning on Affymetrix GSC3000). Expression data were submitted to GeneExpressionOmnibus (<http://www.ncbi.nlm.nih.gov/geo/>), Accession GSE16634. Raw expression data were normalized using Affymetrix Micro Array Suite 5.1. Data analysis was performed using the R bioconductor package (<http://www.bioconductor.org/>) and dChip1.3 (<http://biosun1.harvard.edu/complab/dchip/>), as described in Eichhorn *et al.* (2006). We considered changes >2-fold with a difference between expression values >50 and a corrected p-value <0.01 as significant. For genes displayed by more than one probe set, the probe set giving the strongest signal intensity was chosen. Functional enrichment analyses were performed with the functional distribution tool integrated in the *Ustilago maydis* genome database (<http://mips.gsf.de/cgi-bin/proj/funcatDB/>). Enrichment was considered to be significant with a p-Value below 0.01.

Phylogenetic Analysis

For comparative phylogenetic analyses of Hxt1, the amino acid sequence was aligned with 18 *U. maydis* sugar transporter sequences (see 2.3), 17 *S. cerevisiae* sugar transporter sequences and 6 closely related sugar transporter genes from other fungal species obtained by BLASTP analysis (Figure 2.4-2A). *U. maydis* and *S. cerevisiae* ammonium transporter sequences served as out-group (Figure 2.4-2A). For comparative phylogenetic analyses of Snf1, the amino acid sequence was aligned with Sequences were aligned with 24 fungal, 5 plant and 4 animal derived Snf1 sequences obtained by BLASTP. An *U. maydis* Snf1-like kinase sequence served as outgroup. Alignments were performed using the global alignment G-INS-I of MAFFT version 6 (<http://align.bmr.kyushu-u.ac.jp/mafft/online/server/>). The phylogenetic trees were calculated using the minimum linkage clustering method for

Hxt1 and the Neighbour Joining method for Snf1 (for the latter 1000 bootstraps were performed). Treeillustrator 1.0.1 was used to visualize the Nexus formats of the MAFFT results.

2.4.5 Supplementary Information

A file containing the Supplementary Material of section 2.4 is available on data-CD deposited in section 5 of this thesis. The file includes Figures 2.4-S1 to S2 and Tables 2.4-S1 and S7.

Figure 2.4-S1: Comparative alignment of Snf1 proteins from various fungi.

Figure 2.4-S2: Comparative phylogenetic analysis of *U. maydis* Snf1.

Table 2.4-S1: Accession numbers, gene- and species names of the sugar transport proteins used to calculate the phylogenetic tree shown in Figure 2.4-2A.

Table 2.4-S2A: *U. maydis* genes that are Hxt1-dependently expressed on glucose.

Table 2.4-S2B: *U. maydis* genes that are Hxt1-dependently expressed on xylose.

Table 2.4-S2C: *U. maydis* genes that are carbon source-dependently expressed in SG200.

Table 2.4-S2D: *U. maydis* genes that are carbon source-dependently expressed in SG200 Δ *hxt1*.

Table 2.4-S3: Enrichment analysis of functional categories.

Table 2.4-S4: Xylose-induced genes and xylose-induced genes repressed by Hxt1.

Table 2.4-S5: Most genes (de)-repressed in SG200 Δ *hxt1* are also (de)-repressed on the plant surface.

Table 2.4-S6: *con7* and genes involved in remodeling the fungal cell wall are induced in SG200 Δ *hxt1*.

Table 2.4-S7A: Pheromone-induced genes differentially expressed in *hxt1* deletion mutants.

Table 2.4-S7B: *prf1* and genes that are connected to the pheromone pathway are induced in SG200 Δ *hxt1*.

Acknowledgements

This work was funded by a grant from the German Research Foundation (FOR666) to N. Sauer and J. Kämpfer. Microarray analysis was supported by grant 0312738 from BMBF to R. Kahmann and J. Kämpfer. We wish to thank R. Kahmann and the Max-Planck-Institute for terrestrial Microbiology for support, V. Vincon for excellent technical assistance and K. HeimeI, M. Vranes and A. Zahiri for critical comments on the manuscript.

3. Research Perspectives

This discussion will focus on the contribution of the results given in sections 2.1 - 2.4 to the broader context of “mechanisms of compatibility”, and will provide a general outlook for the respective research projects.

3.1 b-mediated Transcriptome Adaptation during Biotrophic Development

The importance of the b heterodimer to initiate pathogenicity of *U. maydis* has been studied intensively (Kämper *et al.*, 1995; Romeis *et al.*, 2000; Brachmann *et al.*, 2003). Time course expression analysis after b induction in axenic culture revealed about 350 directly or indirectly b-regulated genes and led to the identification of several pathogenicity factors, including Clp1 and the transcription factors Rbf1 and Biz1 (Scherer *et al.*, 2006; Flor-Parra *et al.*, 2006; M. Scherer and J. Kämper, unpublished data). However, all of these factors were shown to be required before, during and/or immediately after plant penetration. Only a minor overlap between b-dependently regulated genes in axenic culture and *in planta*-expressed genes was observed (M. Vranes and J. Kämper, personal communication), arguing that b-mediated transcriptional regulation is altered within the plant. I was able to show that b-mediated transcription in *U. maydis* is not only essential for the initiation, but also for the maintenance of pathogenic development (section 2.1). Therefore, I believe that the b-mediated transcription profile is adapted to the different stages of pathogenic development.

The b-dependent adaption of the transcriptome is most likely triggered by sensing plant-derived environmental cues. Hydrophobic surfaces and cutin-monomers for example were reported to trigger the formation of appressoria on the plant surface (Mendoza-Mendoza *et al.*, 2009). Moreover, under starvation conditions the monosaccharide transporter and receptor Hxt1 positively influences pheromone signaling and the expression of transcription factors like prf1 and rbf1, which are necessary for pathogenic development (section 2.4). However, plant-derived signals that modify the b-dependent transcription cascade during *in planta* proliferation of *U. maydis* have not been discovered yet. As expression of many secreted effectors is regulated by b only during biotrophic development, their expression is most likely dependent on environmental cues. Suggesting an environment-dependent fine-tuning of the abilities to manipulate the host plant. Several of these secreted proteins were found to influence pathogenic development of *U. maydis* (Kämper *et al.*, 2006; Doehlemann *et al.*, 2009); however, a specific function could not be addressed so far.

In section 2.2 it is reported that upon sensing of *U. maydis* on the plant surface, basic defense responses are induced by the host, which are suppressed after penetration by *U. maydis* (Doehlemann *et al.*, 2008a). Similar to their function in other plant pathogens, it is likely that the observed suppression of basal plant defense responses is actively mediated by small secreted effector proteins of *U. maydis*.

The importance of the b-heterodimer during fungal proliferation and for the expression of secreted proteins *in planta* reveals new perspectives to analyze the regulation of pathogenic development. We identified three genes coding for putative transcription factors as b dependently expressed during biotrophic growth (Section 2.1). Since these transcription factors are exclusively expressed within the plant, they most likely integrate additional environmental cues into the b-dependent regulatory cascade. The characterization of such b-dependent transcription factors enables not only to discover the environmental cues that modify the b-dependent transcriptome, but also to investigate the regulation of secreted effectors. By examining the b-dependent transcription cascade *in planta*, it should be possible to identify secreted proteins that are regulated in a similar manner, which might therefore share similar functions. To functionally classify these small secreted effector proteins is the major future challenge (see section 1.3.2). The possibility to analyze the expression profiles of the *U. maydis* effectors by dissecting the b-mediated transcription cascade is a valuable starting point to identify common motives.

Besides the regulatory characterization of secreted proteins, the b-heterodimer also paves the way for the investigation of non-secreted, strictly *in planta* expressed *U. maydis* genes, like *srt1* and *suc2*. Both genes are expressed only after plant penetration, and their expression pattern was found to be similar (section 2.3; Horst *et al.*, 2008) Since sucrose is the substrate of both gene products, one can assume a common regulatory circuit. Interestingly, both genes are down-regulated when the b heterodimer is inactive *in planta* (see section 2.1; below cut-off, *suc2* -1.9-fold and *srt1* -1.6-fold). It is well feasible that one of the transcription factors down-regulated after b inactivation accounts for the down-regulation of *srt1* and *suc2* *in planta*. In conclusion, the investigation of b-dependent regulation allows to dissect the specific molecular pathways and processes, which are restricted to *in planta* development and were previously difficult to access.

3.2 Fungal Sugar Transporters and Their Contribution to Feed *U. maydis* and to Reprogram the Host Metabolism

In general, one could imagine two main strategies a pathogen might use to access plant-derived carbon sources during phytopathogenic development. One possibility is the degradation of carbon backbones of plant cell walls and subsequent uptake of hexoses and/or pentoses by the pathogen. The other strategy would be to nourish on the plants primary metabolism by either metabolizing the plants photosynthesis products or the plants transport and storage carbohydrates.

The first strategy is unlikely to play a major role within the *Ustilago maydis*/maize pathosystem. Maize cell walls consist mainly of cellulose and arabinoxylan, which are composed of glucose and xylose backbones respectively (Carpita, 1996; Carpita *et al.*, 2001; Abedon *et al.*, 2006). Thus, degradation of both cell wall structures to the respective monomers would be a prerequisite for *U. maydis* to feed on cell wall derived carbon sources. However, Doehlemann *et al.* (2008) reported that *U. maydis* is poorly equipped with plant cell wall degrading enzymes. In addition, *U. maydis* lacks the enzymes cellobiohydrolase and β -xylosidase, which are both required for the complete degradation of maize cell wall structures into the monomers glucose and xylose (Doehlemann *et al.*, 2008b). Therefore, it appears unlikely that *U. maydis* feeds on plant cell wall products, a strategy often used by necrotrophic fungi, which possess numerous cell wall degrading enzymes to dissolve the plant cells.

For biotrophic fungi like *U. maydis* it is more effective to nourish on the hosts primary metabolism to access its carbon sources; most likely by interfering with the carbon transport system of the plant. This hypothesis is supported by several findings of this work and of others. Firstly, *U. maydis* prefers to infect young meristematic sink tissue that is not yet photosynthetically active (Wenzler and Meins, 1987). Secondly, *U. maydis* infected tissues retain sink characteristics and do not differentiate into photosynthetic active source tissue (2.2; (Horst *et al.*, 2008; Doehlemann *et al.*, 2008a). Thirdly, carbon export from healthy leaves is increased after infection, while it was found to be reduced in *U. maydis* infected tissues (Billett and Burnett, 1978). Fourthly, carbon supply of *U. maydis* infected sink tissue is mediated via sucrose import, indicated by an increased expression of transcripts related to sucrose degradation, and by increased levels of free hexoses derived from sucrose cleavage (2.2; Horst *et al.*, 2008; Doehlemann *et al.*, 2008a). In conclusion, the uptake of sucrose and its cleavage products appears to be essential for pathogenic development of *U. maydis* (2.3 and 2.4).

The sink characteristics of the infected plant tissue apparently support the biotrophic lifestyle of *U. maydis*. Pathogen induced sink tissues are typically induced by increased plant and/or pathogen derived invertase activities, leading to higher hexose to sucrose ratios, a subsequent repression of photosynthesis and the induction of defense related genes (Kocal *et al.*, 2008; Roitsch *et al.*, 2003; Rolland *et al.*, 2006; Voegelé *et al.*, 2006; Horst *et al.*, 2008). The preference of *U. maydis* to infect young meristematic tissues, which are still in a sink state (Wenzler and Meins, 1987) would suggest that no secreted fungal invertases are required to promote the induction of a sink. This hypothesis is supported by the finding that deletion of *suc2*, the only gene encoding a secreted invertase, has no impact on pathogenic development of *U. maydis* (data not shown).

U. maydis rather relies on sugar transporters like Srt1 and Hxt1 to maintain sink character of the infected tissue. By their high substrate affinities these two transporters have the potential to transform the growing hyphae into a strong fungal sink *in planta*, maintaining sucrose import into infected areas. This constant sucrose import should lead to plant cell wall invertase activity, and high levels of free hexoses, which trigger suppression of photosynthesis, as described previously (Kocal *et al.*, 2008; Roitsch *et al.*, 2003; Rolland *et al.*, 2006; Voegelé *et al.*, 2006; Horst *et al.*, 2008). Therefore, these two transporters seem to promote fungal growth by providing enough energy for pathogenic development, and by redirecting the host metabolism to favor *U. maydis* infection. Yet, we cannot exclude that in addition to transport of carbohydrates other functions of Srt1 and Hxt1, like for example carbohydrate perception influence pathogenic development of *U. maydis*.

The following outlook will provide ideas, how to investigate the contribution of Srt1 and Hxt1 towards successful biotrophic development of *U. maydis* in more detail. To analyze substrate specificity and function of Srt1 and Hxt1 during biotrophic growth, their respective genes should be replaced with genes of well-characterized transporters. The complementation of Srt1 by different plant transporters, exhibiting different affinities towards sucrose, might verify if its extreme high substrate affinity renders Srt1 a virulence factor.

By complementing Hxt1 with different yeast transporters it is possible to separate its transport and its sensing function. Its transport function can be investigated by complementation with Hxt1 of *S. cerevisiae*, a strict glucose transporter; whereas its sensor function can be investigated by complementation with Rgt2 of *S. cerevisiae* (or its derivative with truncated C-terminal tail; Moriya and Johnston, 2004), a strict

glucose sensor. In addition it might be possible to separate sensing and transport function of Hxt1 by directed mutation of the arginine at amino acid position 164 to lysine. Similar mutations at orthologous positions in Rgt2 and Snf3 transform the proteins to permanent sensors (Ozcan *et al.*, 1996). As the corresponding arginine is conserved in all known sugar transporters its mutation is likely to also interfere with sugar transport (Ozcan *et al.*, 1996). In accordance the mutation of arginine 164 to lysine in Hxt1 might render it a permanent glucose sensor without transport ability. Determining which features of Srt1 and Hxt1 play a major role during biotrophic development will clarify the importance of their substrates for fungal growth *in planta*.

To understand the contribution of fungal enzymes in intra- and/or extracellular sucrose cleavage during pathogenic development, alternative sucrose-degrading enzymes have to be investigated in more detail. In addition to *Suc2*, *U. maydis* harbors a potential alpha glucosidase (Um02740), which is predicted as secreted. However, unlike *suc2*, *um02740* expression *in planta* is below the detection limit of the microarrays, arguing for a minor role in extra cellular sucrose degradation (DNA array data not shown). Thus, if extracellular sucrose cleavage is important for biotrophic development of *U. maydis*, it is most probably performed by plant-derived invertases, such as *incw2* of maize (Horst *et al.*, 2008). Furthermore, *U. maydis* harbors two cytoplasmatically localized alpha-glucosidases (Um01943, Um03692) and a sucrose-6-phosphate hydrolase (Um03605), likely to be involved in sucrose degradation after uptake by Srt1. At least multiple deletion mutants of combinations of invertases and alpha-glucosidases should disrupt intracellular sucrose cleavage resulting in similar effects on pathogenicity as deletion of *srt1*.

Furthermore, the temporal and spatial expression of Hxt1 and Srt1 has to be analyzed. Localization of the respective proteins by fusion to GFP, should determine if the proteins are expressed at a specific time, in specific cells, and in specific plant tissues. Of particular interest is to analyze the local response of plant cells to an *U. maydis* infection. A central question is how different plant tissues respond towards strains altered in their ability to take up sucrose and glucose. Previously, such an approach has been performed via expression analysis of infected laser-microdissected plant tissues (Tang *et al.*, 2006). Another focus will be the identification of pathogen induced plant sugar transporters that are either involved in local nutrient supply of the fungus or in local depletion of carbon sources to restrict fungal growth. Two potential candidate genes of maize coding for putative homologs of the *Arabidopsis thaliana* monosaccharide transporter STP4 have already been identified to be up-regulated upon *U. maydis* infection (see section 2.2; Table 2.2-S2;

ZmAfx.7.1.S1_at; Zm.18239.1.S1_at). STP4 is induced in response to elicitor-treatment and infection with *Erysiphe cichoracearum* (Fotopoulos *et al.*, 2003). The pathogen-dependent expression of these STP4-like plant transporters points towards their possible function, either in starving the pathogen or supplying it with carbohydrates.

Plant transporters that are induced to deplete carbon availability during pathogenic interactions are interesting targets to develop plants that are more resistant towards pathogen attacks. Even better suited for the production of resistant plants is the *U. maydis* transporter Srt1. Its very high sucrose affinity is discussed to outcompete the plant sucrose transporters during *U. maydis* infection. Plants over-expressing the fungal *srt1* gene in turn should be capable to reduce the carbohydrate availability in the plant/fungus interface to a higher extent. Thus, Srt1 might be an interesting target to enhance plant resistance towards pathogens without introducing harmful and toxic compounds that usually kill the pathogen and might have unpredictable side effects.

4. Literature

- Abedon, B.G., Hatfield, R.D., and Tracy, W.F.** (2006) Cell wall composition in juvenile and adult leaves of maize (*Zea mays L.*). *J Agric Food Chem* **54**: 3896-3900.
- Abramovitch, R.B., and Martin, G.B.** (2004) Strategies used by bacterial pathogens to suppress plant defenses. *Curr Opin Plant Biol* **7**: 356-364.
- Ahuatzi, D., Riera, A., Peláez, R., Herrero, P., and Moreno, F.** (2007) Hxk2 regulates the phosphorylation state of Mig1 and therefore its nucleocytoplasmic distribution. *J Biol Chem* **282**: 4485-4493.
- Alvarez, M.E., Pennell, R.I., Meijer, P.J., Ishikawa, A., Dixon, R.A., and Lamb, C.** (1998) Reactive oxygen intermediates mediate a systemic signal network in the establishment of plant immunity. *Cell* **92**: 773-784.
- Alves, S.L., Herberts, R.A., Hollatz, C., Trichez, D., Miletti, L.C., de Araujo, P.S., and Stambuk, B.U.** (2008) Molecular analysis of maltotriose active transport and fermentation by *Saccharomyces cerevisiae* reveals a determinant role for the AGT1 permease. *Appl Environ Microbiol* **74**: 1494-1501.
- Ayres, P.G., Press, M.C., and Spencer-Phillips, P.T.N.** (1996) Effects of pathogens and parasitic plants on source-sink relationships. *Photoassimilate Distribution in Plants and Crops, Source-Sink Relationships* : 479-499.
- Banuett, F.** (1995) Genetics of *Ustilago maydis*, a fungal pathogen that induces tumors in maize. *Annu Rev Genet* **29**: 179-208.
- Banuett, F., and Herskowitz, I.** (1989) Different a alleles of *Ustilago maydis* are necessary for maintenance of filamentous growth but not for meiosis. *Proc Natl Acad Sci USA* **86**: 5878-5882.
- Banuett, F., and Herskowitz, I.** (1994) Morphological transitions in the life cycle of *Ustilago maydis* and their genetic control by the a and b loci. *Exp. Mycology* **18**: 247-266.
- Banuett, F., and Herskowitz, I.** (1996) Discrete developmental stages during teliospore formation in the corn smut fungus, *Ustilago maydis*. *Development* **122**: 2965-2976.
- Basse, C.W.** (2005) Dissecting defense-related and developmental transcriptional responses of maize during *Ustilago maydis* infection and subsequent tumor formation. *Plant Physiol* **138**: 1774-1784.
- Bauer, R., Oberwinkler, F., and Vanky, K.** (1997) Ultrastructural markers and systematics in smut fungi and allied taxa. *Can J Bot* **75**: 1273 - 1314.
- Baureithel, K., Felix, G., and Boller, T.** (1994) Specific, high affinity binding of chitin fragments to tomato cells and membranes. Competitive inhibition of binding by derivatives of chitooligosaccharides and a Nod factor of *Rhizobium*. *J Biol Chem* **269**: 17931-17938.

- Belenghi, B., Acconcia, F., Trovato, M., Perazzolli, M., Bocedi, A., Polticelli, F., et al.** (2003) AtCYS1, a cystatin from *Arabidopsis thaliana*, suppresses hypersensitive cell death. *Eur J Biochem* **270**: 2593-2604.
- Bendtsen, J.D., Nielsen, H., von Heijne, G., and Brunak, S.** (2004) Improved prediction of signal peptides: SignalP 3.0. *J Mol Biol* **340**: 783-795.
- Bergmeyer, H.U.** Methoden der enzymatischen Analyse. Verlag Chemie.
- Biemelt, S., and Sonnewald, U.** (2006) Plant-microbe interactions to probe regulation of plant carbon metabolism. *J Plant Physiol* **163**: 307-318.
- Billett, E.E., and Burnett, J.H.** (1978) Physiological plant pathology. .
- Birch, P.R., Boevink, P.C., Gilroy, E.M., Hein, I., Pritchard, L., and Whisson, S.C.** (2008) Oomycete RXLR effectors: delivery, functional redundancy and durable disease resistance. *Curr Opin Plant Biol* **11**: 373-379.
- Birch, P.R., Rehmany, A.P., Pritchard, L., Kamoun, S., and Beynon, J.L.** (2006) Trafficking arms: oomycete effectors enter host plant cells. *Trends Microbiol* **14**: 8-11.
- Bohlmann, R., Schauwecker, F., Basse, C., and Kahmann, R.** (1994) Genetic regulation of mating and dimorphism in *Ustilago maydis*, In Advances in Molecular Genetics of Plant-Microbe Interactions. Daniels, M.J. (eds). Dordrecht: Kluwer Acad. Publ., pp. 239-245.
- Bolton, M.D., van Esse, H.P., Vossen, J.H., de Jonge, R., Stergiopoulos, I., Stulemeijer, I.J., et al.** (2008) The novel *Cladosporium fulvum* lysin motif effector Ecp6 is a virulence factor with orthologues in other fungal species. *Mol Microbiol* **69**: 119-136.
- Bos, J.I., Kanneganti, T.D., Young, C., Cakir, C., Huitema, E., Win, J., et al.** (2006) The C-terminal half of *Phytophthora infestans* RXLR effector AVR3a is sufficient to trigger R3a-mediated hypersensitivity and suppress INF1-induced cell death in *Nicotiana benthamiana*. *Plant J* **48**: 165-176.
- Bölker, M., Genin, S., Lehmler, C., and Kahmann, R.** (1995) Genetic regulation of mating, and dimorphism in *Ustilago maydis*. *Can J Bot* **73**: 320-325.
- Bölker, M., Urban, M., and Kahmann, R.** (1992) The a mating type locus of *U. maydis* specifies cell signaling components. *Cell* **68**: 441-450.
- Brachmann, A., König, J., Julius, C., and Feldbrügge, M.** (2004) A reverse genetic approach for generating gene replacement mutants in *Ustilago maydis*. *Mol Genet Genomics* **272**: 216-226.
- Brachmann, A., Schirawski, J., Müller, P., and Kahmann, R.** (2003) An unusual MAP kinase is required for efficient penetration of the plant surface by *Ustilago maydis*. *EMBO J* **22**: 2199-2210.
- Brachmann, A., Weinzierl, G., Kämper, J., and Kahmann, R.** (2001) Identification of genes in the bW/bE regulatory cascade in *Ustilago maydis*. *Mol Microbiol* **42**: 1047-1063.
- Brader, G., Tas E, and Palva, E.T.** (2001) Jasmonate-dependent induction of indole glucosinolates in *Arabidopsis* by culture filtrates of the nonspecific pathogen *Erwinia carotovora*. *Plant Physiol* **126**: 849-860.

- Brown, V., Sabina, J., and Johnston, M.** (2009) Specialized sugar sensing in diverse fungi. *Curr Biol* **19**: 436-441.
- Brown, V., Sexton, J.A., and Johnston, M.** (2006) A glucose sensor in *Candida albicans*. *Eukaryot Cell* **5**: 1726-1737.
- Bruce, R.J., and West, C.A.** (1989) Elicitation of Lignin Biosynthesis and Isoperoxidase Activity by Pectic Fragments in Suspension Cultures of Castor Bean. *Plant Physiol* **91**: 889-897.
- Büttner, M.** (2007) The monosaccharide transporter(-like) gene family in Arabidopsis. *FEBS Lett* **581**: 2318-2324.
- Büttner, M., and Sauer, N.** (2000) Monosaccharide transporters in plants: structure, function and physiology. *Biochim Biophys Acta* **1465**: 263-274.
- Callow, J.A., and Ling, I.T.** (1973) Histology of neoplasms and chlorotic lesions in maize seedlings following the injection of sporidia of *Ustilago maydis* (DC) Corda. *Physiol Plant Pathol* **3**: 489-494.
- Carlson, M., Osmond, B.C., and Botstein, D.** (1981) Mutants of yeast defective in sucrose utilization. *Genetics* **98**: 25-40.
- Carpita, N.C.** (1996) Structure and biogenesis of the cell walls of grasses. *Annu Rev Plant Physiol Plant Mol Biol* **47**: 445-476.
- Carpita, N.C., Defernez, M., Findlay, K., Wells, B., Shoue, D.A., Catchpole, G., et al.** (2001) Cell wall architecture of the elongating maize coleoptile. *Plant Physiol* **127**: 551-565.
- Catanzariti, A.M., Dodds, P.N., Lawrence, G.J., Ayliffe, M.A., and Ellis, J.G.** (2006) Haustorially expressed secreted proteins from flax rust are highly enriched for avirulence elicitors. *Plant Cell* **18**: 243-256.
- Cánovas, D., and Pérez-Martín, J.** (2009) Sphingolipid biosynthesis is required for polar growth in the dimorphic phytopathogen *Ustilago maydis*. *Fungal Genet Biol* **46**: 190-200.
- Chalker-Scott, L.** (1999) Environmental significance of anthocyanins in plant stress responses. *Photochemistry and Photobiology* **70**: 1-9.
- Chang, J.H., Goel, A.K., Grant, S.R., and Dangl, J.L.** (2004) Wake of the flood: ascribing functions to the wave of type III effector proteins of phytopathogenic bacteria. *Curr Opin Microbiol* **7**: 11-18.
- Cheng, Q., and Michels, C.A.** (1991) MAL11 and MAL61 encode the inducible high-affinity maltose transporter of *Saccharomyces cerevisiae*. *J Bacteriol* **173**: 1817-1820.
- Chinchilla, D., Zipfel, C., Robatzek, S., Kemmerling, B., Nürnberger, T., Jones, J.D., et al.** (2007) A flagellin-induced complex of the receptor FLS2 and BAK1 initiates plant defence. *Nature* **448**: 497-500.
- Chisholm, S.T., Coaker, G., Day, B., and Staskawicz, B.J.** (2006) Host-microbe interactions: shaping the evolution of the plant immune response. *Cell* **124**: 803-814.

- Chou, H.M., Bundock, N., Rolfe, S.A., and Scholes, J.D.** (2000) Infection of *Arabidopsis thaliana* leaves with *Albugo candida* (white blister rust) causes a reprogramming of host metabolism. *Molecular Plant Pathology* **1**: 99-113.
- Christensen, J.J.** (1963) Corn smut induced by *Ustilago maydis*. *Amer Phytopathol Soc Monogr* **2**.
- Cohen, S.A., and Michaud, D.P.** (1993) Synthesis of a fluorescent derivatizing reagent, 6-aminoquinolyl-N-hydroxysuccinimidyl carbamate, and its application for the analysis of hydrolysate amino acids via high-performance liquid chromatography. *Analytical biochemistry* **211**: 279-287.
- Cziferszky, A., Seiboth, B., and Kubicek, C.P.** (2003) The Snf1 kinase of the filamentous fungus *Hypocrea jecorina* phosphorylates regulation-relevant serine residues in the yeast carbon catabolite repressor Mig1 but not in the filamentous fungal counterpart Cre1. *Fungal Genet Biol* **40**: 166-175.
- Dangl, J.L., and Jones, J.D.** (2001) Plant pathogens and integrated defence responses to infection. *Nature* **411**: 826-833.
- David, H., Krogh, A.M., Roca, C., Akesson, M., and Nielsen, J.** (2005) CreA influences the metabolic fluxes of *Aspergillus nidulans* during growth on glucose and xylose. *Microbiology* **151**: 2209-2221.
- Dean, R.A., Talbot, N.J., Ebbole, D.J., Farman, M.L., Mitchell, T.K., Orbach, M.J., et al.** (2005) The genome sequence of the rice blast fungus *Magnaporthe grisea*. *Nature* **434**: 980-986.
- Deising, H.B., Werner, S., and Wernitz, M.** (2000) The role of fungal appressoria in plant infection. *Microbes Infect* **2**: 1631-1641.
- Dodds, P.N., Lawrence, G.J., Catanzariti, A.M., Teh, T., Wang, C.I., Ayliffe, M.A., et al.** (2006) Direct protein interaction underlies gene-for-gene specificity and coevolution of the flax resistance genes and flax rust avirulence genes. *Proc Natl Acad Sci U S A* **103**: 8888-8893.
- Doehlemann, G., van der Linde, K., Assmann, D., Schwammbach, D., Hof, A., Mohanty, A., et al.** (2009) Pep1, a secreted effector protein of *Ustilago maydis*, is required for successful invasion of plant cells. *PLoS Pathog* **5**: e1000290.
- Doehlemann, G., Wahl, R., Horst, R.J., Voll, L.M., Usadel, B., Poree, F., et al.** (2008a) Reprogramming a maize plant: transcriptional and metabolic changes induced by the fungal biotroph *Ustilago maydis*. *Plant J* **56**: 181-195.
- Doehlemann, G., Wahl, R., Vranes, M., de Vries, R.P., Kämper, J., and Kahmann, R.** (2008b) Establishment of compatibility in the *Ustilago maydis*/maize pathosystem. *J Plant Physiol* **165**: 29-40.
- Dudler, R., Hertig, C., Rebmann, G., Bull, J., and Mauch, F.** (1991) A pathogen-induced wheat gene encodes a protein homologous to glutathione-S-transferases. *Mol Plant Microbe Interact* **4**: 14-18.
- Eddy, A.A.** (1982) Mechanisms of solute transport in selected eukaryotic microorganisms. *Adv Microb Physiol* **23**: 1-78, 269-70.
- Egea, C., Ahmed, A.S., Candela, M., and Candela, M.E.** (2001) Elicitation of peroxidase activity and lignin biosynthesis in pepper suspension cells by *Phytophthora capsici*. *Journal of Plant Physiology* **158**: 151-158.

- Ehness, R., Ecker, M., Godt, D.E., and Roitsch, T.** (1997) Glucose and stress independently regulate source and sink metabolism and defense mechanisms via signal transduction pathways involving protein phosphorylation. *Plant Cell* **9**: 1825-1841.
- Eichhorn, H., Lessing, F., Winterberg, B., Schirawski, J., Kamper, J., Muller, P., and Kahmann, R.** (2006) A ferroxidation/permeation iron uptake system is required for virulence in *Ustilago maydis*. *Plant Cell* **18**: 3332-3345.
- Eichmann, R., Schultheiss, H., Kogel, K.H., and Huckelhoven, R.** (2004) The barley apoptosis suppressor homologue BAX inhibitor-1 compromises nonhost penetration resistance of barley to the inappropriate pathogen *Blumeria graminis f. sp. tritici*. *Mol Plant Microbe Interact* **17**: 484-490.
- Emanuelsson, O., Nielsen, H., Brunak, S., and von Heijne, G.** (2000) Predicting subcellular localization of proteins based on their N-terminal amino acid sequence. *J Mol Biol* **300**: 1005-1016.
- Emr, S.D., Schekman, R., Flessel, M.C., and Thorner, J.** (1983) An MF alpha 1-SUC2 (alpha-factor-invertase) gene fusion for study of protein localization and gene expression in yeast. *Proc Natl Acad Sci U S A* **80**: 7080-7084.
- Espinosa, A., and Alfano, J.R.** (2004) Disabling surveillance: bacterial type III secretion system effectors that suppress innate immunity. *Cell Microbiol* **6**: 1027-1040.
- Feldbrügge, M., Kämper, J., Steinberg, G., and Kahmann, R.** (2004) Regulation of mating and pathogenic development in *Ustilago maydis*. *Curr Opin Microbiol* **7**: 666-672.
- Felix, G., Duran, J.D., Volko, S., and Boller, T.** (1999) Plants have a sensitive perception system for the most conserved domain of bacterial flagellin. *Plant J* **18**: 265-276.
- Feuillet, C., Travella, S., Stein, N., Albar, L., Nublát, A., and Keller, B.** (2003) Map-based isolation of the leaf rust disease resistance gene Lr10 from the hexaploid wheat (*Triticum aestivum* L.) genome. *Proc Natl Acad Sci U S A* **100**: 15253-15258.
- Flor-Parra, I., Vranes, M., Kämper, J., and Pérez-Martín, J.** (2006) Biz1, a zinc finger protein required for plant invasion by *Ustilago maydis*, regulates the levels of a mitotic cyclin. *Plant Cell* **18**: 2369-2387.
- Forsberg, H., and Ljungdahl, P.O.** (2001) Sensors of extracellular nutrients in *Saccharomyces cerevisiae*. *Curr Genet* **40**: 91-109.
- Fotopoulos, V., Gilbert, M.J., Pittman, J.K., Marvier, A.C., Buchanan, A.J., Sauer, N., et al.** (2003) The monosaccharide transporter gene, AtSTP4, and the cell-wall invertase, Atbetafruct1, are induced in Arabidopsis during infection with the fungal biotroph *Erysiphe cichoracearum*. *Plant Physiol* **132**: 821-829.
- Fu, Z.Q., Guo, M., Jeong, B.R., Tian, F., Elthon, T.E., Cerny, R.L., et al.** (2007) A type III effector ADP-ribosylates RNA-binding proteins and quells plant immunity. *Nature* **447**: 284-288.

- Fuchs, U., Hause, G., Schuchardt, I., and Steinberg, G.** (2006) Endocytosis is essential for pathogenic development in the corn smut fungus *Ustilago maydis*. *Plant Cell* **18**: 2066-2081.
- Gancedo, J.M.** (2008) The early steps of glucose signalling in yeast. *FEMS Microbiology Reviews* **32**: 673-704.
- García-Muse, T., Steinberg, G., and Pérez-Martín, J.** (2003) Pheromone-induced G2 arrest in the phytopathogenic fungus *Ustilago maydis*. *Eukaryot Cell* **2**: 494-500.
- Garrido, E., Voss, U., Müller, P., Castillo-Lluva, S., Kahmann, R., and Pérez-Martín, J.** (2004) The induction of sexual development and virulence in the smut fungus *Ustilago maydis* depends on Crk1, a novel MAPK protein. *Genes Dev* **18**: 3117-3130.
- Gietz, D., St Jean, A., Woods, R.A., and Schiestl, R.H.** (1992) Improved method for high efficiency transformation of intact yeast cells. *Nucleic Acids Res* **20**: 1425.
- Gillissen, B., Bergemann, J., Sandmann, C., Schroeer, B., Bölker, M., and Kahmann, R.** (1992) A two-component regulatory system for self/non-self recognition in *Ustilago maydis*. *Cell* **68**: 647-657.
- Glazebrook, J.** (2005) Contrasting mechanisms of defense against biotrophic and necrotrophic pathogens. *Annu Rev Phytopathol* **43**: 205-227.
- Glazebrook, J., Chen, W., Estes, B., Chang, H.S., Nawrath, C., Métraux, J.P., et al.** (2003) Topology of the network integrating salicylate and jasmonate signal transduction derived from global expression phenotyping. *Plant J* **34**: 217-228.
- Gomez, L.D., Noctor, G., Knight, M.R., and Foyer, C.H.** (2004) Regulation of calcium signalling and gene expression by glutathione. *J Exp Bot* **55**: 1851-1859.
- Göhre, V., and Robatzek, S.** (2008) Breaking the barriers: microbial effector molecules subvert plant immunity. *Annu Rev Phytopathol* **46**: 189-215.
- Gómez-Ariza, J., Campo, S., Rufat, M., Estopà, M., Messeguer, J., San Segundo, B., and Coca, M.** (2007) Sucrose-mediated priming of plant defense responses and broad-spectrum disease resistance by overexpression of the maize pathogenesis-related PRms protein in rice plants. *Mol Plant Microbe Interact* **20**: 832-842.
- Granado, J., Felix, G., and Boller, T.** (1995) Perception of Fungal Sterols in Plants (Subnanomolar Concentrations of Ergosterol Elicit Extracellular Alkalinization in Tomato Cells). *Plant Physiol* **107**: 485-490.
- Greenberg, J.T., and Yao, N.** (2004) The role and regulation of programmed cell death in plant-pathogen interactions. *Cell Microbiol* **6**: 201-211.
- Greenberg, J.T., Guo, A., Klessig, D.F., and Ausubel, F.M.** (1994) Programmed cell death in plants: a pathogen-triggered response activated coordinately with multiple defense functions. *Cell* **77**: 551-563.
- Guillemain, G., Loizeau, M., Pinçon-Raymond, M., Girard, J., and Leturque, A.** (2000) The large intracytoplasmic loop of the glucose transporter GLUT2 is involved in glucose signaling in hepatic cells. *J Cell Sci* **113** (Pt 5): 841-847.

- Guillemain, G., Muñoz-Alonso, M.J., Cassany, A., Loizeau, M., Faussat, A.M., Burnol, A.F., and Leturque, A.** (2002) Karyopherin alpha2: a control step of glucose-sensitive gene expression in hepatic cells. *Biochem J* **364**: 201-209.
- Hahn, K., and Strittmatter, G.** (1994) Pathogen-defence gene *prp1-1* from potato encodes an auxin-responsive glutathione S-transferase. *Eur J Biochem* **226**: 619-626.
- Hahn, M., and Mendgen, K.** (2001) Signal and nutrient exchange at biotrophic plant-fungus interfaces. *Curr Opin Plant Biol* **4**: 322-327.
- Hahn, M., Neef, U., Struck, C., Gottfert, M., and Mendgen, K.** (1997) A putative amino acid transporter is specifically expressed in haustoria of the rust fungus *Uromyces fabae*. *Mol Plant Microbe Interact* **10**: 438-445.
- Hane, J.K., Lowe, R.G., Solomon, P.S., Tan, K.C., Schoch, C.L., Spatafora, J.W., et al.** (2007) Dothideomycete plant interactions illuminated by genome sequencing and EST analysis of the wheat pathogen *Stagonospora nodorum*. *Plant Cell* **19**: 3347-3368.
- Harris, L.J., Saparno, A., Johnston, A., Prusic, S., Xu, M., Allard, S., et al.** (2005) The maize An2 gene is induced by Fusarium attack and encodes an ent-copalyl diphosphate synthase. *Plant Mol Biol* **59**: 881-894.
- Hartmann, H.A., Kahmann, R., and Bölker, M.** (1996) The pheromone response factor coordinates filamentous growth and pathogenicity in *Ustilago maydis*. *EMBO J.* **15**: 1632-1641.
- Hartmann, H.A., Kruger, J., Lottspeich, F., and Kahmann, R.** (1999) Environmental signals controlling sexual development of the corn smut fungus *Ustilago maydis* through the transcriptional regulator Prf1. *Plant Cell* **11**: 1293-1306.
- Häusler, R.E., Fischer, K.L., and Flügge, U.I.** (2000) Determination of low-abundant metabolites in plant extracts by NAD (P) H fluorescence with a microtiter plate reader. *Analytical Biochemistry* **281**: 1-8.
- Heineke, D., Sonnewald, U., Büssis, D., Günter, G., Leidreiter, K., Wilke, I., et al.** (1992) Apoplastic expression of yeast-derived invertase in potato: effects on photosynthesis, leaf solute composition, water relations, and tuber composition. *Plant Physiol* **100**: 301-308.
- Heisteruber, D., Schulte, P., and Moerschbacher, B.M.** (1994) Soluble carbohydrates and invertase activity in stem rust-infected, resistant and susceptible near-isogenic wheat leaves. *Physiological and Molecular Plant Pathology (United Kingdom)* .
- Herbers, K., Meuwly, P., Frommer, W.B., Metraux, J.P., and Sonnewald, U.** (1996a) Systemic acquired resistance mediated by the ectopic expression of invertase: possible hexose sensing in the secretory pathway. *Plant Cell* **8**: 793-803.
- Herbers, K., Meuwly, P., Métraux, J.P., and Sonnewald, U.** (1996b) Salicylic acid-independent induction of pathogenesis-related protein transcripts by sugars is dependent on leaf developmental stage. *FEBS Lett* **397**: 239-244.

- Hipskind, J.D., Nicholson, R.L., and Goldsbrough, P.B.** (1996) Isolation of a cDNA encoding a novel leucine-rich repeat motif from *Sorghum bicolor* inoculated with fungi. *Mol Plant Microbe Interact* **9**: 819-825.
- Holliday, R.** (1974) *Ustilago maydis*, In Handbook of Genetics. King, R.C. (eds). New York, USA: Plenum Press, pp. 575-595.
- Holliday, R.** (2004) Early studies on recombination and DNA repair in *Ustilago maydis*. *DNA Repair (Amst)* **3**: 671-682.
- Horst, R.J., Engelsdorf, T., Sonnewald, U., and Voll, L.M.** (2008) Infection of maize leaves with *Ustilago maydis* prevents establishment of C4 photosynthesis. *J Plant Physiol* **165**: 19-28.
- Hu, G., Cheng, P.Y., Sham, A., Perfect, J.R., and Kronstad, J.W.** (2008) Metabolic adaptation in *Cryptococcus neoformans* during early murine pulmonary infection. *Mol Microbiol* **69**: 1456-1475.
- Huang, Y.H., and Hartman, G.L.** (1998) Reaction of selected soybean genotypes to isolates of *Fusarium solani* f. sp. glycines and their culture filtrates. *Plant Disease* **82**: 999-1002.
- Hückelhoven, R.** (2005) Powdery mildew susceptibility and biotrophic infection strategies. *FEMS Microbiol Lett* **245**: 9-17.
- Ito, Y., Kaku, H., and Shibuya, N.** (1997) Identification of a high-affinity binding protein for N-acetylchitooligosaccharide elicitor in the plasma membrane of suspension-cultured rice cells by affinity labeling. *Plant J* **12**: 347-356.
- Jia, Y., McAdams, S.A., Bryan, G.T., Hershey, H.P., and Valent, B.** (2000) Direct interaction of resistance gene and avirulence gene products confers rice blast resistance. *Embo J* **19**: 4004-4014.
- Jiang, R., and Carlson, M.** (1996) Glucose regulates protein interactions within the yeast SNF1 protein kinase complex. *Genes Dev* **10**: 3105-3115.
- Jobic, C., Boisson, A.M., Gout, E., Rasclé, C., Fèvre, M., Cotton, P., and Bligny, R.** (2007) Metabolic processes and carbon nutrient exchanges between host and pathogen sustain the disease development during sunflower infection *Sclerotinia sclerotiorum* 7. *Planta* **226**: 251-265.
- Johnson, L.N., Noble, M.E., and Owen, D.J.** (1996) Active and inactive protein kinases: structural basis for regulation. *Cell* **85**: 149-158.
- Jones, D.A., and Takemoto, D.** (2004) Plant innate immunity - direct and indirect recognition of general and specific pathogen-associated molecules. *Curr Opin Immunol* **16**: 48-62.
- Jones, J.D., and Dangl, J.L.** (2006) The plant immune system. *Nature* **444**: 323-329.
- Kamoun, S.** (2006) A catalogue of the effector secretome of plant pathogenic oomycetes. *Annu Rev Phytopathol* **44**: 41-60.
- Kamoun, S.** (2007) Groovy times: filamentous pathogen effectors revealed. *Curr Opin Plant Biol* **10**: 358-365.

- Kay, S., and Bonas, U.** (2009) How *Xanthomonas* type III effectors manipulate the host plant. *Curr Opin Microbiol* **12**: 37-43.
- Kay, S., Hahn, S., Marois, E., Hause, G., and Bonas, U.** (2007) A bacterial effector acts as a plant transcription factor and induces a cell size regulator. *Science* **318**: 648-651.
- Kämper, J.** (2004) A PCR-based system for highly efficient generation of gene replacement mutants in *Ustilago maydis*. *Mol Genet Genomics* **271**: 103-110.
- Kämper, J., Kahmann, R., Bölker, M., Ma, L.J., Brefort, T., Saville, B.J., et al.** (2006) Insights from the genome of the biotrophic fungal plant pathogen *Ustilago maydis*. *Nature* **444**: 97-101.
- Kämper, J., Reichmann, M., Romeis, T., Bölker, M., and Kahmann, R.** (1995) Multiallelic recognition: nonself-dependent dimerization of the bE and bW homeodomain proteins in *Ustilago maydis*. *Cell* **81**: 73-83.
- Kemen, E., Kemen, A.C., Rafiqi, M., Hempel, U., Mendgen, K., Hahn, M., and Voegelé, R.T.** (2005) Identification of a protein from rust fungi transferred from haustoria into infected plant cells. *Mol Plant Microbe Interact* **18**: 1130-1139.
- Kemmerling, B., Schwedt, A., Rodriguez, P., Mazzotta, S., Frank, M., Qamar, S.A., et al.** (2007) The BRI1-associated kinase 1, BAK1, has a brassinolide-independent role in plant cell-death control. *Curr Biol* **17**: 1116-1122.
- Keon, J.P., White, G.A., and Hargreaves, J.A.** (1991) Isolation, characterization and sequence of a gene conferring resistance to the systemic fungicide carboxin from the maize smut pathogen, *Ustilago maydis*. *Curr Genet* **19**: 475-481.
- Kikot, G.E., Hours, R.A., and Alconada, T.M.** (2008) Contribution of cell wall degrading enzymes to pathogenesis of *Fusarium graminearum*: a review. *J Basic Microbiol* .
- Klarzynski, O., Plesse, B., Joubert, J.M., Yvin, J.C., Kopp, M., Kloareg, B., and Fritig, B.** (2000) Linear beta-1,3 glucans are elicitors of defense responses in tobacco. *Plant Physiol* **124**: 1027-1038.
- Kliebenstein, D.J., and Rowe, H.C.** (2008) Ecological costs of biotrophic versus necrotrophic pathogen resistance, the hypersensitive response and signal transduction. *Plant Science* **174**: 551-556.
- Klosterman, S.J., Perlin, M.H., Garcia-Pedrajas, M., Covert, S.F., and Gold, S.E.** (2007) Genetics of morphogenesis and pathogenic development of *Ustilago maydis*. *Adv Genet* **57**: 1-47.
- Kocal, N., Sonnewald, U., and Sonnewald, S.** (2008) Cell wall-bound invertase limits sucrose export and is involved in symptom development and inhibition of photosynthesis during compatible interaction between tomato and *Xanthomonas campestris* pv *vesicatoria*. *Plant Physiol* **148**: 1523-1536.
- Koch, K.** (2004) Sucrose metabolism: regulatory mechanisms and pivotal roles in sugar sensing and plant development. *Curr Opin Plant Biol* **7**: 235-246.
- Komor, E., Haass, D., and Tanner, W.** (1972) Unusual features of the active hexose uptake system of *Chlorella vulgaris*. *Biochim Biophys Acta* **266**: 649-660.

- Kronstad, J.W., and Staben, C.** (1997) Mating type in filamentous fungi. *Annu Rev Genet* **31**: 245-276.
- Lange, B.M., Lapierre, C., and Sandermann, H.** (1995) Elicitor-Induced Spruce Stress Lignin (Structural Similarity to Early Developmental Lignins). *Plant Physiol* **108**: 1277-1287.
- Leandro, M.J., Gonçalves, P., and Spencer-Martins, I.** (2006) Two glucose/xylose transporter genes from the yeast *Candida intermedia*: first molecular characterization of a yeast xylose-H⁺ symporter. *Biochem J* **395**: 543-549.
- Lee, S.H., Lee, J., Lee, S., Park, E.H., Kim, K.W., Kim, M.D., et al.** (2009) GzSNF1 is required for normal sexual and asexual development in the ascomycete *Gibberella zeae*. *Eukaryot Cell* **8**: 116-127.
- Leturque, A., Brot-Laroche, E., and Le Gall, M.** (2009) GLUT2 mutations, translocation and receptor function in diet-sugar managing. *Am J Physiol Endocrinol Metab* .
- Levine, A., Tenhaken, R., Dixon, R., and Lamb, C.** (1994) H₂O₂ from the oxidative burst orchestrates the plant hypersensitive disease resistance response. *Cell* **79**: 583-593.
- Loubradou, G., Brachmann, A., Feldbrügge, M., and Kahmann, R.** (2001) A homologue of the transcriptional repressor Ssn6p antagonizes cAMP signalling in *Ustilago maydis*. *Mol Microbiol* **40**: 719-730.
- Loyall, L., Uchida, K., Braun, S., Furuya, M., and Frohnmeyer, H.** (2000) Glutathione and a UV light-induced glutathione S-transferase are involved in signaling to chalcone synthase in cell cultures. *Plant Cell* **12**: 1939-1950.
- M'batchi, B., and Delrot, S.** (1984) Parachloromercuribenzenesulfonic acid: A potential tool for differential labeling of the sucrose transporter. *Plant Physiol* **75**: 154-160.
- Madi, L., McBride, S.A., Bailey, L.A., and Ebbole, D.J.** (1997) *rco-3*, a gene involved in glucose transport and conidiation in *Neurospora crassa*. *Genetics* **146**: 499-508.
- Marrs, K.A.** (1996) The functions and regulation of glutathione S-transferases in plants. *Annu Rev Plant Physiol Plant Mol Biol* **47**: 127-158.
- Martinez-Espinoza, A.D., Garcia-Pedrajas, M.D., and Gold, S.E.** (2002) The Ustilaginales as plant pests and model systems. *Fungal Genet Biol* **35**: 1-20.
- Mauch, F., and Dudler, R.** (1993) Differential induction of distinct glutathione-S-transferases of wheat by xenobiotics and by pathogen attack. *Plant Physiol* **102**: 1193-1201.
- McCartney, R.R., and Schmidt, M.C.** (2001) Regulation of Snf1 kinase. Activation requires phosphorylation of threonine 210 by an upstream kinase as well as a distinct step mediated by the Snf4 subunit. *J Biol Chem* **276**: 36460-36466.
- Mendgen, K., and Hahn, M.** (2002) Plant infection and the establishment of fungal biotrophy. *Trends Plant Sci* **7**: 352-356.

- Mendoza-Mendoza, A., Berndt, P., Djamei, A., Weise, C., Linne, U., Marahiel, M., et al.** (2009) Physical-chemical plant-derived signals induce differentiation in *Ustilago maydis*. *Mol Microbiol* **71**: 895-911.
- Meyer, S., Melzer, M., Truernit, E., Hümmer, C., Besenbeck, R., Stadler, R., and Sauer, N.** (2000) AtSUC3, a gene encoding a new Arabidopsis sucrose transporter, is expressed in cells adjacent to the vascular tissue and in a carpel cell layer. *Plant J* **24**: 869-882.
- Momcilovic, M., Iram, S.H., Liu, Y., and Carlson, M.** (2008) Roles of the glycogen-binding domain and Snf4 in glucose inhibition of SNF1 protein kinase. *J Biol Chem* **283**: 19521-19529.
- Monod, M., Capoccia, S., Léchenne, B., Zaugg, C., Holdom, M., and Jousson, O.** (2002) Secreted proteases from pathogenic fungi. *Int J Med Microbiol* **292**: 405-419.
- Morgan, W., and Kamoun, S.** (2007) RXLR effectors of plant pathogenic oomycetes. *Curr Opin Microbiol* **10**: 332-338.
- Moriya, H., and Johnston, M.** (2004) Glucose sensing and signaling in *Saccharomyces cerevisiae* through the Rgt2 glucose sensor and casein kinase I. *Proc Natl Acad Sci U S A* **101**: 1572-1577.
- Morris, S.W., Vernooij, B., Titatarn, S., Starrett, M., Thomas, S., Wiltse, C.C., et al.** (1998) Induced resistance responses in maize. *Mol Plant Microbe Interact* **11**: 643-658.
- Murillo, I., Roca, R., Bortolotti, C., and Segundo, B.S.** (2003) Engineering photoassimilate partitioning in tobacco plants improves growth and productivity and provides pathogen resistance. *Plant J* **36**: 330-341.
- Müller, O., Kahmann, R., Aguilar, G., Trejo-Aguilar, B., Wu, A., and de Vries, R.P.** (2008) The secretome of the maize pathogen *Ustilago maydis*. *Fungal Genet Biol* **45 Suppl 1**: S63-S70.
- Müller, P., Leibbrandt, A., Teunissen, H., Cubasch, S., Aichinger, C., and Kahmann, R.** (2004) The Gbeta-subunit-encoding gene *bpp1* controls cyclic-AMP signaling in *Ustilago maydis*. *Eukaryot Cell* **3**: 806-814.
- Mysore, K.S., and Ryu, C.M.** (2004) Nonhost resistance: how much do we know? *Trends Plant Sci* **9**: 97-104.
- Nadwodnik, J., and Lohaus, G.** (2008) Subcellular concentrations of sugar alcohols and sugars in relation to phloem translocation in *Plantago major*, *Plantago maritima*, *Prunus persica*, and *Apium graveolens*. *Planta* **227**: 1079-1089.
- Nehls, U., Wiese, J., Guttenberger, M., and Hampp, R.** (1998) Carbon allocation in ectomycorrhizas: identification and expression analysis of an *Amanita muscaria* monosaccharide transporter. *Mol Plant Microbe Interact* **11**: 167-176.
- Nicholson, R.L., and Epstein, L.** (1991) Adhesion of fungi to the plant surface: prerequisite for pathogenesis, In *The Fungal Spore and Disease Initiation in Plants and Animals*. Cole, G.T., and Hoch, H.C. (eds). New York: Plenum, pp. 3-23.
- Nikawa, J., Tsukagoshi, Y., and Yamashita, S.** (1991) Isolation and characterization of two distinct myo-inositol transporter genes of *Saccharomyces cerevisiae*. *J Biol Chem* **266**: 11184-11191.

- Nürnberg, T., and Lipka, V.** (2005) Non-host resistance in plants: new insights into an old phenomenon. *Molecular plant pathology* **6**: 335-345.
- O'Connell, R.J., and Panstruga, R.** (2006) Tete a tete inside a plant cell: establishing compatibility between plants and biotrophic fungi and oomycetes. *New Phytol* **171**: 699-718.
- Odenbach, D., Breth, B., Thines, E., Weber, R.W., Anke, H., and Foster, A.J.** (2007) The transcription factor Con7p is a central regulator of infection-related morphogenesis in the rice blast fungus *Magnaporthe grisea*. *Mol Microbiol* **64**: 293-307.
- Ogawa, K.** (2005) Glutathione-associated regulation of plant growth and stress responses. *Antioxid Redox Signal* **7**: 973-981.
- Ospina-Giraldo, M.D., Mullins, E., and Kang, S.** (2003) Loss of function of the *Fusarium oxysporum* SNF1 gene reduces virulence on cabbage and Arabidopsis. *Curr Genet* **44**: 49-57.
- Ostling, J., and Ronne, H.** (1998) Negative control of the Mig1p repressor by Snf1p-dependent phosphorylation in the absence of glucose. *Eur J Biochem* **252**: 162-168.
- Ozcan, S., and Johnston, M.** (1999) Function and regulation of yeast hexose transporters. *Microbiol Mol Biol Rev* **63**: 554-569.
- Ozcan, S., Dover, J., Rosenwald, A.G., Wölfli, S., and Johnston, M.** (1996) Two glucose transporters in *Saccharomyces cerevisiae* are glucose sensors that generate a signal for induction of gene expression. *Proc Natl Acad Sci U S A* **93**: 12428-12432.
- Panstruga, R.** (2003) Establishing compatibility between plants and obligate biotrophic pathogens. *Curr Opin Plant Biol* **6**: 320-326.
- Papamichos-Chronakis, M., Gligoris, T., and Tzamaras, D.** (2004) The Snf1 kinase controls glucose repression in yeast by modulating interactions between the Mig1 repressor and the Cyc8-Tup1 co-repressor. *EMBO Rep* **5**: 368-372.
- Parniske, M.** (2008) Arbuscular mycorrhiza: the mother of plant root endosymbioses. *Nat Rev Microbiol* **6**: 763-775.
- Penninckx, I.A., Thomma, B.P., Buchala, A., Métraux, J.P., and Broekaert, W.F.** (1998) Concomitant activation of jasmonate and ethylene response pathways is required for induction of a plant defensin gene in Arabidopsis. *Plant Cell* **10**: 2103-2113.
- Perfect, S.E., Hughes, H.B., O'Connell, R.J., and Green, J.R.** (1999) *Colletotrichum*: A model genus for studies on pathology and fungal-plant interactions. *Fungal Genet Biol* **27**: 186-198.
- Polidori, E., Ceccaroli, P., Saltarelli, R., Guescini, M., Menotta, M., Agostini, D., et al.** (2007) Hexose uptake in the plant symbiotic ascomycete *Tuber borchii* Vittadini: biochemical features and expression pattern of the transporter TBHXT1. *Fungal Genet Biol* **44**: 187-198.
- Prathumpai, W., McIntyre, M., and Nielsen, J.** (2004) The effect of CreA in glucose and xylose catabolism in *Aspergillus nidulans*. *Appl Microbiol Biotechnol* **63**: 748-753.

- Prisic, S., Xu, M., Wilderman, P.R., and Peters, R.J.** (2004) Rice contains two disparate ent-copalyl diphosphate synthases with distinct metabolic functions. *Plant Physiol* **136**: 4228-4236.
- Puhalla, J.E.** (1968) Compatibility reactions on solid medium and interstrain inhibition in *Ustilago maydis*. *Genetics* **60**: 461-474.
- Quadbeck-Seeger, C., Wanner, G., Huber, S., Kahmann, R., and Kämper, J.** (2000) A protein with similarity to the human retinoblastoma binding protein 2 acts specifically as a repressor for genes regulated by the b mating type locus in *Ustilago maydis*. *Mol Microbiol* **38**: 154-66..
- Regenfelder, E., Spellig, T., Hartmann, A., Lauenstein, S., Bölker, M., and Kahmann, R.** (1997) G proteins in *Ustilago maydis*: transmission of multiple signals? *EMBO J* **16**: 1934-1942.
- Rehmany, A.P., Gordon, A., Rose, L.E., Allen, R.L., Armstrong, M.R., Whisson, S.C., et al.** (2005) Differential recognition of highly divergent downy mildew avirulence gene alleles by RPP1 resistance genes from two Arabidopsis lines. *Plant Cell* **17**: 1839-1850.
- Reinders, A., and Ward, J.M.** (2001) Functional characterization of the alpha-glucoside transporter Sut1p from *Schizosaccharomyces pombe*, the first fungal homologue of plant sucrose transporters. *Mol Microbiol* **39**: 445-454.
- Reineke, G., Heinze, B., Schirawski, J., Buettner, H., Kahmann, R., and Basse, C.W.** (2008) Indole-3-acetic acid (IAA) biosynthesis in the smut fungus *Ustilago maydis* and its relevance for increased IAA levels in infected tissue and host tumour formation. *Mol Plant Pathol* **9**: 339-355.
- Ridout, C.J., Skamnioti, P., Porritt, O., Sacristan, S., Jones, J.D., and Brown, J.K.** (2006) Multiple avirulence paralogues in cereal powdery mildew fungi may contribute to parasite fitness and defeat of plant resistance. *Plant Cell* **18**: 2402-2414.
- Roitsch, T., and González, M.C.** (2004) Function and regulation of plant invertases: sweet sensations. *Trends Plant Sci* **9**: 606-613.
- Roitsch, T., Balibrea, M.E., Hofmann, M., Proels, R., and Sinha, A.K.** (2003) Extracellular invertase: key metabolic enzyme and PR protein. *J Exp Bot* **54**: 513-524.
- Rolland, F., Baena-Gonzalez, E., and Sheen, J.** (2006) Sugar sensing and signaling in plants: conserved and novel mechanisms. *Annu Rev Plant Biol* **57**: 675-709.
- Romeis, T., Brachmann, A., Kahmann, R., and Kämper, J.** (2000) Identification of a target gene for the bE-bW homeodomain protein complex in *Ustilago maydis*. *Mol Microbiol* **37**: 54-66.
- Ronne, H.** (1995) Glucose repression in fungi. *Trends Genet* **11**: 12-17.
- Rooney, H.C., Van't Klooster, J.W., van der Hoorn, R.A., Joosten, M.H., Jones, J.D., and de Wit, P.J.** (2005) Cladosporium Avr2 inhibits tomato Rcr3 protease required for Cf-2-dependent disease resistance. *Science* **308**: 1783-1786.

- Rosebrock, T.R., Zeng, L., Brady, J.J., Abramovitch, R.B., Xiao, F., and Martin, G.B.** (2007) A bacterial E3 ubiquitin ligase targets a host protein kinase to disrupt plant immunity. *Nature* **448**: 370-374.
- Rowell, J.B.** (1955) Functional role of compatibility factors and an in vitro test for sexual incompatibility with haploid lines of *Ustilago zea*. *Phytopathology* **45**: 370-374.
- Römer, P., Hahn, S., Jordan, T., Strauss, T., Bonas, U., and Lahaye, T.** (2007) Plant pathogen recognition mediated by promoter activation of the pepper Bs3 resistance gene. *Science* **318**: 645-648.
- Sambrook, J., Frisch, E.F., and Maniatis, T.** (1989) *Molecular Cloning: A Laboratory Manual*. Cold Spring Harbour, New York: Cold Spring Harbour Laboratory Press.
- Santangelo, G.M.** (2006) Glucose signaling in *Saccharomyces cerevisiae*. *Microbiol Mol Biol Rev* **70**: 253-282.
- Sauer, N.** (2007) Molecular physiology of higher plant sucrose transporters. *FEBS Lett* **581**: 2309-2317.
- Sauer, N., and Stolz, J.** (1994) SUC1 and SUC2: two sucrose transporters from *Arabidopsis thaliana*; expression and characterization in baker's yeast and identification of the histidine-tagged protein. *Plant J* **6**: 67-77.
- Schaarschmidt, S., Kopka, J., Ludwig-Müller, J., and Hause, B.** (2007) Regulation of arbuscular mycorrhization by apoplastic invertases: enhanced invertase activity in the leaf apoplast affects the symbiotic interaction. *Plant J* **51**: 390-405.
- Schauwecker, F., Wanner, G., and Kahmann, R.** (1995) Filament-specific expression of a cellulase gene in the dimorphic fungus *Ustilago maydis*. *Biol. Chem. Hoppe-Seyler* **376**: 617-625.
- Schenk, P.M., Kazan, K., Wilson, I., Anderson, J.P., Richmond, T., Somerville, S.C., and Manners, J.M.** (2000) Coordinated plant defense responses in *Arabidopsis* revealed by microarray analysis. *Proc Natl Acad Sci U S A* **97**: 11655-11660.
- Scherer, M., Heimel, K., Starke, V., and Kämper, J.** (2006) The Clp1 protein is required for clamp formation and pathogenic development of *Ustilago maydis*. *Plant Cell* **18**: 2388-2401.
- Schlesinger, R., Kahmann, R., and Kämper, J.** (1997) The homeodomains of the heterodimeric bE and bW proteins of *Ustilago maydis* are both critical for function. *Mol Gen Genet* **254**: 514-519.
- Schmidt, M.C., McCartney, R.R., Zhang, X., Tillman, T.S., Solimeo, H., Wölfel, S., et al.** (1999) Std1 and Mth1 proteins interact with the glucose sensors to control glucose-regulated gene expression in *Saccharomyces cerevisiae*. *Mol Cell Biol* **19**: 4561-4571.
- Schmitt, M.E., Brown, T.A., and Trumppower, B.L.** (1990) A rapid and simple method for preparation of RNA from *Saccharomyces cerevisiae*. *Nucleic Acids Res* **18**: 3091-3092.

- Scholes, J.D., Lee, P.J., Horton, P., and Lewis, D.H.** (1994) Invertase: understanding changes in the photosynthetic and carbohydrate metabolism of barley leaves infected with powdery mildew. *New Phytologist* : 213-222.
- Schornack, S., Meyer, A., Römer, P., Jordan, T., and Lahaye, T.** (2006) Gene-for-gene-mediated recognition of nuclear-targeted AvrBs3-like bacterial effector proteins. *J Plant Physiol* **163**: 256-272.
- Schulz, B., Banuett, F., Dahl, M., Schlesinger, R., Schäfer, W., Martin, T., et al.** (1990) The b alleles of *U. maydis*, whose combinations program pathogenic development, code for polypeptides containing a homeodomain-related motif. *Cell* **60**: 295-306.
- Schüssler, A., Martin, H., Cohen, D., Fitz, M., and Wipf, D.** (2006) Characterization of a carbohydrate transporter from symbiotic glomeromycotan fungi. *Nature* **444**: 933-936.
- Senda, K., and Ogawa, K.** (2004) Induction of PR-1 accumulation accompanied by runaway cell death in the *lsd1* mutant of *Arabidopsis* is dependent on glutathione levels but independent of the redox state of glutathione. *Plant Cell Physiol* **45**: 1578-1585.
- Seo, H.S., Song, J.T., Cheong, J.J., Lee, Y.H., Lee, Y.W., Hwang, I., et al.** (2001) Jasmonic acid carboxyl methyltransferase: a key enzyme for jasmonate-regulated plant responses. *Proc Natl Acad Sci U S A* **98**: 4788-4793.
- Shi, Z., Christian, D., and Leung, H.** (1998) Interactions between spore morphogenetic mutations affect cell types, sporulation, and pathogenesis in *Magnaporthe grisea*. *Mol Plant Microbe Interact* **11**: 199-207.
- Shindo, T., and Van der Hoorn, R.A.** (2008) Papain-like cysteine proteases: key players at molecular battlefields employed by both plants and their invaders. *Mol Plant Pathol* **9**: 119-125.
- Simmons, C.R., Fridlender, M., Navarro, P.A., and Yalpani, N.** (2003) A maize defense-inducible gene is a major facilitator superfamily member related to bacterial multidrug resistance efflux antiporters. *Plant Mol Biol* **52**: 433-446.
- Singh, R.P., Hodson, D.P., Jin, Y., Huerta-Espino, J., Kinyua, M.G., Wanyera, R., et al.** (2006) Current status, likely migration and strategies to mitigate the threat to wheat production from race Ug99 (TTKS) of stem rust pathogen. *CAB Reviews: Perspectives in Agriculture, Veterinary Science, Nutrition and Natural Resources* **1**: 1-13.
- Smith, F.C., Davies, S.P., Wilson, W.A., Carling, D., and Hardie, D.G.** (1999) The SNF1 kinase complex from *Saccharomyces cerevisiae* phosphorylates the transcriptional repressor protein Mig1p in vitro at four sites within or near regulatory domain 1. *FEBS Lett* **453**: 219-223.
- Snetselaar, K.M., and Mims, C.W.** (1992) Sporidial fusion and infection of maize seedlings by the smut fungus *Ustilago maydis*. *Mycologia* **84**: 193-203.
- Snetselaar, K.M., and Mims, C.W.** (1993) Infection of maize stigmas by *Ustilago maydis*: Light and electron microscopy. *Phytopathology* **83**: 843.

- Solomon, M., Belenghi, B., Delledonne, M., Menachem, E., and Levine, A.** (1999) The involvement of cysteine proteases and protease inhibitor genes in the regulation of programmed cell death in plants. *Plant Cell* **11**: 431-444.
- Sonnewald, U., Brauer, M., von Schaewen, A., Stitt, M., and Willmitzer, L.** (1991) Transgenic tobacco plants expressing yeast-derived invertase in either the cytosol, vacuole or apoplast: a powerful tool for studying sucrose metabolism and sink/source interactions. *Plant J* **1**: 95-106.
- Sonnhammer, E.L.L., von Heijne, G., and Krgh, A.** (1998) A hidden Markov model for predicting transmembrane helices in protein sequences. In: Glasgow J., editor. Proceedings of the sixth international conference of intelligent systems for molecular biology (ISMB98). Menlo Park, AAAI Press. pp. 175-182.
- Spellig, T., Bölker, M., Lottspeich, F., Frank, R.W., and Kahmann, R.** (1994a) Pheromones trigger filamentous growth in *Ustilago maydis*. *EMBO J.* **13**: 1620-1627.
- Spellig, T., Regenfelder, E., Reichmann, M., Schauwecker, F., Bohlmann, R., Urban, M., et al.** (1994b) Control of mating and development in *Ustilago maydis*. *Antonie Van Leeuwenhoek* **65**: 191-197.
- Stambuk, B.U., Batista, A.S., and De Araujo, P.S.** (2000) Kinetics of active sucrose transport in *Saccharomyces cerevisiae*. *J Biosci Bioeng* **89**: 212-214.
- Stambuk, B.U., da Silva, M.A., Panek, A.D., and de Araujo, P.S.** (1999) Active alpha-glucoside transport in *Saccharomyces cerevisiae*. *FEMS Microbiol Lett* **170**: 105-110.
- Stavrinos, J., McCann, H.C., and Guttman, D.S.** (2008) Host-pathogen interplay and the evolution of bacterial effectors. *Cell Microbiol* **10**: 285-292.
- Struck, C., Mueller, E., Martin, H., and Lohaus, G.** (2004) The *Uromyces fabae* UfAAT3 gene encodes a general amino acid permease that prefers uptake of in planta scarce amino acids. *Molecular Plant Pathology* **5**: 183-189.
- Struck, C., Ernst, M., and Hahn, M.** (2002) Characterization of a developmentally regulated amino acid transporter (AAT1p) of the rust fungus *Uromyces fabae*. *Molecular Plant Pathology* **3**: 23-30.
- Sugio, A., Yang, B., Zhu, T., and White, F.F.** (2007) Two type III effector genes of *Xanthomonas oryzae* pv. *oryzae* control the induction of the host genes *OsTFIIAgamma1* and *OsTFX1* during bacterial blight of rice. *Proc Natl Acad Sci U S A* **104**: 10720-10725.
- Tang, G.Q., Lüscher, M., and Sturm, A.** (1999) Antisense repression of vacuolar and cell wall invertase in transgenic carrot alters early plant development and sucrose partitioning. *Plant Cell* **11**: 177-189.
- Tang, W., Coughlan, S., Crane, E., Beatty, M., and Duvick, J.** (2006) The application of laser microdissection to in planta gene expression profiling of the maize anthracnose stalk rot fungus *Colletotrichum graminicola*. *Mol Plant Microbe Interact* **19**: 1240-1250.
- Tang, X., Rolfe, S.A., and Scholes, J.D.** (1996) The effect of *Albugo candida* (white blister rust) on the photosynthetic and carbohydrate metabolism of leaves of *Arabidopsis thaliana*. *Plant, Cell and Environment* **19**: 967-975.

- Tani, T., Sobajima, H., Okada, K., Chujo, T., Arimura, S., Tsutsumi, N., et al.** (2008) Identification of the *OsOPR7* gene encoding 12-oxophytodienoate reductase involved in the biosynthesis of jasmonic acid in rice. *Planta* **227**: 517-526.
- Tetlow, I.J., and Farrar, J.F.** (1992) Sucrose-metabolizing enzymes from leaves of barley infected with brown rust (*Puccinia hordei* Otth.). *New Phytologist* : 475-480.
- Thimm, O., Bläsing, O., Gibon, Y., Nagel, A., Meyer, S., Krüger, P., et al.** (2004) MAPMAN: a user-driven tool to display genomics data sets onto diagrams of metabolic pathways and other biological processes. *Plant J* **37**: 914-939.
- Thomma, B.P., Eggermont, K., Penninckx, I.A., Mauch-Mani, B., Vogelsang, R., Cammue, B.P., and Broekaert, W.F.** (1998) Separate jasmonate-dependent and salicylate-dependent defense-response pathways in *Arabidopsis* are essential for resistance to distinct microbial pathogens. *Proc Natl Acad Sci U S A* **95**: 15107-15111.
- Tonukari, N.J., Scott-Craig, J.S., and Walton, J.D.** (2000) The *Cochliobolus carbonum* SNF1 gene is required for cell wall-degrading enzyme expression and virulence on maize. *Plant Cell* **12**: 237-248.
- Toth, I.K., and Birch, P.R.** (2005) Rotting softly and stealthily. *Curr Opin Plant Biol* **8**: 424-429.
- Treitel, M.A., Kuchin, S., and Carlson, M.** (1998) Snf1 protein kinase regulates phosphorylation of the Mig1 repressor in *Saccharomyces cerevisiae*. *Mol Cell Biol* **18**: 6273-6280.
- Tsukuda, T., Carleton, S., Fotheringham, S., and Holloman, W.K.** (1988) Isolation and characterization of an autonomously replicating sequence from *Ustilago maydis*. *Mol Cell Biol* **8**: 3703-3709.
- Turgeon, R., and Gowan, E.** (1990) Phloem loading in *Coleus blumei* in the absence of carrier-mediated uptake of export sugar from the apoplast. *Plant Physiol* **94**: 1244-1249.
- Turian, G., and Hamilton, R.H.** (1960) Chemical detection of 3-indolylacetic acid in *Ustilago zaeae* tumors. *Biochem Biophys Acta* **41**: 148-150.
- Tyler, B.M.** (2009) Entering and breaking: virulence effector proteins of oomycete plant pathogens. *Cell Microbiol* **11**: 13-20.
- Urban, M., Kahmann, R., and Bölker, M.** (1996) Identification of the pheromone response element in *Ustilago maydis*. *Mol Gen Genet* **251**: 31-37.
- Vagnoli, P., Coons, D.M., and Bisson, L.F.** (1998) The C-terminal domain of Snf3p mediates glucose-responsive signal transduction in *Saccharomyces cerevisiae*. *FEMS microbiology letters* **160**: 31-36.
- van Loon, L.C., Rep, M., and Pieterse, C.M.** (2006) Significance of inducible defense-related proteins in infected plants. *Annu Rev Phytopathol* **44**: 135-162.
- VanEtten, H.D., Mansfield, J.W., Bailey, J.A., and Farmer, E.E.** (1994) Two classes of plant antibiotics: phytoalexins versus "phytoanticipins". *Plant Cell* **6**: 1191-1192.

- Viigand, K., Tammus, K., and Alamäe, T.** (2005) Clustering of *MAL* genes in *Hansenula polymorpha*: cloning of the maltose permease gene and expression from the divergent intergenic region between the maltose permease and maltase genes. *FEMS Yeast Res* **5**: 1019-1028.
- Voegelé, R.T.** (2006) *Uromyces fabae*: development, metabolism, and interactions with its host *Vicia faba*. *FEMS Microbiol Lett* **259**: 165-173.
- Voegelé, R.T., Struck, C., Hahn, M., and Mendgen, K.** (2001) The role of haustoria in sugar supply during infection of broad bean by the rust fungus *Uromyces fabae*. *Proc Natl Acad Sci U S A* **98**: 8133-8138.
- Voegelé, R.T., Wirsal, S., Möll, U., Lechner, M., and Mendgen, K.** (2006) Cloning and characterization of a novel invertase from the obligate biotroph *Uromyces fabae* and analysis of expression patterns of host and pathogen invertases in the course of infection. *Mol Plant Microbe Interact* **19**: 625-634.
- Voll, L., Häusler, R.E., Hecker, R., Weber, A., Weissenböck, G., Fiene, G., et al.** (2003) The phenotype of the *Arabidopsis cue1* mutant is not simply caused by a general restriction of the shikimate pathway. *Plant J* **36**: 301-317.
- von Schaewen, A., Stitt, M., Schmidt, R., Sonnewald, U., and Willmitzer, L.** (1990) Expression of a yeast-derived invertase in the cell wall of tobacco and *Arabidopsis* plants leads to accumulation of carbohydrate and inhibition of photosynthesis and strongly influences growth and phenotype of transgenic tobacco plants. *EMBO J* **9**: 3033-3044.
- Vorwerk, S., Somerville, S., and Somerville, C.** (2004) The role of plant cell wall polysaccharide composition in disease resistance. *Trends Plant Sci* **9**: 203-209.
- Wagner, U., Edwards, R., Dixon, D.P., and Mauch, F.** (2002) Probing the diversity of the *Arabidopsis* glutathione S-transferase gene family. *Plant Mol Biol* **49**: 515-532.
- Wahl, R.** (2005) Konstruktion von temperatursensitiven bE/bW-Heterodimeren in *Ustilago maydis*. Diploma Thesis, Philipps-University Marburg.
- Walters, D.R., and McRoberts, N.** (2006) Plants and biotrophs: a pivotal role for cytokinins? *Trends Plant Sci* **11**: 581-586.
- Walton, J.D.** (2001) Secondary metabolites: killing pathogens. *Encyclopedia Life Science*: 1-5.
- Wang, D., Pajeroska-Mukhtar, K., Culler, A.H., and Dong, X.** (2007) Salicylic acid inhibits pathogen growth in plants through repression of the auxin signaling pathway. *Curr Biol* **17**: 1784-1790.
- Wasternack, C.** (2007) Jasmonates: an update on biosynthesis, signal transduction and action in plant stress response, growth and development. *Ann Bot (Lond)* **100**: 681-697.
- Weinzierl, G.** (2001) Isolierung und Charakterisierung von Komponenten der b-vermittelten Regulationskaskade in *Ustilago maydis*. Thesis, Philipps-University Marburg.
- Wenzler, H., and Meins, F.J.R.** (1987) Persistent changes in the proliferative capacity of maize leaf tissues induced by *Ustilago* infection. *Physiological and molecular plant pathology* **30**: 309-319.

- Westerink, N., Brandwagt, B.F., de Wit, P.J., and Joosten, M.H.** (2004) *Cladosporium fulvum* circumvents the second functional resistance gene homologue at the *Cf-4* locus (Hcr9-4E) by secretion of a stable avr4E isoform. *Mol Microbiol* **54**: 533-545.
- Whisson, S.C., Boevink, P.C., Moleleki, L., Avrova, A.O., Morales, J.G., Gilroy, E.M., et al.** (2007) A translocation signal for delivery of oomycete effector proteins into host plant cells. *Nature* **450**: 115-118.
- Wieczorke, R., Krampe, S., Weierstall, T., Freidel, K., Hollenberg, C.P., and Boles, E.** (1999) Concurrent knock-out of at least 20 transporter genes is required to block uptake of hexoses in *Saccharomyces cerevisiae*. *FEBS Lett* **464**: 123-128.
- Win, J., Morgan, W., Bos, J., Krasileva, K.V., Cano, L.M., Chaparro-Garcia, A., et al.** (2007) Adaptive evolution has targeted the C-terminal domain of the RXLR effectors of plant pathogenic oomycetes. *Plant Cell* **19**: 2349-2369.
- Winter, H., and Huber, S.C.** (2000) Regulation of sucrose metabolism in higher plants: localization and regulation of activity of key enzymes. *Crit Rev Biochem Mol Biol* **35**: 253-289.
- Wolberger, C., Vershon, A.K., Liu, B., Johnson, A.D., and Pabo, C.O.** (1991) Crystal structure of a MAT alpha 2 homeodomain-operator complex suggests a general model for homeodomain-DNA interactions. *Cell* **67**: 517-528.
- Wösten, H.A., Bohlmann, R., Eckerskorn, C., Lottspeich, F., Bölker, M., and Kahmann, R.** (1996) A novel class of small amphipathic peptides affect aerial hyphal growth and surface hydrophobicity in *Ustilago maydis*. *EMBO J.* **15**: 4274-4281.
- Xia, Y.** (2004) Proteases in pathogenesis and plant defence. *Cell Microbiol* **6**: 905-913.
- Yamaguchi, T., Yamada, A., Hong, N., Ogawa, T., Ishii, T., and Shibuya, N.** (2000) Differences in the recognition of glucan elicitor signals between rice and soybean: beta-glucan fragments from the rice blast disease fungus *Pyricularia oryzae* that elicit phytoalexin biosynthesis in suspension-cultured rice cells. *Plant Cell* **12**: 817-826.
- Yang, B., Sugio, A., and White, F.F.** (2006) Os8N3 is a host disease-susceptibility gene for bacterial blight of rice. *Proc Natl Acad Sci U S A* **103**: 10503-10508.
- Yi, M., Park, J.H., Ahn, J.H., and Lee, Y.H.** (2008) MoSNF1 regulates sporulation and pathogenicity in the rice blast fungus *Magnaporthe oryzae*. *Fungal Genet Biol* **45**: 1172-1181.
- Zaman, S., Lippman, S.I., Zhao, X., and Broach, J.R.** (2008) How *Saccharomyces* responds to nutrients. *Annu Rev Genet* **42**: 27-81.
- Zarnack, K., Eichhorn, H., Kahmann, R., and Feldbrügge, M.** (2008) Pheromone-regulated target genes respond differentially to MAPK phosphorylation of transcription factor Prf1. *Mol Microbiol* **69**: 1041-1053.
- Zheng, Y., Kief, J., Auffarth, K., Farfsing, J.W., Mahlert, M., Nieto, F., and Basse, C.W.** (2008) The *Ustilago maydis* Cys2His2-type zinc finger transcription factor

Mzr1 regulates fungal gene expression during the biotrophic growth stage. *Mol Microbiol* **68**: 1450-1470.

Zhou, J.M., and Chai, J. (2008) Plant pathogenic bacterial type III effectors subdue host responses. *Curr Opin Microbiol* **11**: 179-185.

Zipfel, C., Kunze, G., Chinchilla, D., Caniard, A., Jones, J.D., Boller, T., and Felix, G. (2006) Perception of the bacterial PAMP EF-Tu by the receptor EFR restricts Agrobacterium-mediated transformation. *Cell* **125**: 749-760.

Zipfel, C., Robatzek, S., Navarro, L., Oakeley, E.J., Jones, J.D., Felix, G., and Boller, T. (2004) Bacterial disease resistance in Arabidopsis through flagellin perception. *Nature* **428**: 764-767.

Zor, T., and Selinger, Z. (1996) Linearization of the Bradford protein assay increases its sensitivity: theoretical and experimental studies. *Analytical biochemistry* **236**: 302-308.

5. Supplementary Material

Data-CD:

Table of Contents: CD/

▼	data-CD – 5. Supplementary Material	22.5 MB
▼	Supplementary Material of 2.1	1.8 MB
	Supplementary Material of 2.1.pdf	1.8 MB
▼	Supplementary Material of 2.2	7.3 MB
	Supplementary Material of 2.2.pdf	4.9 MB
	Table 2.2-S1.xls	20 KB
	Table 2.2-S2.xls	1.1 MB
	Table 2.2-S3.xls	80 KB
	Table 2.2-S4.xls	20 KB
	Table 2.2-S5.xls	40 KB
	Table 2.2-S6.xls	564 KB
	Table 2.2-S7.xls	524 KB
	Table 2.2-S8.xls	24 KB
	Table 2.2-S9.xls	16 KB
	Table 2.2-S10.xls	16 KB
▼	Supplementary Material of 2.3	4 MB
	Supplementary Material of 2.3.pdf	4 MB
▼	Supplementary Material of 2.4	9.3 MB
	Supplementary Material of 2.4.pdf	9.3 MB

Authors Contributions

The research on which this dissertation is based is either published (Section 2.2), submitted (Section 2.1; 2.3) or will be submitted for publication in peer-reviewed journals (Section 2.4). This declaration is intended to clarify the contribution by the author of this thesis (Ramon Wahl).

Section 2.1 (The *Ustilago maydis* *b* Mating Type Locus Controls Hyphal Proliferation and Expression of Secreted Virulence Factors *in Planta* – submitted to Molecular Microbiology, 2009) is based on the work of the authors Ramon Wahl and Jörg Kämper. R.W. performed the underlying research. The generation of the temperature sensitive *b* alleles and first infection studies were already carried out in the diploma thesis of R.W. (Wahl, 2005). R.W. isolated the single mutation causing the temperature sensitivity of *b* as part of this dissertation. R.W. performed the time-course analysis after *b* inactivation *in planta* as part of this thesis. R.W. constructed NLS:GFP expressing strains and investigated the cell division defect after *b* inactivation *in planta* as part of this thesis. R.W. constructed compatible strains forming a temperature-sensitive dikaryon and performed the subsequent DNA array analysis *in planta* as part of this thesis. R.W. and J.K. designed the experiments and wrote the manuscript.

Section 2.2. (Reprogramming a Maize Plant: Transcriptional and Metabolic Changes Induced by the Fungal Biotroph *Ustilago maydis* - published in The Plant Journal, 2008) is based on the work of Gunther Doehlemann, Ramon Wahl, Robin J. Horst, Lars M. Voll, Björn Usadel, Fabien Poree, Mark Stitt, Jörn Pons-Kühnemann, Uwe Sonnewald, Regine Kahmann and Jörg Kämper. The two first authors G.D. and R.W. contributed equally. R.J.H., L.M.V and U.S. performed the metabolic profiling of the provided plant material. B.U., F.P. and M.S. developed MapMan a whole pathway analyses tool adjusted to display maize expression data. G.D. and R.W. produced the plant material, extracted the RNA and performed the DNA array expression analysis. G.D. did the microscopy. R.W. performed most of the bioinformatic analysis. J.P.-K. wrote the “R”-script for statistical analysis. G.D., R.W., R.K. and J.K. designed the experiments and wrote the manuscript.

Section 2.3 (A Novel High Affinity Sucrose Transporter is Required for Fungal Virulence and Avoids Extracellular Glucose Signaling in Biotrophic Interactions – submitted to PLoS Biology, 2009) is based on the work of Ramon Wahl, Kathrin Wippel, Jörg Kämper and Norbert Sauer. The two first authors R. W. and K.W.

contributed equally. R.W. and J.K. identified Srt1 as virulence factor. R.W. isolated the gene and performed expression analyses in *U. maydis*. R.W. performed growth and infection experiments of *srt1* deletion mutants. K.W. and R.W. generated yeast constructs, K.W. and N.S. performed the functional and kinetic characterization of Srt1. R.W., K.W. and N.S. did the phylogenetic analyses. J.K. and N.S. wrote the manuscript.

Section 2.4 (Hxt1, a Monosaccharide Transporter and Sensor Required for Virulence of the Maize Pathogen *Ustilago maydis* - unpublished) is based on the work of Ramon Wahl, Kathrin Wippel, Sarah Goos, M. Vranes, Norbert Sauer and Jörg Kämper. R.W. identified Hxt1 as virulence factor. R.W. constructed single deletion mutants of *hxt1* and *srt1* as well as the double deletion mutant *srt1/hxt1* and performed infection experiments. R.W. performed real-time PCR expression analysis of *hxt1* and DNA array expression analysis comparing SG200 and SG200 Δ *hxt1* on different carbon sources. R.W. isolated the *hxt1* gene, generated yeast constructs and complemented yeast growth of EBYVW.4000 on different hexoses by heterologous *hxt1* expression. K.W. and N.S. performed the kinetic characterization of Hxt1. R.W. did the phylogenetic analyses of Hxt1. S.G. and R.W. generated the deletion mutants of *snf1* and the double deletion mutants of *snf1/hxt1* and performed the characterizations of these strains. M.V. provided the DNA-array data of *U. maydis* during infection. R.W. and J.K. designed the experiments and wrote the manuscript.

R.W. wrote the dissertation.

Ramon Wahl

Karlsruhe, June 30th, 2009

Danksagung

Ich möchte mich zunächst bei Frau Renkawitz-Pohl und Herrn Batschauer für die freundliche Übernahme der Gutachten bedanken. Bei Michael Feldbrügge möchte ich mich zudem für die guten Ratschläge und die gute Zeit beim Squasch bedanken. Ich wünsch Dir alles gute für Düsseldorf.

Mein größter Dank an dieser Stelle geht an Jörg. Ich danke Dir für dein Vertrauen und die Freiheiten die Du mir für meine Arbeit gegeben hast, und für deinen Einsatz während der letzten Monaten - Ich denke, der Stress hat sich gelohnt.

Mein besonderer Dank gilt allen Co-Autoren und Helfern, die für das Entstehen dieser Arbeit essentiell waren.

Regine Kahmann danke Ich für die freundliche und gute Zusammenarbeit während des "Zentral Experimentes". Robin Horst und besonders Gunther Doehlemann danke ich für die gute Zeit beim pflanzen, infizieren, schnippeln, mörsern, präpen, synthetisieren, hybridisieren, waschen, scannen...: Ne lange Liste, aber wir haben es gepackt! ;) Ohne Björn Usadel, Fabien Poree und Mark Stitt wäre die darauf folgende Analyse wohl unmöglich gewesen - danke für MapMan. Danke auch an die Mitstreiter aus Erlangen, Lars Voll und Uwe Sonnewald, sowie an Joern für die Hilfe bei statistischen Fragen. Norbert Sauer und Kathrin Wippel möchte ich vielmals für Ihre Mitarbeit und Ihr "Know-How" innerhalb des Transportprojektes danken - die Funktion von Srt1 war eine der wichtigsten Entdeckung für diese Arbeit. Magnus Rath möchte Ich dafür danken, dass er so viel Mühe in die Pflanzenschnitte und Färbungen investiert hat – ich bin sicher es wird sich noch auszahlen. ;)

Das Kämper-Lab, was soll ich sagen? Dank Euch!

Vor allem danke ich Kai und Miro. Wie lange machen Wir das jetzt schon zusammen - 5, 6 Jahre? Danke für die Zeit, den Spaß, und eure Hilfe, uva. - bleibt einfach wie Ihr seid. Al, Alex, Ali? Lets call u "The Great". As fourth year PhD-student I wanna thank u for lots of fun and good discussions - miss u at Kaiserallee 40. Kai und Nikola euch gehört die Zukunft. Es gilt ne schwere Bürde zu tragen – bin sicher Ihr schafft das. ;) Sarah, vielen Dank für Deine Hilfe während der letzten Monate, du hast mir ne Menge Arbeit abgenommen. An dieser Stelle geht noch mal ein dicker Kuss nach Marburg. Volker, auch wenn Du nicht mehr zur Gruppe gehörst, Danke für die vielen Pflanzen. Janine, Evelyn, Arne, Ronny und Mauri, Ich dank Euch für alles. Ohne Euch wäre das Projekt "Promotion" um einiges schwieriger gewesen. Ich vermisse euch hier in Karlsruhe.

Zu guter letzt möchte Ich mich noch bei zwei Menschen bedanken, die mir sehr am Herzen liegen.

Mum, Ich hab`s endlich geschafft. Danke für`s zuhören und Mut machen - Du bist die Größte.

Edyta - Danke, das Du die ganze Zeit für mich da warst Ich freu mich auf unsere Zukunft. Du bist das Beste was mir je passiert ist. Ich liebe Dich.

Lebenslauf

Persönliche Angaben

Ramon Wahl

Geburtsdatum: 07. August 1980
Geburtsort: Kreuztal
Geschlecht: männlich
Nationalität: deutsch

Schulbildung

07/1987-06/1991 Besuch der Grundschule Aue-Wingeshausen
07/1991-05/2000 Besuch des Johannes-Althusius-Gymnasium Bad Berleburg
Abschluss: Abitur

Studium

10/2000-09/2005 Studium der Biologie an der Philipps-Universität in Marburg
Hauptfächer: Genetik, Mikrobiologie, Biochemie
12/2004-09/2005 Anfertigung der Diplomarbeit am
Max-Planck Institut für terrestrische Mikrobiologie in Marburg
Thema: "Konstruktion von temperatursensitiven b-Heterodimeren in
Ustilago maydis"
Abschluss: Diplom in Biologie

Promotion

09/2005-04/2008 Untersuchungen zur Anfertigung der Doktorarbeit am
Max-Planck-Institut für terrestrische Mikrobiologie in Marburg
04/2008-06/2009 Abschließende Untersuchungen und Anfertigung der Dissertation am
Karlsruher Institut für Technologie
06/2009 Dissertation am Fachbereich Biologie der Philipps-Universität
in Marburg
Betreuer: Prof. Dr. Jörg Kämper
Thema: "Biotrophic Development of *Ustilago maydis* and the
Response of Its Host Plant Maize"